

1. Report No. FHWA/TX-11/0-5627-3		2. Government Accession No.		3. Recipient's Catalog No.	
4. Title and Subtitle FIELD EVALUATION OF ASPHALT MIXTURE SKID RESISTANCE AND ITS RELATIONSHIP TO AGGREGATE CHARACTERISTICS				5. Report Date September 2010 Published: August 2011	
				6. Performing Organization Code	
7. Author(s) Eyad Masad, Arash Rezaei, and Arif Chowdhury				8. Performing Organization Report No. Report 0-5627-3	
9. Performing Organization Name and Address Texas Transportation Institute The Texas A&M University System College Station, Texas 77843-3135				10. Work Unit No. (TRAIS)	
				11. Contract or Grant No. Project 0-5627	
12. Sponsoring Agency Name and Address Texas Department of Transportation Research and Technology Implementation Office P.O. Box 5080 Austin, Texas 78763-5080				13. Type of Report and Period Covered Technical Report: September 2009–August 2010	
				14. Sponsoring Agency Code	
15. Supplementary Notes Project performed in cooperation with the Texas Department of Transportation and the Federal Highway Administration. Project Title: Aggregate Resistance to Polishing and Its Relationship to Skid Resistance URL: http://tti.tamu.edu/documents/0-5627-3.pdf					
16. Abstract This report documents the findings from the research that was carried out as part of Phase II of TxDOT Project 0-5627. The research included measurements and analysis of mechanical and physical properties of aggregates used in surface mixes in the state of Texas. These properties were aggregate shape characteristics measured using the Aggregate Imaging System (AIMS), British Pendulum value, coarse aggregate acid insolubility, Los Angeles weight loss, Micro-Deval weight loss, and Magnesium sulfate weight loss. In addition, a database of field skid number measurements that were collected over a number of years using the skid trailer was developed. The Dynamic Friction Tester (DFT) and Circular Texture Meter (CTMeter) were used to measure friction and texture, respectively, of selected asphalt pavement sections. These data and measurements were used to carry out comprehensive statistical analyses of the influence of aggregate properties and mixture design on skid resistance value and its variability. Consequently, a method and software were developed for predicting asphalt pavement skid resistance. This method requires inputs that describe aggregate resistance to polishing, mixture gradation, and traffic. The developed software can be used to select the mixture type and aggregate source that are needed to achieve the required level of skid resistance for a given service life.					
17. Key Words Skid Resistance, Asphalt Mixture, Aggregate Characteristics			18. Distribution Statement No restrictions. This document is available to the public through NTIS: National Technical Information Service Alexandria, Virginia 22312 http://www.ntis.gov		
19. Security Classif.(of this report) Unclassified		20. Security Classif.(of this page) Unclassified		21. No. of Pages 118	22. Price

**FIELD EVALUATION OF ASPHALT MIXTURE
SKID RESISTANCE AND ITS RELATIONSHIP TO
AGGREGATE CHARACTERISTICS**

by

Eyad Masad, Ph.D., P.E.
Professor
Zachry Department of Civil Engineering
Texas A&M University

Arash Rezaei
Graduate Research Assistant
Zachry Department of Civil Engineering
Texas A&M University

and

Arif Chowdhury, P.E.
Assistant Research Engineer
Texas Transportation Institute

Report 0-5627-3

Project 0-5627

Project Title: Aggregate Resistance to Polishing and Its Relationship to Skid Resistance

Performed in cooperation with the
Texas Department of Transportation
and the
Federal Highway Administration

September 2010

Published: August 2011

TEXAS TRANSPORTATION INSTITUTE
The Texas A&M University System
College Station, Texas 77843-3135

DISCLAIMER

The contents of this report reflect the views of the authors, who are responsible for the facts and accuracy of the data presented herein. The contents do not necessarily reflect the official view or policies of the Texas Department of Transportation (TxDOT) or Federal Highway Administration (FHWA). This report does not constitute a standard, specification, or regulation. The engineer in charge was Eyad Masad, Ph.D., P.E. #96368.

ACKNOWLEDGMENTS

This project was made possible by the Texas Department of Transportation. Many personnel made possible the coordination and accomplishment of the work presented herein. Dr. German Claros, P.E., is the research engineer, and Ms. Caroline Herrera, P.E., is the project director for this research project. Mr. Edward Morgan and Ms. Zyna Polanski are members of the project monitoring committee (PMC). The authors are thankful to the PMC members for their guidance and directions. Numerous engineers, laboratory supervisors, and inspectors at the Texas Department of Transportation Districts and Pavement Division assisted by providing information, traffic control, material samples, and also by helping in some field testing. Without their cordial cooperation it would not be possible to complete this project.

TABLE OF CONTENTS

LIST OF FIGURES	viii
LIST OF TABLES	ix
CHAPTER I – INTRODUCTION	1
PROBLEM STATEMENT	3
OBJECTIVES	3
SCOPE OF THE STUDY	3
ORGANIZATION OF THE REPORT	4
CHAPTER II – SUMMARY OF PHASE I	5
INTRODUCTION	5
EXPERIMENTAL DESIGN	5
ANALYSIS OF AGGREGATE TEXTURE AND GRADATION	7
ANALYSIS OF ASPHALT MIXTURE FRICTION AND SKID RESISTANCE	8
CHAPTER III – ANALYSIS OF SKID RESISTANCE DATA	13
INTRODUCTION	13
SUMMARY OF THE ANALYSIS OF SKID RESISTANCE DATA	13
CHAPTER IV – ANALYSIS OF DFT AND CTMETER MEASUREMENTS ON ASPHALT PAVEMENTS	19
INTRODUCTION	19
SELECTION OF THE FIELD SECTIONS	19
ANALYSIS OF FIELD MEASUREMENTS	23
CHAPTER V – A SYSTEM FOR PREDICTING SKID NUMBER OF ASPHALT PAVEMENTS	31
INTRODUCTION	31
DEVELOPMENT OF SYSTEM FOR PREDICTING SKID NUMBER	31
SENSITIVITY ANALYSIS OF PREDICTION SYSTEM	38
RECOMMENDED SYSTEM FOR PREDICTING SKID NUMBER	42
ILLUSTRATION OF AN AGGREGATE CLASSIFICATION SYSTEM BASED ON PROPOSED MODEL	42
SKID ANALYSIS OF ASPHALT PAVEMENTS (SAAP)	44
CHAPTER VI – CONCLUSIONS AND RECOMMENDATIONS	53
SUMMARY OF THE RESULTS OF THE FIELD DATA ANALYSIS	53
RECOMMENDATIONS	54
REFERENCES	57
APPENDIX A – STANDARD PROCEDURES FOR MEASURING DEGRADATION OF AGGREGATE BY MICRO-DEVAL ABRASION AND TEXTURE MEASUREMENT BY AIMS	63
APPENDIX B – SAMPLE ILLUSTRATION OF SURFACE CHARACTERISTICS FOR DIFFERENT MIX TYPES	95
APPENDIX C – EXAMPLE DATA AND SENSITIVITY ANALYSIS	103

LIST OF FIGURES

Figure 1. Weibull Distribution Function.....	8
Figure 2. Different Modules of the Predictive Model of IFI.	10
Figure 3. IFI Model Input Parameters.....	11
Figure 4. Layout of the Measurement Section (a) Schematic of Measurement Plan (b) CTMeter Measurement.	22
Figure 5. Layout of the Measurement Section: DFT Measurement.	23
Figure 6. Measured MPD Values for Different Mix Types.....	25
Figure 7. Mean Profile Depth vs. Measured Skid Number.....	26
Figure 8. Mean Dynamic Friction at 20 km/h for Different Aggregates.....	27
Figure 9. Mean Dynamic Friction at 20 km/h for Different Aggregate Types.....	28
Figure 10. Dynamic Friction at 20 km/h vs. Measured Skid Number for Different Mix Types.	29
Figure 11. TMF vs. Number of Polishing Cycles.....	35
Figure 12. Measured Skid Number vs. Calculated Skid Number Using PIARC Equation.	36
Figure 13. Measured Skid Number vs. Calculated Skid Number Using Modified PIARC Equation.	37
Figure 14. Relationship between Measured and Calculated MPD Values.	38
Figure 15. Terminal Friction Values for Different Aggregates and Mix Designs.....	39
Figure 16. Polishing Rate for Different Aggregates.	40
Figure 17. IFI Values as a Function of TMF for Sample 1.....	41
Figure 18. SN Values as a Function of TMF for Sample 1.	41
Figure 19. Initial Window of the Program.....	45
Figure 20. Aggregate Gradation Input.	45
Figure 21. Manual Aggregate Gradation.	46
Figure 22. AIMS Texture Data Input Window.....	47
Figure 23. Texture Data Points Select.	47
Figure 24. Two Point Texture Measurement.	48
Figure 25. Three Point Texture Measurement.	48
Figure 26. Input MPD Value.	49
Figure 27. Traffic Data Input.	49
Figure 28. Analysis Type.....	50
Figure 29. A Sample Plot of Skid Number over the Service Years.....	51
Figure 30. Classification Setting Values.....	52
Figure 31. Classification Sample.....	52

LIST OF TABLES

Table 1. Aggregate Sources Used in Pavement Sections.	15
Table 2. Measured Field Sections.	20
Table 3. Lane Distribution Factor.	23
Table 4. Calculated Scale and Shape Factors for Different Mixes.	33
Table 5. Selected Aggregates Based on Terminal Texture.	38
Table 6. Selected Aggregates Based on Polishing Rate.	39
Table 7. Skid Number Threshold Values after Five Years of Service.	43
Table 8. Aggregate Classification for Different Roads.	44

CHAPTER I – INTRODUCTION

In 2005, 6.1 million traffic crashes, 43,443 traffic fatalities, and approximately 2.7 million traffic-related injuries throughout the United States were reported by the National Highway Traffic Safety Administration (1). Nationwide studies showed that between 15 to 18 percent of crashes occur on wet pavements (2-4), and many researchers indicated that there is a relationship between wet weather accidents and pavement skid resistance (5-7). Accident rates can be reduced greatly by implementing corrective measures to improve the skid resistance of asphalt pavements in hazardous areas.

Pavement skid resistance is primarily a function of the surface macrotexture and microtexture (8). Macrotexture refers to the large irregularities on the road surface (coarse-scale texture) that are associated with voids between aggregate particles. The magnitude of the macrotexture depends on the size, shape, and distribution of coarse aggregates used in pavement construction as well as the particular construction techniques used in the placement of the pavement surface layer (1,9). Microtexture refers to small irregularities on the pavement surface (fine-scale texture), and it is related mostly to aggregate surface texture and the ability of the aggregate to maintain this texture against the polishing action of traffic and environmental factors (1,10).

Road surfaces will attain their peak skid resistance condition after a few weeks of traffic action due to wearing of the surface asphalt binder. This is followed by polishing of the surface aggregates and loss of both microtexture and macrotexture (11-14). The loss of skid resistance usually starts at a high rate followed by a slower rate until an equilibrium skid resistance state is reached (15-17).

The well-documented influence of aggregate on skid resistance has encouraged the development of several methods for evaluating the abrasion and polishing resistance of aggregates and classifying aggregates based on these characteristics. Some researchers used petrographic examination to evaluate aggregate mineralogy and put forward guidelines for the use of aggregates in asphalt pavement construction (18). For example, Bloem (19) stated that sandstone aggregate has an excellent frictional performance because it is composed of hard quartz particles cemented together with brittle binder.

These particles are exposed when the cement is worn away by traffic. Goodman et al. (20) indicated that rocks containing igneous and metamorphic constituents are less susceptible to polishing than sedimentary rocks. Other studies stated that synthetic aggregates, e.g., slag or expanded lightweight aggregate (fabricated by heating natural clay), can also improve pavement frictional resistance (21,22). Csathy et al. (23) reported that limestone, which is the most common type of aggregate used in road construction, is the most susceptible aggregate type to polishing, and polish susceptibility of the limestone depends on calcite and dolomite contents (24). Some researchers attributed the differences among aggregates in resisting polishing to the content of wear-resistant minerals such as silica (19,25). Bloem (19) stated that the siliceous particle content should be at least 25 percent to have satisfactory polish resistance. These studies demonstrated that petrographic analysis is very useful to understand the influence of mineralogy on polishing resistance. However, the significant variation in mineralogy and structure among aggregates would prohibit classifying aggregates based on their geological group (i.e., sedimentary, metamorphic, and igneous). In addition, petrographic analysis does not lend itself easy to the development of specifications that can be used by aggregate suppliers and highway agencies.

Many studies proposed test methods such as the Los Angeles (LA) abrasion test, Magnesium sulfate soundness, and British pendulum test to evaluate the aggregate's resistance to polishing (26). For example Crouch et al. (26) used a modified version of AASHTO TP33 procedure to measure the uncompacted voids in coarse aggregates that were subjected to various times of abrasion in the LA test. Other studies, however, reported that the LA abrasion test and other physical tests (e.g., freeze and thaw test) do not yield good predictions of field friction (27,28). Although the British pendulum test is probably the most common method used to assess frictional resistance of aggregates, many studies have reported that the results from this test are a function of many other factors (e.g., magnitude and number of gaps between the aggregates' coupon curvature, the arrangement of aggregate particles in a coupon), and this test has a high variability (29-31). More recently, Prowell et al. (32) suggested the use of the Micro-Deval test as a surrogate to determine an aggregate resistance to weathering and abrasion instead of a sulfate soundness and LA abrasion tests. Mahmoud and Masad (33) recommended the

use of the aggregate imaging system (AIMS) to measure loss of texture of aggregates subjected to polishing in the Micro-Deval. Despite recent progress in the development of new aggregate tests, there has been little progress in applying the results of these tests in models that can be used to predict the skid resistance of asphalt pavements.

PROBLEM STATEMENT

The texture characteristics of aggregate and asphalt mixture design are important factors that influence the skid resistance of asphalt pavements. There is a need for developing a comprehensive system for selecting aggregates and asphalt mixture design such that the required level of skid resistance is achieved, and for predicting the skid resistance of asphalt pavements throughout their service life. This system will contribute to the construction of safe asphalt pavements and reduce the cost of maintenance and rehabilitation.

OBJECTIVES

The objectives of this project were to (1) study the influence of aggregate properties and mix types on asphalt pavement skid resistance and (2) develop a system for predicting asphalt pavement skid resistance during its service life. These objectives were achieved by measuring and analyzing skid trailer data over a number of years, measuring friction and pavement texture of asphalt pavements using Dynamic Friction Tester (DFT) and Circular Texture Meter (CTMeter), and measuring aggregate characteristics.

SCOPE OF THE STUDY

The literature survey shows that aggregate characteristics affect frictional properties of flexible pavements to a high degree. The hypothesis behind this study is that it is possible to measure the frictional characteristics of different aggregate types and improve the frictional performance of the pavement surface by the selection of polish-resistant aggregates with certain shape and texture characteristics.

The scope of this project included measuring and analyzing various characteristics of aggregates used in surface mixes in the state of Texas. These characteristics were aggregate shape, angularity and texture measured using the Aggregate Imaging System (AIMS); British Pendulum value, coarse aggregate acid insolubility; Los Angeles weight loss; Micro-Deval weight loss, and magnesium sulfate weight loss. In addition, this project included developing a database of the annual field skid resistance data, conducting field measurements of the selected sites, and developing a relationship to predict skid resistance as a function of aggregate characteristics and mixture design.

ORGANIZATION OF THE REPORT

Chapter II of this report includes a summary of the results of Phase I of TxDOT Project 0-5627. Chapter III describes the work that was conducted as part of Phase II of the project and data analysis results. Chapter IV presents the results of measuring asphalt pavement frictional properties. The system for predicting asphalt pavement skid number as a function of aggregate properties and mixture design is presented in Chapter V. The last chapter, Chapter VI, includes the conclusions and recommendations of this study.

Appendix A presents two standard test procedures suggested by this project to characterize the texture of aggregates. These tests include aggregate polishing by Micro-Deval device and texture measurement by AIMS. Appendix B depicts some typical pictures taken during the field testing. The corresponding friction, texture, and skid number will provide some basis for comparison. Research Report 0-5627-2 also describes partial efforts carried out in Phase II of this research study.

CHAPTER II – SUMMARY OF PHASE I

INTRODUCTION

TxDOT Project 5-1707 developed a method to measure aggregate shape, angularity, texture, and the changes of these characteristics as a function of polishing time. Research Project 0-5627 was initiated to produce a new aggregate classification system based on relating the results of the new test method developed in Project 5-1707 for measuring aggregate characteristics to real-life field pavement skid resistance. The following tasks were carried out in Phase I on Project 0-5627 and presented in Research Report 0-5627-1:

- Completed a comprehensive literature survey to determine available tests for measuring aggregate characteristics related to asphalt pavement skid resistance.
- Conducted laboratory and field tests for directly or indirectly measuring asphalt pavement skid resistance.
- Developed models for predicting skid resistance as a function of material properties and mixture gradation.

EXPERIMENTAL DESIGN

The laboratory experiments involved the use of five different aggregate sources and a blend of two sources from the state of Texas. The mineralogy and relative hardness (Mohs hardness scale) of these aggregates can be found in Report 0-5627-1.

The Micro-Deval device was selected as the main aggregate polishing tool, and aggregate samples were polished in the Micro-Deval for two different time durations: 105 minutes and 180 minutes. The Micro-Deval test was conducted following the ASTM D6928 procedure. In this test, a steel container is loaded with 5000 grams of steel balls and 1500 grams of an aggregate sample in the range of 4.75 mm to 16 mm and 2000 ml tap water. The blend of steel balls and aggregates is subjected to 9600 to 12,000 revolutions, and the sample weight loss (weight of aggregate passed #16 sieve size) is measured and reported. In this research study, the texture of polished aggregate was

measured by AIMS after 105 minutes and 180 minutes polishing in the Micro-Deval device. AIMS is an automated imaging system that determines the angularity, shape, and texture of coarse aggregate as well as the shape and angularity of fine aggregates based on a scanning system and digital image processing. This system is equipped with a digital camera, back-lighting, and top-lighting units that can provide enough light intensity to capture a clear 2-D image of aggregate particles. AIMS quantifies texture by analyzing the variations of gray scale shadows on images using the wavelet analysis method (34). The variations in gray scale increase with an increase in texture. Previous analysis has shown that AIMS is capable of measuring aggregate texture less than 0.5 mm and down to 10 microns (34).

Large asphalt slabs were compacted in the laboratory using three commonly used asphalt mixtures in Texas. These three mixtures were: Type C, Type D, and porous friction course (PFC). The Type C and Type D mixes are dense graded surface mixtures with 16 mm and 9.5 mm nominal maximum aggregate size (NMAS), respectively (35). The third mixture is an open graded mixture or PFC and contains a large proportion of one-sized coarse aggregates typically from 9.0 mm to 12.5 mm in size (35). These slabs were polished at three locations by the three-wheel polishing device originally developed at the National Center for Asphalt Technology (NCAT). This machine is capable of polishing a donut shape area with a mean diameter of 284 mm to accommodate DFT and CTMeter measurements (36). Friction and texture measurements were performed before any polishing and after predefined polishing cycles. The maximum number of polishing cycles was 100,000 cycles for Type C and Type D, and 200,000 cycles for PFC mixtures. All Type D mixtures showed signs of severe raveling after 5000 polishing cycles. Consequently, researchers decided to discontinue polishing these mixtures.

The friction properties of surface were measured using DFT following the ASTM E1911-98 procedure. The DFT device consists of three rubber sliders attached to a rotating 350 mm wheel driven by a motor that can reach to 100 km/h tangential speed (37). In this device, three transducers measure the traction force in each rubber slider while dragging on the pavement. Considering the vertical pressure that is reasonably close to the contact pressure of vehicles, the coefficient of friction of the surface is

determined (38). The DFT measurement at 20 km/h is an indication of surface microtexture (39).

The CTMeter is a texture measuring device equipped with a Charged Couple Device (CCD) laser displacement sensor mounted on an arm above the surface. This test was conducted according to ASTM E2157 procedure (37). A motor at a tangential velocity of 6 mm/min drives the arm. The CCD laser takes 1024 samples of the pavement surface at one round with 0.87 mm spacing. To calculate the mean profile depth (MPD) the data are divided into eight equal 111.5 mm arcs. The calculated MPD for each segment is averaged and presented as MPD for the test surface (40).

ANALYSIS OF AGGREGATE TEXTURE AND GRADATION

As discussed earlier, AIMS was used to measure aggregate texture at three points: before polishing in the Micro-Deval, after 105 minutes of polishing, and after 180 minutes of polishing. The equation proposed by Mahmoud and Masad (33) was then used to describe texture as a function of polishing time (t) in minutes as shown in Equation 1:

$$Texture(t) = a_{agg} + b_{agg} \cdot \exp(-c_{agg} \cdot t) \quad (1)$$

where a_{agg} , b_{agg} , and c_{agg} are regression constants. In this equation a_{agg} , $a_{agg}+b_{agg}$, and c_{agg} are interpreted as the terminal, initial, and rate of texture change, respectively. The coefficients of the texture model were obtained using a non-linear regression analysis.

As reported by many studies, aggregate gradation is an important factor that affects pavement macrotexture and skid resistance. Therefore, it was important to quantitatively describe aggregate gradation of mixtures used in this study. For this purpose, different standard distribution functions were considered, and the cumulative two-parameter Weibull distribution that has the form of Equation 2 was found to fit the standard aggregate size distribution data:

$$F(x; \lambda, \kappa) = 1 - e^{-\left(\frac{x}{\lambda}\right)^\kappa} \quad (2)$$

where x is aggregate size in millimeters, and κ and λ are known as the shape and scale parameters of the Weibull function, respectively. These two parameters change depending on the mixture gradation. Figure 1 demonstrates the effect of shape and scale parameters on Weibull distribution function.

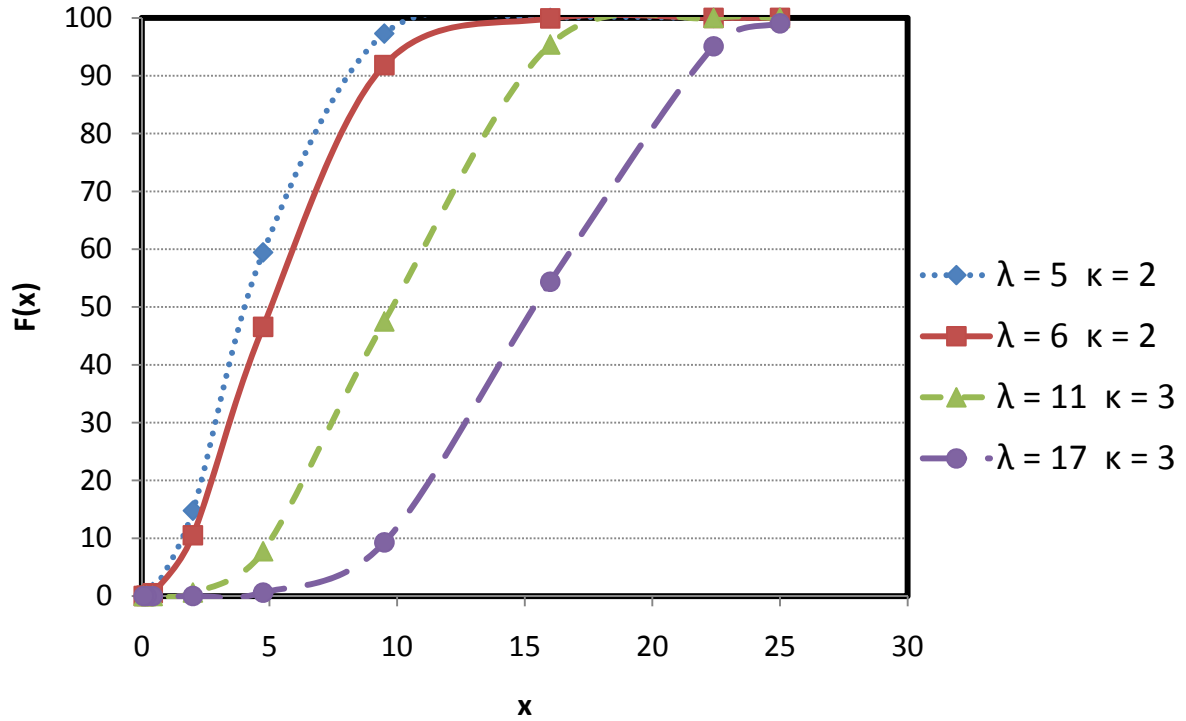


Figure 1. Weibull Distribution Function.

ANALYSIS OF ASPHALT MIXTURE FRICTION AND SKID RESISTANCE

The mixture friction resistance was quantified by the International Friction Index (IFI), which was developed as a universal method for the characterization of pavement surface friction and harmonization of different friction measuring equipment (41,42).

The IFI can be calculated using friction and texture measurements obtained by means of different test methods. The IFI equation includes calibration factors that depend on the test methods used to measure friction and texture. Using DFT and CTMeter measurements, the IFI could be calculated as in Equations 3 and 4:

$$IFI = 0.081 + 0.732 DF_{20} \exp\left(\frac{-40}{S_p}\right) \quad (3)$$

$$S_p = 14.2 + 89.7MPD \quad (4)$$

The IFI is also related to skid resistance measured using smooth tire skid trailer as in Equation 5:

$$IFI = 0.045 + 0.925 \times 0.01 \times SN(50)e^{\frac{20}{S_p}} \quad (5)$$

where, DF20 is the measured dynamic friction at 20 km/h, which is a measure of microtexture; MPD is mean profile depth and is measured by CTMeter; S_p is a function of MPD value; and SN(50) is skid number measured by a smooth tire tow trailer at 50 mph (80 km/h).

Researchers found that the equation proposed by Mahmoud and Masad (33) for describing the loss of aggregate texture (Equation 1) can be used to describe the change of IFI. However, the time in Equation 1 was replaced with increments of 1000 polishing cycles as shown in Equation 6:

$$IFI(N) = a_{mix} + b_{mix} \times \exp(-c_{mix} \cdot N) \quad (6)$$

where a_{mix} , $a_{mix}+b_{mix}$, and c_{mix} are the terminal, initial, and rate of change in IFI. N is the number of increments of 1000 polishing cycles (e.g., N = 60 for 60,000 polishing cycles). The regression coefficients of Equation 6 were determined using nonlinear regression analysis. The high R^2 values obtained for each mix showed that Equation 6 was able to accurately describe the IFI functions for all mixtures.

The coefficients of the IFI equation (Equation 6) were related to the aggregate texture coefficients (Equation 1) and the gradation parameters (Equation 2), and the statistical model that emerged is shown in Equations 7–9:

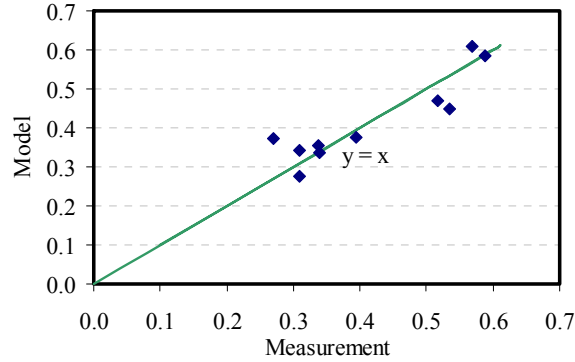
$$a_{mix} = \frac{18.422 + k}{118.936 - 0.0013 \times (AMD)^2} \quad R^2 = 0.96 \quad (7)$$

$$a_{mix} + b_{mix} = 0.4984 \ln \left[5.656 \times 10^{-4} (a_{agg} + b_{agg}) \right. \\ \left. \dots + 5.846 \times 10^{-2} \kappa - 4.985 \times 10^{-2} \lambda \right] \quad R^2 = 0.82 \quad (8)$$

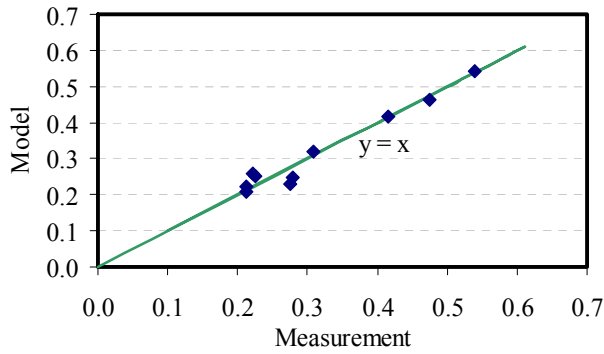
$$c_{mix} = 0.765 \cdot e^{\left(\frac{-7.297 \cdot 10^{-2}}{c_{agg}} \right)} \quad R^2 = 0.90 \quad (9)$$

where, AMD is aggregate texture after Micro-Deval polishing measured by AIMS; $a_{agg}+b_{agg}$ and c_{agg} are the initial and rate of texture change for corresponding

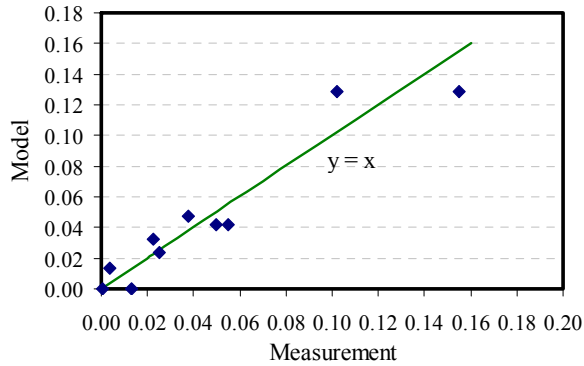
aggregate; and k , λ are Weibull distribution shape and scale factors, respectively. Figure 2 shows that the model does a very good job in representing terminal, initial, and rate of IFI measurements.



(a) Terminal IFI



(b) Initial IFI



(c) Rate of IFI Change

Figure 2. Different Modules of the Predictive Model of IFI.

In summary, Figure 3 and Equations 1 to 9 present the model developed in Phase I of this research project.

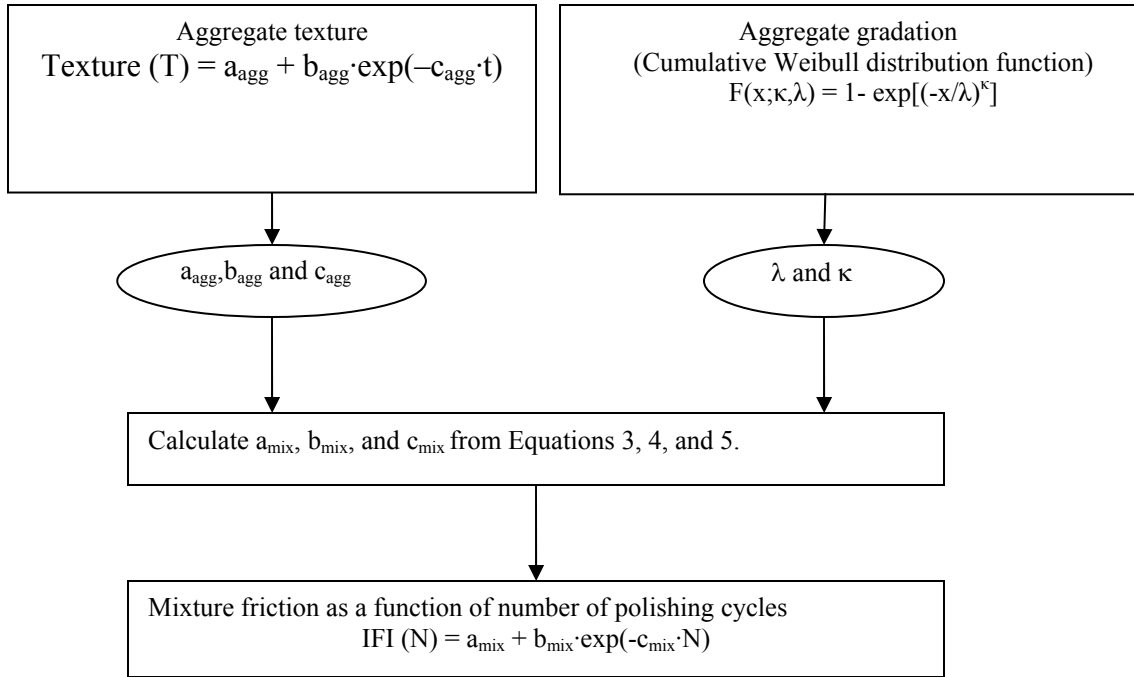


Figure 3. IFI Model Input Parameters.

This model can be used to predict mix friction based on gradation and aggregate resistance to polishing. This model also facilitates selecting appropriate aggregate type for desired mixture friction, and it can be used as a starting point to classify aggregates based on their frictional properties.

CHAPTER III – ANALYSIS OF SKID RESISTANCE DATA

INTRODUCTION

The objective of Phase II was to correlate laboratory measurements of friction and texture of asphalt mixtures as well as aggregate resistance to polishing to field measurements of skid resistance of asphalt pavements. This objective was achieved in two steps. In the first step, data of skid resistance measurements using the skid trailer were collected for many field sections with known construction history. In the second step, CTMeter and DFT measurements were conducted on pavement sections with a record of skid measurements for several years, construction history, and diverse range of weather and traffic conditions.

SUMMARY OF THE ANALYSIS OF SKID RESISTANCE DATA

Skid resistance is typically measured using the friction trailer, which is towed at a constant speed over the pavement. When the test is initiated, water is sprayed in front of the tire so the wet pavement friction can be tested. The wheel is fully locked, and the resulting torque is recorded. Based on the measured torque (converted to a horizontal force) and dynamic vertical load on test wheel, the wet coefficient of friction between the test tire and pavement surface is calculated. The skid number (SN) is then reported as the coefficient of friction multiplied by 100. The same speed should be maintained before the test and when the wheel is locked. The friction trailer is typically equipped with two types of tires: rib tire on the right side according to ASTM E501 and smooth tire on the left side according to ASTM E524. Following the recommendation of the ASTM E-274 specification, the test speed (48, 64, or 80 km/h) and type of tire (R for rib and S for smooth tire) should be cited when the SN is reported. For example, SN(64)S indicates that the test was performed at a speed of 64 km/h (40 mile/h) with the smooth type of tire (SN40S is used if speed is reported in miles per hour). The friction trailer used by TxDOT is equipped with smooth tires and travels at a speed of 80 km/h (50 mile/h).

Researchers conducted extensive data collection and analysis in this project to create a database of sections with different friction characteristics. The initial selection of

sections intended to include the mixes and aggregates that were already tested in the laboratory phase of this research study and to include sections for which the skid performance was available. The initial experimental design was revised several times by the TTI researchers and TxDOT engineers to agree on a sound and inclusive experimental design. Moreover, availability of the skid data, availability of the traffic data, variety of the aggregate lithologies, variety of mix types, and availability of construction and maintenance record were the main factors considered in the selection of sections. The experimental design was then finalized and implemented in Phase II of this project.

A huge amount of skid resistance data was studied to choose and extract the most reliable data. Several meetings with TxDOT research groups were held to decide on the desired sections. Since the skid data and construction record of each project is kept in two different databases, a comprehensive effort was made to select the sections with a wide range of construction history and a long record of skid data. Any discrepancies between the data and field observations were thoroughly investigated. TTI researchers contacted each TxDOT district office to confirm the data integrity and accuracy. Many meetings and conference calls were held with data providers to obtain some details on the collected data (e.g., the exact location of the tested field, date and time, construction date, materials data, etc.). Afterward, the data were analyzed using statistical analysis methods.

After reviewing all data, 65 roads including 1527 Pavement Management Information System (PMIS) sections that cover a wide range of skid performance were identified. Each PMIS section is a particular stretch of roadway with predefined boundaries defined by Texas reference markers. These sections are distributed in the nine TxDOT districts.

These 1527 PMIS sections contain 4068 data records with 21 aggregate types as tabulated in Table 1, and different mix types, e.g., surface treatments Grade 4 aggregate, surface treatment Grade 3, PFC, and Type C.

Table 1. Aggregate Sources Used in Pavement Sections.

<i>No.</i>	<i>Aggregate</i>	<i>Material Type</i>	<i>TxDOT Classification</i>
1	A	Crushed Siliceous Gravel	SAC A
2	B	Crushed Limestone-Dolomite	SAC B
3	C	Crushed Limestone-Dolomite	SAC B
4	D	Crushed Granite	SAC A
5	E	Crushed Limestone-Dolomite	SAC B
6	F	Crushed Limestone-Dolomite	SAC B
7	G	Crushed Limestone-Dolomite	SAC B
8	H	Sandstone	SAC A
9	I	Crushed Siliceous & Limestone Gravel	SAC A
10	J	Crushed Limestone Rock Asphalt	SAC B
11	K	Crushed Limestone-Dolomite	SAC B
12	L	Lightweight Aggregate	SAC A
13	M	Crushed Limestone-Dolomite	SAC B
14	N	Crushed Limestone-Dolomite	SAC B
15	O	Crushed Traprock	SAC A
16	P	Crushed Traprock	SAC A
18	R	50 percent aggregate H + 50 percent aggregate K	N/A
19	S	Crushed Rhyolite	SAC A
20	T	Crushed Granite	SAC A
21	U	Crushed Limestone-Dolomite	

To facilitate comparing different factors affecting pavement skid resistance the following simplifications were made:

- As long as gradation remains the same, regardless of asphalt type, the surface treatment was assumed to be the same, e.g., surface treatment Grade 4 is a combination of size 4 aggregates with AC-15P, AC-20-5TR, AC 20XP, and CRS-2P asphalt types. Furthermore, only two types of surface treatment were considered in the analysis while the effect of binder type on frictional characteristics was not considered.
- In order to compare different road categories in different service years, a new parameter called Traffic Multiplication Factor (TMF) was introduced. As shown in Equation 10, TMF is the multiplication of the Annual Average Daily Traffic (AADT) and number of years in service.

$$TMF = \frac{AADT \times \text{Years in Service} \times 365}{1000} \quad (10)$$

This factor reflects the cumulative effect of both years in service and AADT for the most critical lane in the highway, i.e., outer lane. The results of the data analysis showed the measured skid number decreased as TMF increased. The measured skid numbers had less variation at higher TMF levels. This phenomenon could be attributed to mixtures reaching close to terminal skid condition, which is associated with aggregates approaching their equilibrium (or terminal) state of texture after a high number of polishing or loading cycles.

Field measurement of skid trailer on four surface types (surface treatment Grade 3, surface treatment Grade 4, PFC, and Type C) were included in the analysis. The results showed that the surface treatments had a very high variability in their measured skid number using skid trailer. This variability occurs because the measured skid number for surface treatments is not just a function of aggregate shape characteristics and gradation, but other factors such as overall macrotexture of pavement surface. The spatial variation of pavement macrotexture of surface treatments is significant due to aggregate penetration in the asphalt, asphalt bleeding, and aggregate reorientation under traffic. The results also revealed that surface treatments generally had higher skid numbers than Type C, which is a conventional dense graded mix. Additionally, PFC mixes exhibited better skid resistance than Type C mixes and surface treatment mixes. Although initial skid numbers of surface treatments are very high, they may drop rapidly if the macrotexture of pavement drops by the mechanism mentioned earlier. Moreover, unlike hot-mix asphalt, the quality of surface treatments is more affected by the surface irregularities of the underlying layer. The PFC mixes had the lowest variation in measured skid number.

The effect of aggregate type was studied, and the results showed that there was a high interaction between aggregate performance, mix type in which aggregate is used, and traffic level. In general, it is hard to classify aggregates without specifying mixture type and traffic levels. For instance, aggregate K provided good skid resistance in surface treatment Grade 3 at low TMF, whereas dense graded mixtures (Type C) with this same aggregate showed low skid performance. This poor performance could be attributed to the high polishing rate of aggregate K as was found in the laboratory measurements conducted in Phase I of this project.

The aggregate K that is classified as SAC B (surface aggregate classification B) in the TxDOT classification system and aggregate O, which is classified as SAC A, yield similar skid resistances when they are used in surface treatment Grade 4. Aggregate J, classified as SAC B, provides very high skid resistance level in surface treatment Grade 4 at low and medium TMF. On the other hand, aggregate P, which is a SAC A, provides only good skid resistance in surface treatment Grade 4. Although aggregate J and K both are classified as SAC B, but under similar conditions they show skid numbers of 54 and 29, respectively, when used in surface treatment Grade 4. These results show that the surface aggregate classification system does not always yield consistent skid resistance.

For the most part, the results of the field data analysis, conducted in Phase II, are in agreement with the laboratory findings in Phase I. The same equation form (i.e., Equation 1) that was used to describe aggregate polishing rate can be used to describe skid number versus TMF values in the field and also describe skid number versus polishing cycles in the laboratory.

CHAPTER IV – ANALYSIS OF DFT AND CTMETER MEASUREMENTS ON ASPHALT PAVEMENTS

INTRODUCTION

This chapter presents the analysis and results of field measurements using CTMeter and DFT and development of a theoretical relationship between laboratory and field data. During the field testing, efforts were made to test the same part of the pavement section that was already tested by the TxDOT towed friction trailer.

Friction and macrotexture tests using DFT and CTMeter, respectively, were conducted in the selected sections in such a way that the total number of tests was distributed uniformly within the length of the tested section (section length was about 0.5 mile for the highway).

SELECTION OF THE FIELD SECTIONS

In this study, researchers selected 64 sections for friction and macrotexture evaluation. The sections were selected to cover a wide range of material type and traffic levels; represent different road types (i.e., interstates, state highways, U.S. highways, and farm to market roads); and such that a complete record of the construction and skid measurement were available in the TxDOT database. The pavement age of these sections was between two and 11 years. These sections were distributed on different TxDOT districts. Table 2 shows a list of the sections.

Table 2. Measured Field Sections.

District	County	Highway	Des.	Mix Design	TRM	Dir.
Abilene	Nolan	IH20	L	CRM	247+0.1	WB
	Taylor	IH20	L	PFC	272+0.1	WB
				Superpave 1/2"	280+0.8	WB
				PFC	284-0.55	WB
				US83	L	PFC
Atlanta	Harrison	IH20	R	SMA-C	634+320'	EB
Austin	Bastrop	US290	K	PFC	628+0.53	EB
	Travis	SH71	L	Type C	582-0.61	WB
Beaumont	Hardin	FM421	K	Type C	747+0.7	EB
		US69	K	SMA-D	489+0.1	SB
	Jefferson	SH73	L	PFC	772+0.1	WB
		US69	L	PFC	538-0.05	NB
	Tyler	SH146	K	Type C	422+0.7	NB
Brownwood	Brown	FM2376	K	Type D	460+1.6	NB
		FM2524	K	Type D	340+ 0.4	SB
		FM3064	K	Type D	458+0.9	WB
		SH153	K	Type D	372+0.7	WB
		US67	K	Type D	570+0.4	WB
	Eastland	IH20	L	Type D	362+0.6	WB
		SH36	K	Type C	346+1.6	WB
	McCullough	US87	R	Type D	458+0.2	SB
Bryan	Limestone	US84	K	Type C	736+150'	EB
Corpus Christi	Nueces	IH37	R	PFC	15+0.73	NB
	San Patricio	IH37	R	PFC	17+0.64	NB
Fort Worth	Johnson	IH35	WL	Type D	29-100'	SB
Houston	Brazoria	SH288	R	PFC	496+1.35	SB
	Conroe	IH45	L	PFC	93+0.1	SB
	Fort Bend	SH6	K	PFC	682+0.75	SB
	Waller	SH6	L	PFC	628+1	NB
Lubbock	Crosby	US-62	L	CMHB-C	352+1.7	WB
	Floyd	US-62	R	CMHB-C	386+0.1	EB
	Garza	SH207	K	CMHB-F	254+1.7	SB
		US84	L	CMHB-C	352+1.7	NB
	Lynn	FM1317	K	CMHB-F	296 +80'	EB
		US380	K	CMHB-C	320+1.7	EB
		US87	L	CMHB-C	306+1-400'	NB
Terry	US62	L	Novachip	296+0.5+100'	WB	
Odessa	Ector	IH20	R	CMHB-F	117+0.7	EB
	Midland	IH20	R	PFC	147+0.5+400'	EB

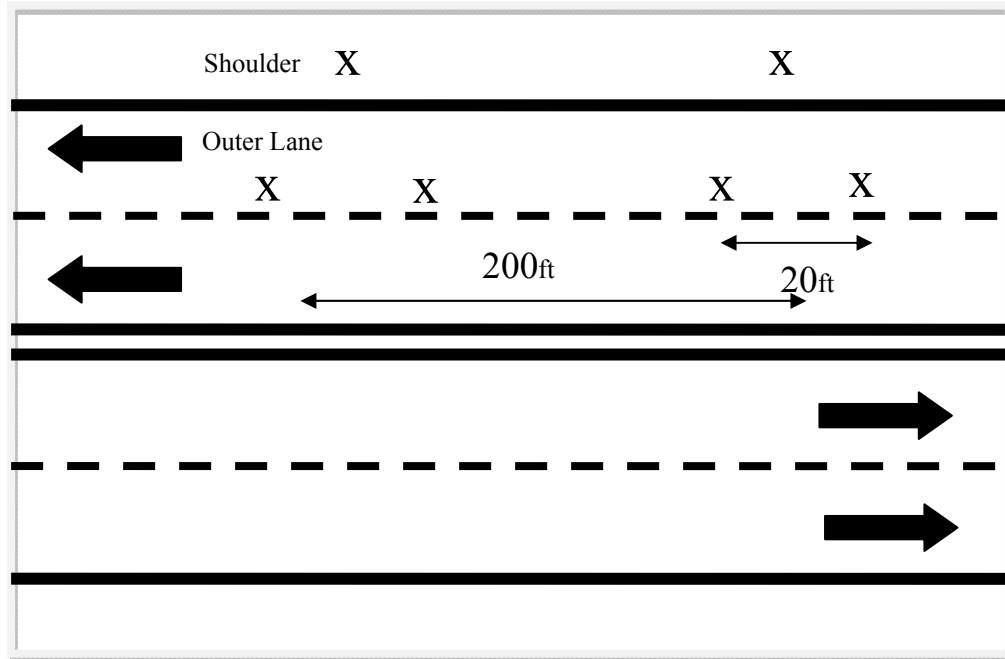
Table 3. Measured Field Sections (Continued).

District	County	Highway	Des.	Mix Design	TRM	Dir.
Paris	Hopkins	IH30	L	PFC	134-.035	WB
		SH154	K	Type D	674-0.74	NB
San Antonio	Bexar	IH35	R	PFC	168+0.8	NB
		SH16	R	Type C	614	SB
		US90	R	Type C	560+1.75	EB
	Wilson	US181	R	Novachip	518	SB
Tyler	Anderson	US287	K	Type D	604+0.1	NB
	Greg	IH20	L	Type D	580+0.7	WB
				Type C	591-200'	WB
	Smith	IH20	L	Type C	550-500'	WB
				Type C	557-500'	WB
	Van Zandt	IH20	L	Type C	518-200'	WB
Waco	Hill	IH35	L	SMA-D	358-200'	SB
	McLennan	SH6	L	PFC	502-0.1	WB
Wichita Falls	Clay	US287	K	PFC	532+0.5	NB
		US287	L	PFC	368 + 1.8	WB
	Wichita	SH240	L	PFC	470-0.85	NB
		SL473	K	PFC	192-0.35	SB
Yoakum	Gonzales	IH10	L	PFC	636+0.2	WB
	Victoria	US59	L	Type C	632+60'	NB
		US59	R	PFC	632+0.5	SB
				PFC	634+120'	SB
	Wharton	US59	L	Type C	562-550'	NB
		US59	R	PFC	560+1+260'	SB
Austin	SH36	K	Type D	612+1.5+200'	SB	

Measurements were conducted on the outer lane as the skid trailer measurements are typically performed at the outside lane (in case of multiple lanes). The outer lane experiences the most polishing because most truck traffic uses this lane. Measurements were completed on a travel lane and shoulder. Since the shoulders are subjected to little or no traffic, skid resistance measurements were assumed to represent the initial skid measurements of travel lane.

The CTMeter and DFT devices were positioned in the left wheelpath in all test sections. Please note that the skid number measured by the trailer is done locking the left wheel. Six locations were tested in each section. Two locations were at the shoulder, and four locations were at the outer lane. Two DFT and six CTMeter readings were

performed at each location. The DFT and CTMeter measurements were conducted at the same exact locations following ASTM E 2157 and ASTM E 1911 procedures, respectively. Figure 4 and Figure 5 show the layout of the measurement locations. During the testing the research team avoided extreme cold ambient temperature or rain. Information about construction, traffic, and skid trailer measurements data were also collected. These sections did not include any surface treatments.



(a)



(b)

Figure 4. Layout of the Measurement Section (a) Schematic of Measurement Plan (b) CTMeter Measurement.



Figure 5. Layout of the Measurement Section: DFT Measurement.

Based on the AADT traffic information, the TMF on the test section was calculated. The following assumptions were made in calculating the TMF:

- The number of vehicles is the same in both directions (AADT was divided by two).
- The TxDOT recommended traffic lane distribution factors, shown in Table 4, are applicable for calculating the percent of traffic on the outer lane.
- All vehicle types have the same polishing effect on the road surface. This assumption was employed since there is no published information available on the difference in polishing effects between trucks and passenger cars.

Table 4. Lane Distribution Factor.

Total Number of Lanes in Both Directions	Lane Distribution Factor
Less than or equal to 4	1
6	0.7
Greater than or equal to 8	0.6

ANALYSIS OF FIELD MEASUREMENTS

This section presents the DFT and CTMeter results and a comparison between the frictional characteristics of field sections and the laboratory slabs that were tested in Phase I of this project. The Permanent International Association of Road Congresses’

(PIARC) model is developed to express the IFI as a function of DFT results obtained according to ASTM E 1911 (Equation 11) and skid number obtained by a skid trailer with a smooth tire according to ASTM E 274 (Equation 12). The S_p value in these two equations is a function of MPD (see Equation 13), which is obtained using the CTMeter device:

$$IFI = 0.081 + 0.732DFT_{20} e^{\frac{-40}{S_p}} \quad (11)$$

$$IFI = 0.045 + 0.925 \times 0.01 \times SN(50) e^{\frac{20}{S_p}} \quad (12)$$

$$S_p = 14.2 + 89.7MPD \quad (13)$$

The measured range of the MPD values using the CTMeter for selected pavement sections was quite wide (from 0.32 mm to 2.65 mm). Figure 6 shows the mean MPD values measured at a shoulder for the different mixes. This figure shows the PFC mixes had higher MPD values compared to Type C and Type D mixes. Type D mixes had the lowest MPD values because the gradation used in this mix is finer than other mixes. Higher macrotexture mixes allows water to drain faster from tire-pavement interface and increases the skid resistance in higher speeds. The porous nature of the PFC surface also expedites the drainage of water from the surface.

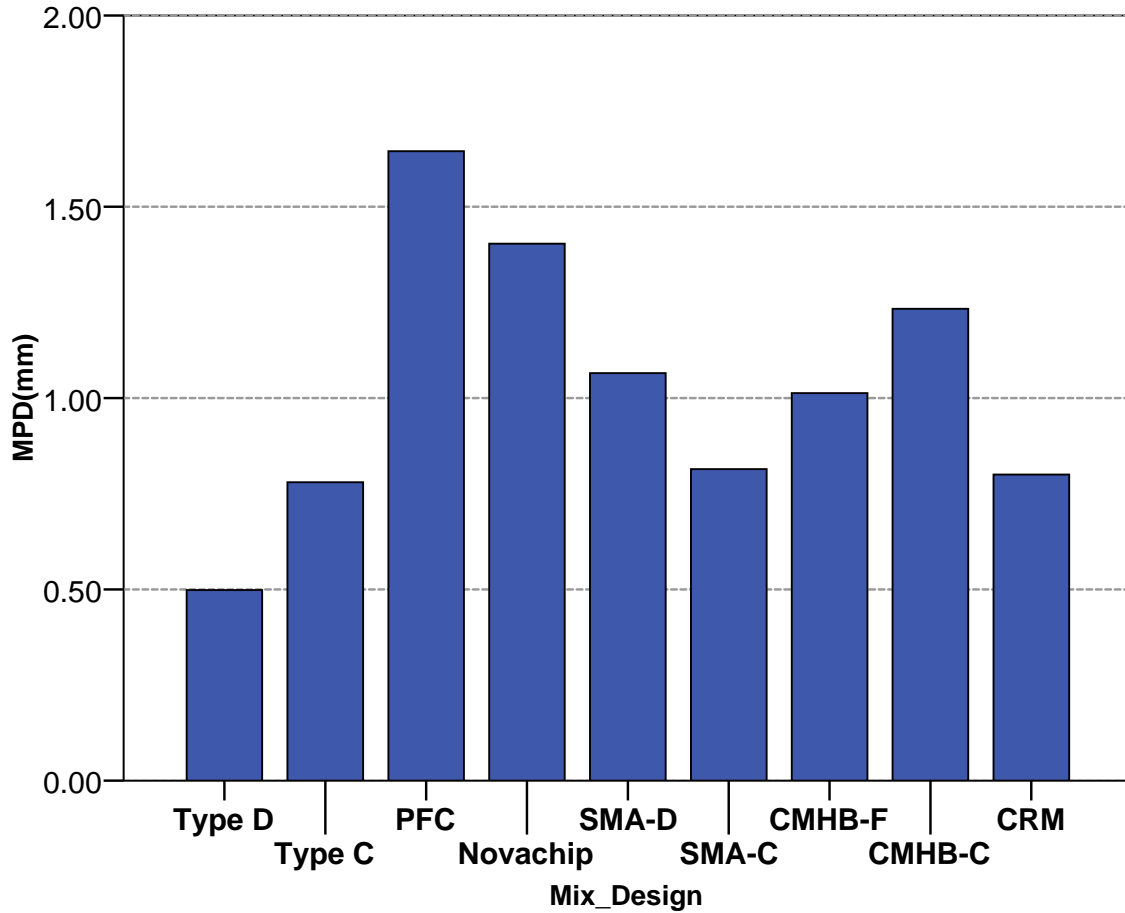


Figure 6. Measured MPD Values for Different Mix Types.

Figure 7 shows very high scatter in the relationship between measured skid number and MPD. The results indicate that there is no direct relationship between MPD and measured skid number.

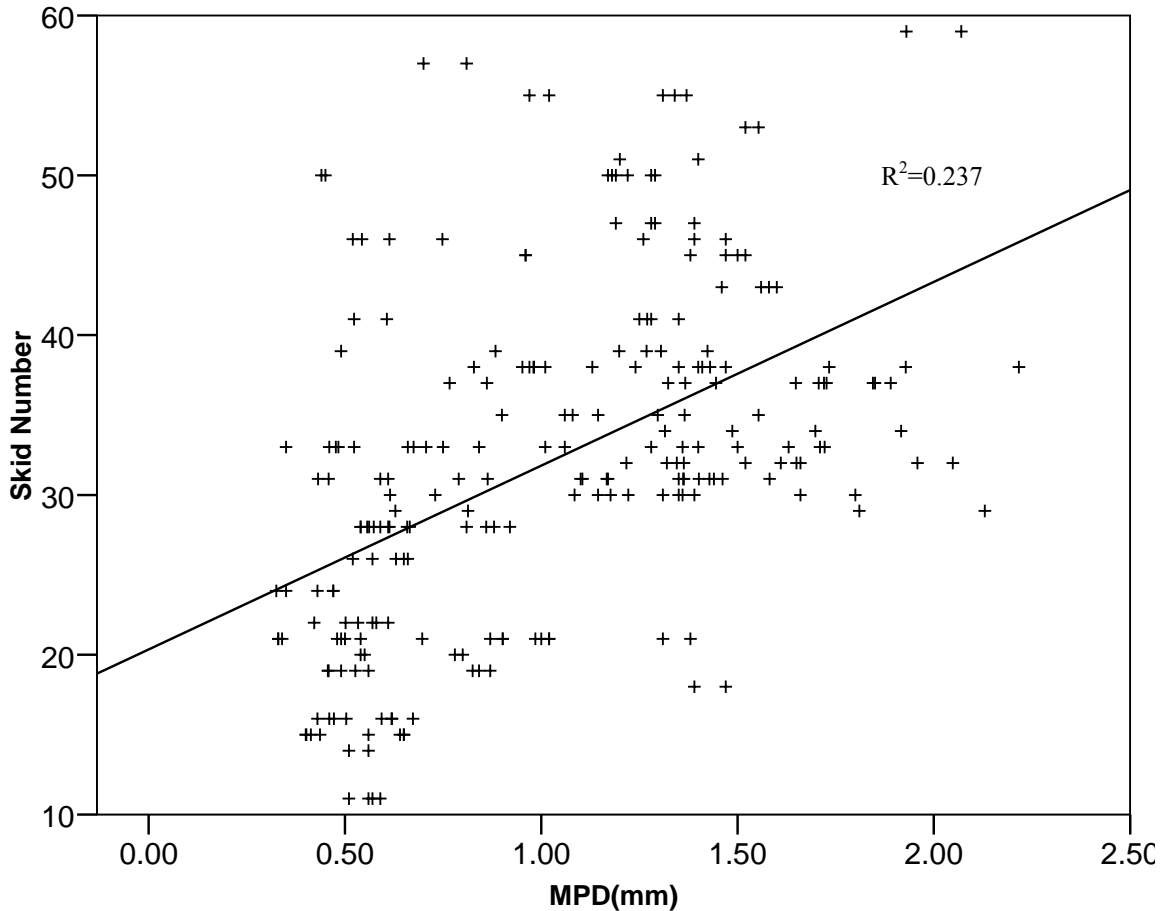


Figure 7. Mean Profile Depth vs. Measured Skid Number.

Figure 8 shows the mean DFT_{20} for the different aggregate types used in constructing pavement sections. Dynamic friction measured at 20 km/h measured by DFT is a measure of microtexture. This figure shows that the initial microtexture level depends on aggregate type. Moreover, sandstone has a very high microtexture compared to other aggregate types. The microtexture of limestone aggregate is generally low and due to a variety of different limestone aggregates; the variability of measured microtexture for this aggregate is high. Figure 8 also shows that combining limestone with other aggregate types such as quartzite or traprock results in a higher microtexture.

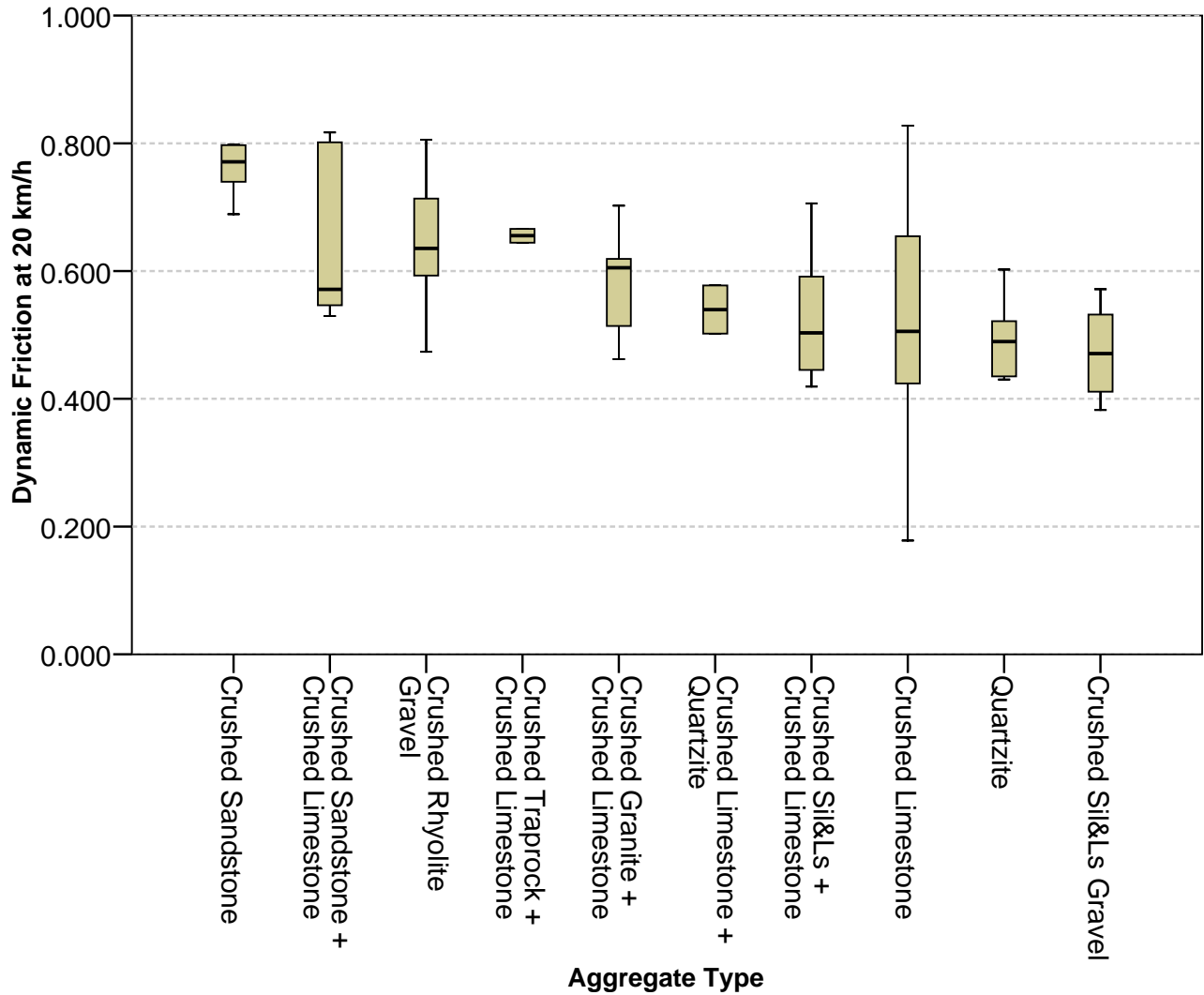


Figure 8. Mean Dynamic Friction at 20 km/h for Different Aggregates.

Figure 9 shows the measured DFT_{20} values at different traffic levels for different aggregate types. Limestone aggregate rapidly loses its initial texture due to the polishing effect of traffic. Other aggregate types such as sandstone, quartzite, and granite are able to maintain their initial texture. Moreover, mixing limestone with other aggregate types such as quartzite and granite can help this aggregate in maintaining the initial texture.

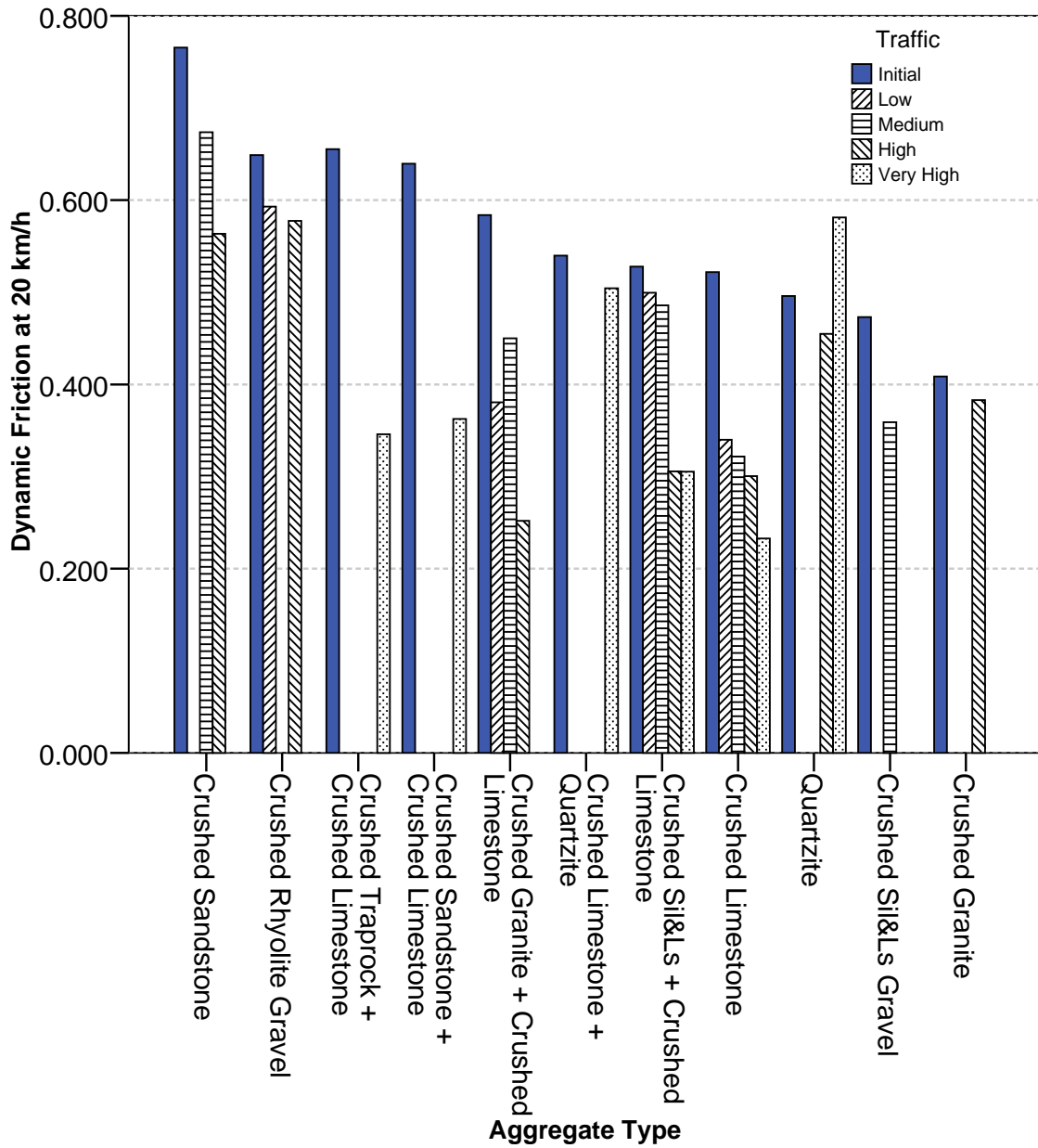


Figure 9. Mean Dynamic Friction at 20 km/h for Different Aggregate Types.

Figure 10 shows that there is high scatter in the relationship between dynamic friction at 20 km/h and measured skid value. This plot shows that the SN value has some correlation to the dynamic friction measured at 20 km/h.

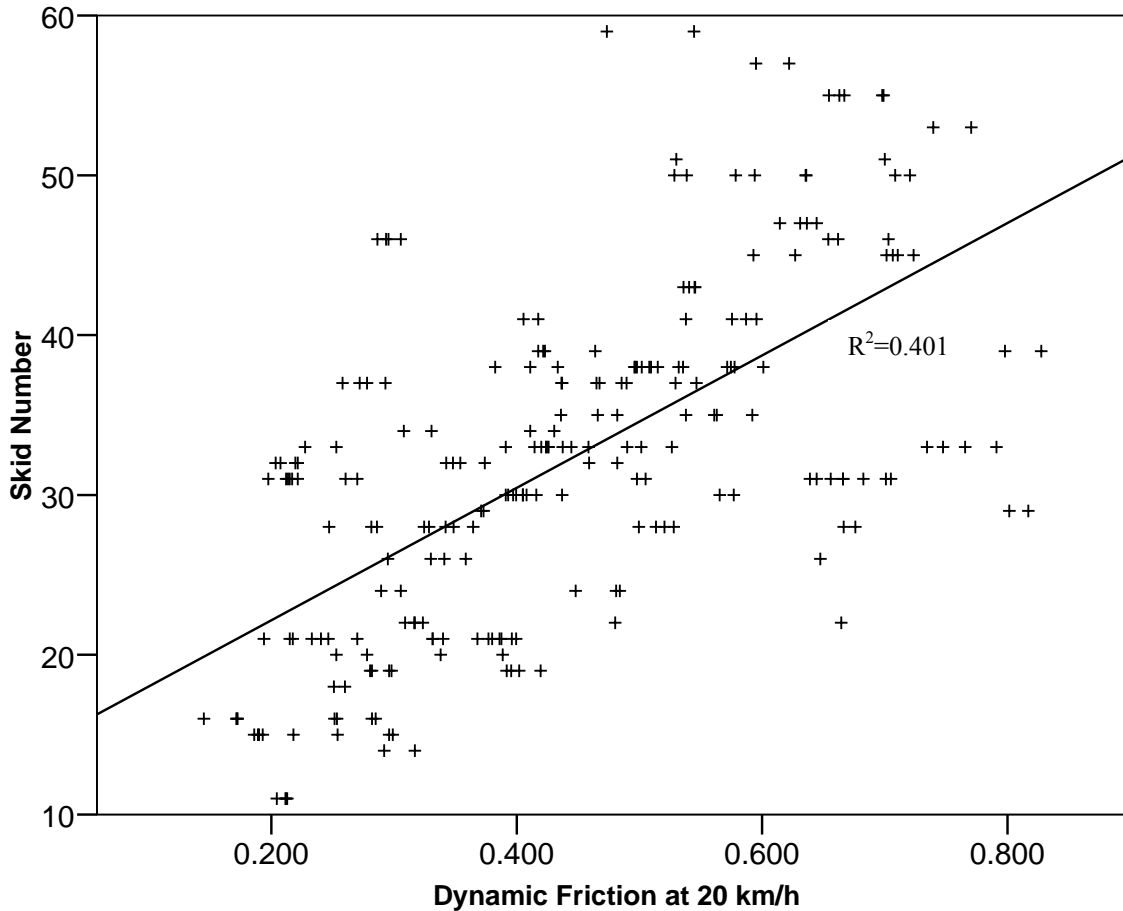


Figure 10. Dynamic Friction at 20 km/h vs. Measured Skid Number for Different Mix Types.

During the analyses of the test results from these 64 field sections, the traffic data were converted into a Traffic Multiplier Factor or TMF. The measured MPD value for different mixtures varied from 0.32 mm to 2.65 mm. There was no correlation between the MPD values and measured skid number. Dynamic friction measured at 20 km/h (measured by DFT) indicates the microtexture. Microtexture depends on aggregate type. Sandstone exhibits high microtexture, and limestone exhibits low microtexture. Limestone rapidly loses its microtexture due to polishing by traffic. Although limestone loses its microtexture rapidly, it can maintain initial microtexture when blended with other aggregates such as granite or quartzite. The results also indicated that there was a fair correlation between friction (DF_{20}) and measured skid number for all mixes.

CHAPTER V – A SYSTEM FOR PREDICTING SKID NUMBER OF ASPHALT PAVEMENTS

INTRODUCTION

The results of Phases I and II of this project have shown that the influence of certain aggregate parameter (aggregate texture) on mixture skid resistance also depends on the type of mixture design. Skid resistance of HMA surface is a function of aggregate gradation, macrotexture, microtexture, and traffic. Therefore, a method is presented in this chapter to predict the skid number of asphalt pavements as a function of traffic based on aggregate characteristics and mixture design gradation. This system will be very valuable to select the optimum combination of aggregate type and mixture design in order to achieve the desired level of skid resistance. Some of the equations presented earlier in this report will also be included in this chapter in order to present a complete procedure for predicting the field skid number without having the reader referred to equations presented in various parts of this report.

DEVELOPMENT OF SYSTEM FOR PREDICTING SKID NUMBER

As discussed in Chapter II of this report, a method was developed in Phase I for predicting the IFI as a function of number of loading cycles (N) using the NCAT polishing device. As shown in Equations 14 to 18, the parameters of the relationship of IFI versus N are dependent on aggregate texture measuring using AIMS before and after polishing in the Micro-Deval and aggregate gradation, which is an indication of the wearing susceptibility of the aggregates.

$$IFI(N) = a_{mix} + b_{mix} \cdot \exp(-c_{mix} \cdot N) \quad (14)$$

$$F(x; \kappa, \lambda) = 1 - \exp[-(x/\lambda)^\kappa] \quad (15)$$

$$a_{mix} = \frac{18.422 + \lambda}{118.936 - 0.0013 \times (AMD)^2} \quad (16)$$

$$a_{mix} + b_{mix} = 0.4984 \ln(5.656 \times 10^{-4} (a_{agg} + b_{agg}) + 5.846 \times 10^{-2} \lambda - 4.985 \times 10^{-2} \kappa) + 0.8619 \quad (17)$$

$$c_{mix} = 0.765 \cdot e^{\left(\frac{-7.297 \cdot 10^{-2}}{c_{agg}} \right)} \quad (18)$$

where:

a_{mix} : terminal IFI value for the mix.

$a_{mix} + b_{mix}$: initial IFI value for the mix.

c_{mix} : rate of change in IFI for the mix.

AMD: aggregate texture after Micro-Deval.

$a_{agg} + b_{agg}$: aggregate initial texture using texture model.

c_{agg} : aggregate texture rate of change using texture model.

k-value: shape factor of Weibull distribution used to describe aggregate gradation.

λ -value: scale factor of Weibull distribution used to describe aggregate gradation.

The $a_{agg} + b_{agg}$ and c_{agg} are obtained from measuring aggregate texture after 105 and 180 minutes time intervals of polishing in the Micro-Deval. It would be desirable to predict these values from only two texture measurements of aggregates using AIMS before Micro-Deval and after Micro-Deval polishing for 105 minutes, which is the standard time currently used by TxDOT. For this purpose, nonlinear regression analysis was used to examine the possibility of predicting a_{agg} , b_{agg} , and c_{agg} from AMD and BMD texture. A total of nine aggregate samples were used in this regression analysis. Moreover, these samples were part of a database of AIMS measurements of aggregates in Phase I and with three other aggregate sources. The following equations can be used to determine the texture model coefficients:

$$a_{agg} + b_{agg} = 0.983BMD + 5.258 \quad R^2 = 0.98 \quad (19)$$

$$a_{agg} = 0.811AMD + 4.258 \quad R^2 = 0.94 \quad (20)$$

$$c_{agg} = \frac{A + TL}{B + C \times ARI} \quad R^2 = 0.74 \quad (21)$$

where BMD and AMD are the AIMS texture indices measured before and after

Micro-Deval polishing of aggregates, respectively. A, B, and C are regression constants and have the value of -0.357 , 20.18 , and -23.676 , respectively. TL and ARI are texture loss and aggregate roughness index and defined as:

$$TL = \frac{BMD - AMD}{AMD} \quad (21a)$$

$$ARI = \frac{AMD/BMD}{\sqrt{1 - (AMD/BMD)^2}} \quad (21b)$$

where ARI is termed Aggregate Roughness Index and TL is denoted Texture Loss.

The polishing rate (c_{mix}) and the terminal friction value (a_{mix}) of an asphalt mixture can be determined using Equations 19 to 21 along with Equations 16 and 18. Since the scale and shape parameter (λ and κ) of the Weibull cumulative distribution function are also required in Equations 16 and 18, a nonlinear regression analysis can be used. Researchers included eight Texas mix designs in this analysis as shown in Table 5. The gradation boundaries for these mix designs were extracted from TxDOT specification manual, and the scale and shape parameter (λ and κ) of the cumulative Weibull distribution was calculated using SOLVER function of Microsoft[®] Excel. For most cases, the coefficient of determination of the regression was more than 0.95.

Table 5. Calculated Scale and Shape Factors for Different Mixes.

Mix Design	Scale Parameter λ	Shape Parameter κ
Type C	5.605	0.830
Type D	4.052	0.864
PFC	10.054	3.954
SMA_D	9.201	1.494
Crack Attenuating Mixture (CAM)	3.168	1.000
SMA_C	9.431	1.276
CMHB_C	8.578	1.077
CMHB_F	5.574	1.415

Next, the results of the lab measurements and field measurement were used to develop a relationship between lab polishing and field polishing in terms of number of polishing cycle in lab (N) and TMF. Equation 14 was developed for predicting the IFI

values in a mixture as a function of N (number of the cycles in terms of 1000 cycles in NCAT polishing device). Based on the measured DFT_{20} values and macrotexture measurements by CTMeter, the IFI values were determined for each section using Equations 11 and 13 for each road section.

Then, Equation 14 was used to determine the N value that would give the same IFI that is calculated using Equation 11. The coefficients a_{mix} , b_{mix} , and c_{mix} that were substituted in Equation 14 were for the same mixtures that were tested in the field. A statistical analysis was performed to determine the outliers that were removed from the analysis. Researchers performed a non-linear regression analysis to find the relationship between TMF and number of polishing cycles (N) as in Equation 22 and Figure 29.

$$N = TMF \times 10^{\frac{1}{A+B \times c_{mix} + \frac{C}{c_{mix}}}} \quad R^2 = 0.74 \quad (22)$$

where A, B, and C are regression coefficients and have the value of -0.452, -58.95, and 5.834×10^{-6} , respectively. The relationship between N and TMF is not only a function of traffic but also a function of mixture polishing characteristics. Figure 11 shows the relationship between measured and calculated number of polishing cycles. The proposed equation has a high R-squared value and can be used to estimate the variation of IFI in the field in terms of TMF.

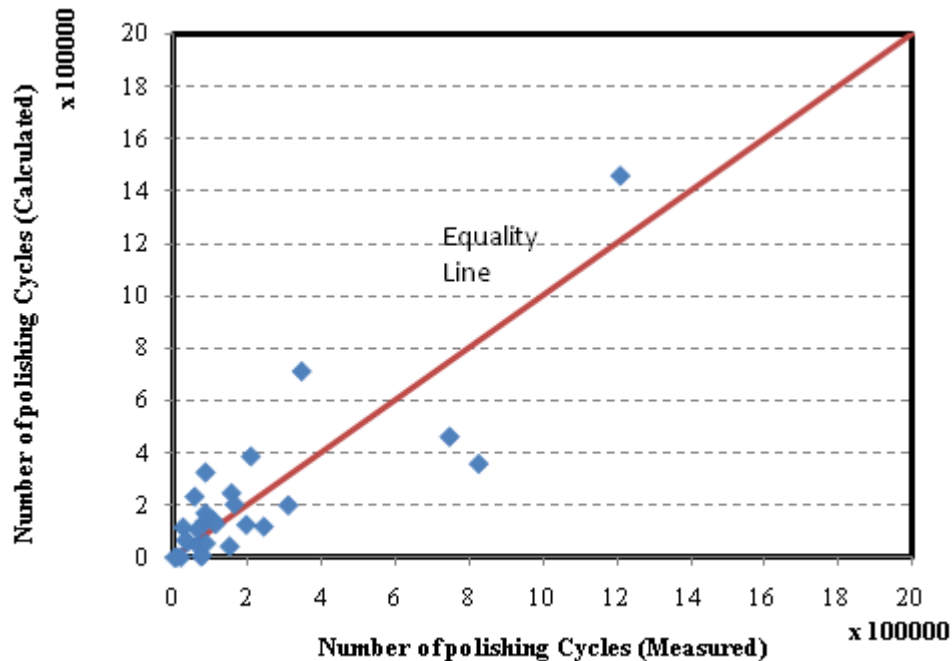


Figure 11. TMF vs. Number of Polishing Cycles.

The last step in the analysis was to predict the SN value given the IFI. In order to obtain the relationship between measured skid resistance by skid trailer and DFT/CTMeter combination, the PIARC procedure for finding the IFI value was used, and the IFI values were calculated using DFT, CTMeter, and skid number using Equations 11 to 13.

In principle, Equations 11 and 12 should give the same value for the IFI. Therefore, IFI calculated from Equation 11 can be substituted in Equation 12 to find the SN(50). As illustrated in Figure 12 the measured values of SN by skid trailer is greater than the calculated value using the PIARC equation. The R-squared value for the relation is 0.76 and is relatively high. There are two main factors that could explain this difference between SN(50) obtained from Equation 12 and measured values. The first is the propagation of errors. Error is present in the PIARC regression equation and is propagated during the mathematical manipulation required to backcalculate the SN. The second factor is experimental error. Each friction measuring device will generate some experimental error due to the equipment design and human factors and different

simplifying assumptions made in this research. The presence of these errors could account for the differences between the measured and calculated SN.

Based on the relationship between measured and calculated SN values, Equation 12 was modified to account for the difference between calculated and measured skid numbers. Equation 23 shows the modified form of Equation 12 to predict the field skid number:

$$SN(50) = 1.41 + 143.19(IFI - 0.045)e^{\frac{-20}{S_r}} \quad (23)$$

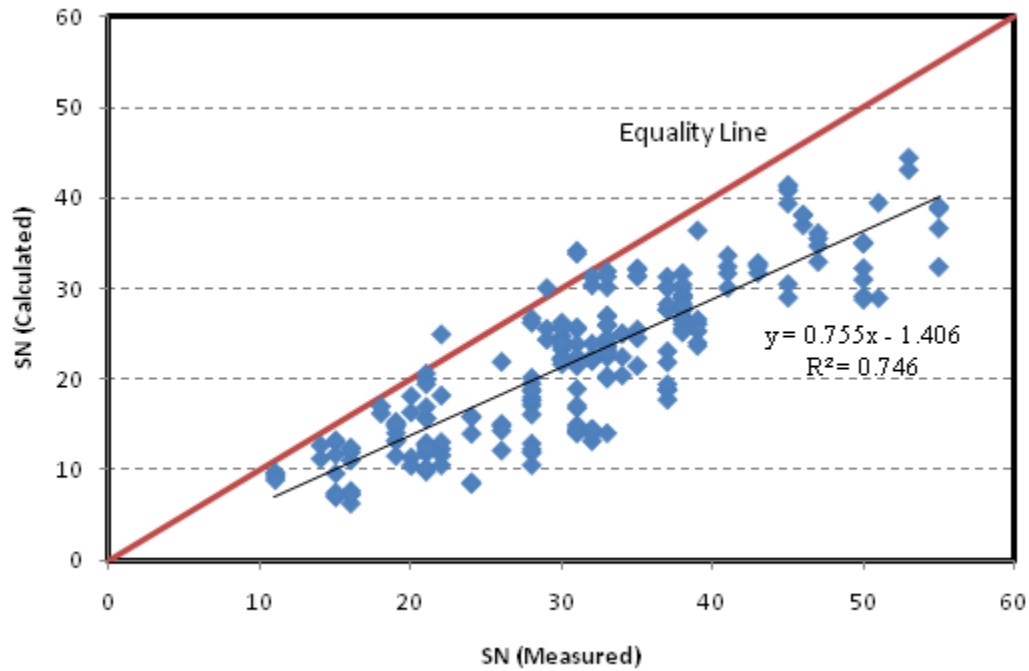


Figure 12. Measured Skid Number vs. Calculated Skid Number Using PIARC Equation.

Figure 13 shows the measured and calculated skid number values using the modified PIARC equation (Equation 23). The calculated and measured values are relatively close, and the modified equation can be used to predict the measured skid number.

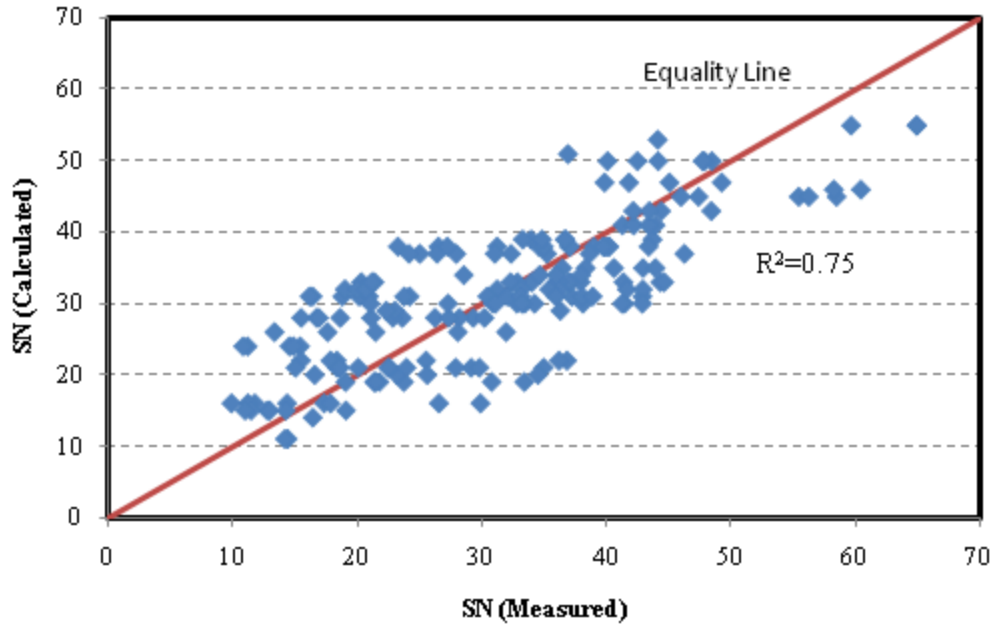


Figure 13. Measured Skid Number vs. Calculated Skid Number Using Modified PIARC Equation.

Equation 23 includes the S_p value, which is a function of MPD. Macrottexture, which is represented by MPD, is a function primarily of mixture gradation. Therefore, nonlinear regression analysis was conducted to determine MPD as a function of the gradation parameters λ and κ . The best correction found between measured MPD and Equation 24 shows these gradation parameters. Figure 14 shows the relationship between measured and calculated MPD values.

$$MPD_0 = 0.139\lambda + 0.086\kappa - \frac{0.041}{\kappa^4} \quad R^2 = 0.79 \quad (24)$$

where λ and κ are Weibull distribution function coefficients.

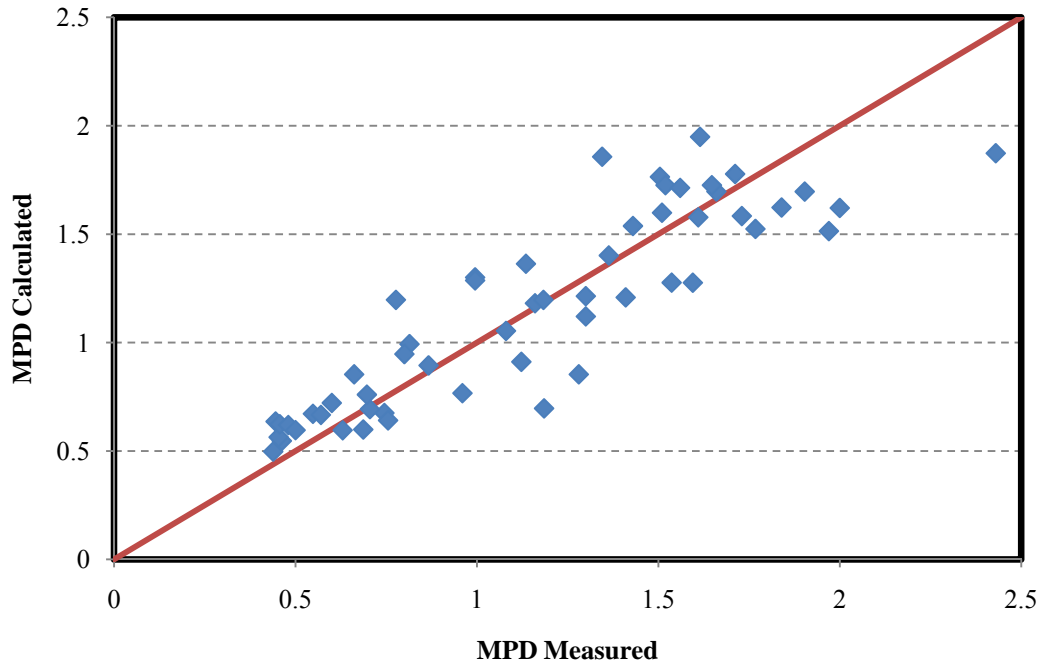


Figure 14. Relationship between Measured and Calculated MPD Values.

SENSITIVITY ANALYSIS OF PREDICTION SYSTEM

The sensitivity analysis was conducted using several aggregate types and mixture designs. Aggregates were selected to represent a wide spectrum of texture values representing the minimum, maximum, first quartile, second quartile, and third quartiles of terminal texture (a_{agg}) and polishing rate (c_{agg}) as shown in Tables 6 and 7, respectively.

Table 6. Selected Aggregates Based on Terminal Texture.

Sample	Quartile	Terminal Texture a_{mix}	Polish Rate	Material Type	Material Group
1	Minimum	26.67	0.0233	Crushed Limestone	3. LS-Dolomites
2	1st	56.34	0.0094	Crushed Limestone	3. LS-Dolomites
3	Median	72.46	0.0145	Crushed Limestone	3. LS-Dolomites
4	3rd	92.43	0.0049	Crushed Sandstone	2. Sandstone
5	Maximum	216.34	0.0298	Crushed LS Rock Asphalt	6. Miscellaneous

Table 7. Selected Aggregates Based on Polishing Rate.

Sample	Quartile	Polish Rate c_{mix}	Terminal Texture a_{mix}	Aggregate Type	TxDOT Aggregate Group
6	Minimum	0.0001	84.55	Crushed Sil. & LS Gravel	4. Gravels
7	1 st Quarter	0.0182	216.34	Crushed LS Rock Asphalt	6. Miscellaneous
8	Median	0.0227	109.58	Crushed Limestone	3. LS-Dolomites
9	3 rd Quarter	0.0253	69.17	Crushed Limestone	3. LS-Dolomites
10	Maximum	0.0364	279.45	Crushed LS Rock Asphalt	6. Miscellaneous

Using Equations 16 and 18 the terminal friction value and polish rate were calculated. Figure 15 shows the terminal friction values for different aggregates and mix designs.

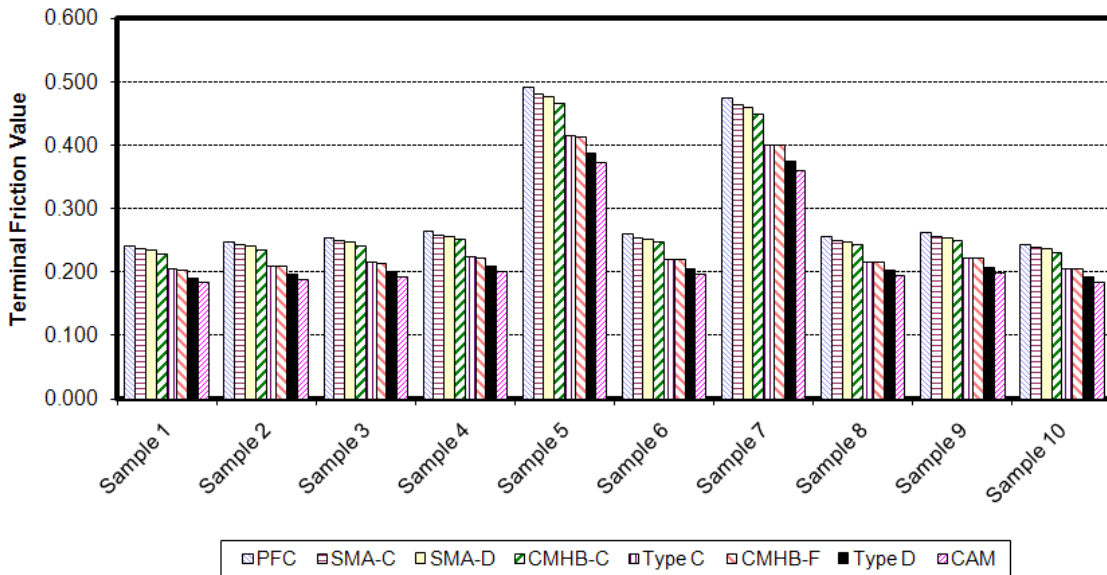


Figure 15. Terminal Friction Values for Different Aggregates and Mix Designs.

The PFC mixes have the highest terminal friction values. SMA-C, SMA-D, and CMHB-C are the next mixes in the list. The terminal polish values of the Type C and CHMB-F mixes are almost the same. Type D mix and CAM mix have the lowest terminal friction among all mixes. Among the aggregates, sample 10 and sample 5 have the highest terminal friction values. These values can be attributed to the high texture index after Micro-Deval. The difference among other aggregates is not significant. Figure 16 shows the polishing rate for different aggregates.

Given polishing rate and initial and terminal friction values, IFI can be calculated using Equations 14 and 22 as a function of TMF. For instance, Figures 17 and 18 illustrate the IFI values for sample 1. The SN values were calculated using Equation 23 as a function of TMF and plotted in Figure 18. These figures indicate the use of the model to predict the variation of skid number as a function of traffic.

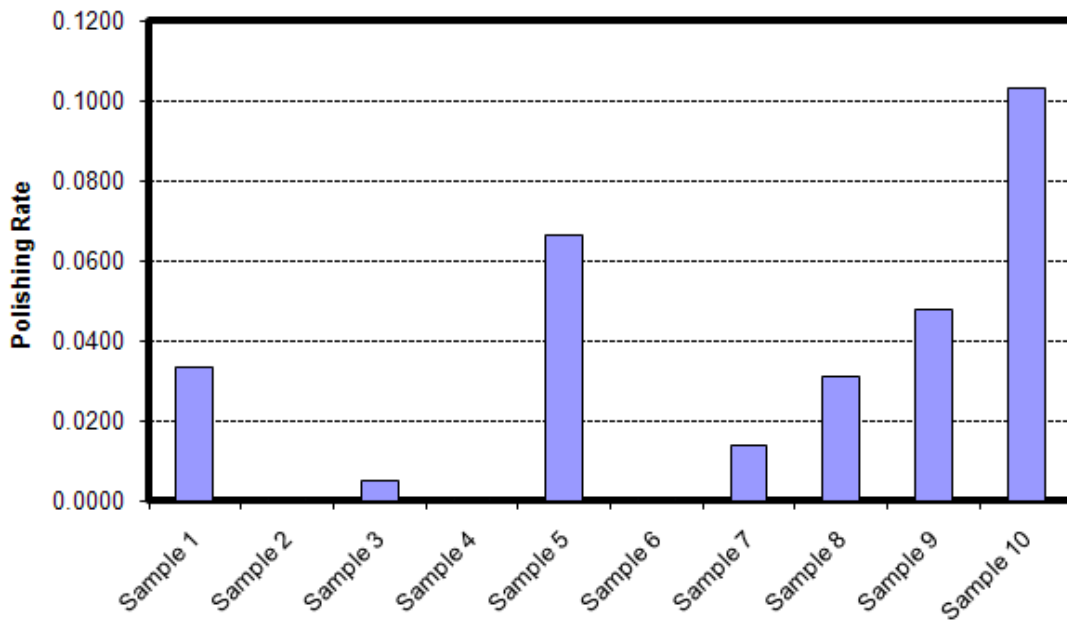


Figure 16. Polishing Rate for Different Aggregates.

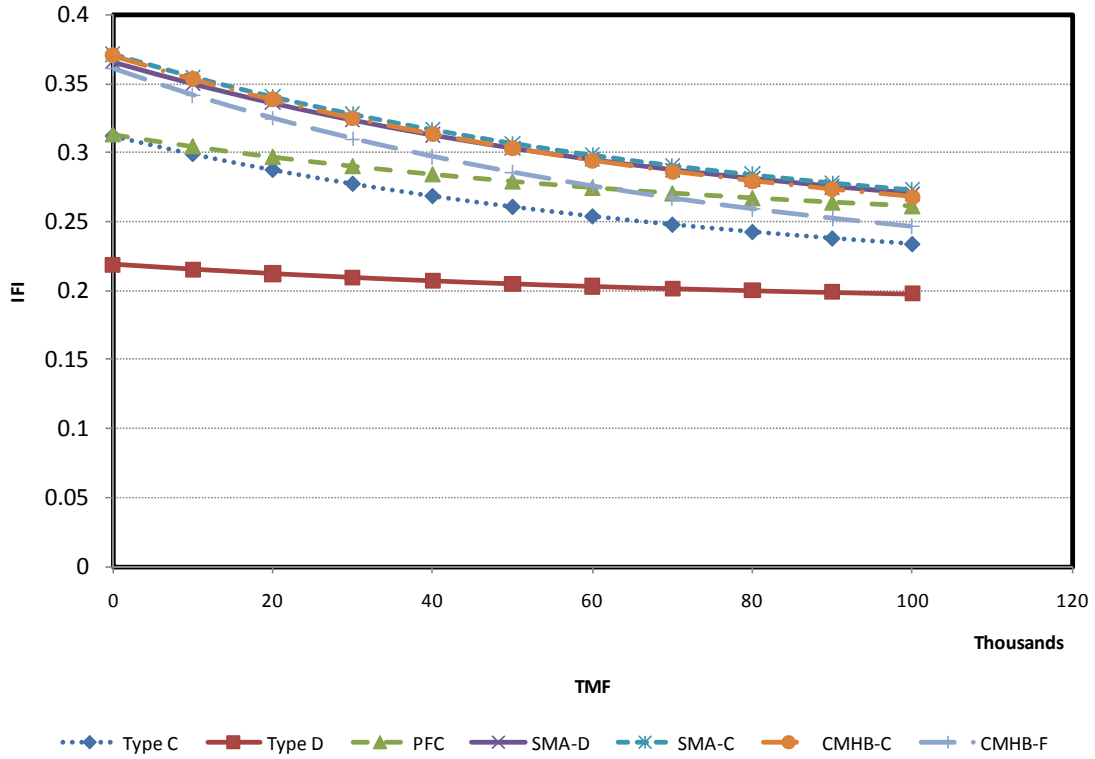


Figure 17. IFI Values as a Function of TMF for Sample 1.

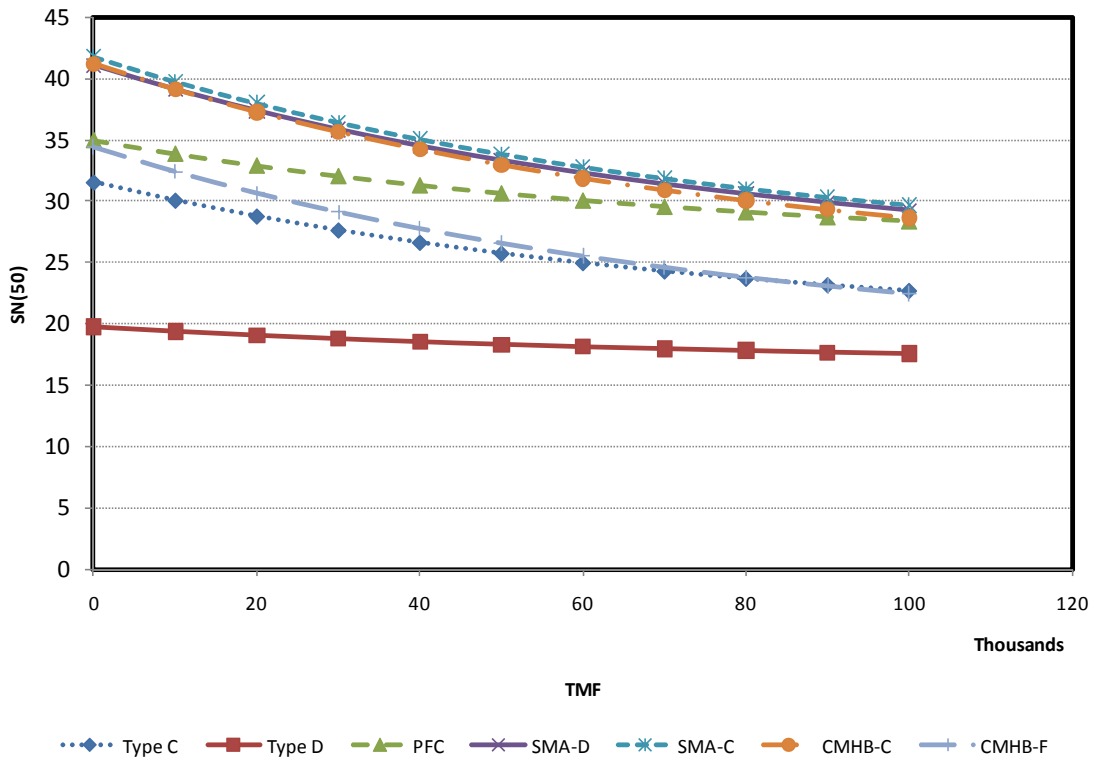


Figure 18. SN Values as a Function of TMF for Sample 1.

RECOMMENDED SYSTEM FOR PREDICTING SKID NUMBER

This chapter presented a system for predicting the skid number of asphalt mixtures. This system consists of the following steps:

- Measure aggregate texture using AIMS before Micro-Deval (BMD).
- Measure aggregate texture using AIMS after Micro-Deval (AMD).
- Calculate $a_{agg}+b_{agg}$ using Equation 19.
- Calculate a_{agg} using Equation 20.
- Calculate Texture Loss (TL) using Equation 21a.
- Calculate Aggregate Roughness Index (ARI) using Equation 21b.
- Calculate c_{agg} using Equation 21.
- Determine the gradation parameters (λ and κ) from Table 4 or by fitting the cumulative Weibull function (Equation 2) to the gradation curve.
- Calculate a_{mix} using Equation 16.
- Calculate $a_{mix}+b_{mix}$ using Equation 17.
- Calculate c_{mix} using Equation 18.
- Calculate MPD using Equation 24.
- Calculate S_p using Equation 13.
- Calculate International Friction Index (IFI) as a function of N using Equation 11.
- Calculate TMF in terms of N using Equation 22.
- Calculate Skid Number (SN) using Equation 23.

ILLUSTRATION OF AN AGGREGATE CLASSIFICATION SYSTEM BASED ON PROPOSED MODEL

In this section, the model is used to illustrate the influence of aggregate characteristics and aggregate gradation on skid resistance. In addition, the results presented herein demonstrate how this model can be used to select the optimum aggregate characteristics and gradation such that the required skid resistance level is achieved given a certain traffic level.

The analysis involved the use of four AADT/lane levels representing interstate, U.S. highway and state highway, and farm to market sections from the state of Texas. Four different mix types commonly used in the state of Texas were selected, and scale and shape parameters of the corresponding Weibull function were determined. The analysis utilized the texture characteristics of aggregates K, H, and M listed in Table 1. In order to facilitate the comparison between the various sections, the SN(50) values in Table 8 were used to classify the pavement sections after 5 years of service.

Table 8. Skid Number Threshold Values after Five Years of Service.

Aggregate Class	SN Threshold Value
High	SN(50)>30
Medium	21 < SN(50) < 29
Low	SN(50)<20

Table 8 shows the classification of the various pavement sections. All types of mixtures with aggregate H achieved high skid resistance (level H after five years) for all mixtures and all traffic levels. However, the performance of mixtures incorporating aggregates K and M was dependent on the mixture type and traffic level. Another observation is that mixtures PFC and SMA with aggregate K maintained level H of skid resistance irrespective of the traffic level; while mixture M with the same aggregate experienced a reduction in skid resistance from H to M when the AADT/lane reached 5800. These results clearly demonstrate how the proposed model provides flexibility for engineers to select an aggregate source and a mixture design that achieves the required skid number after a certain traffic level.

Table 9. Aggregate Classification for Different Roads.

AADT/Lane	Mix Type			
	Type C	Type D	PFC	SMA
Aggregate K				
550	H	L	H	H
5800	M	L	H	H
16800	M	L	H	H
34000	M	L	H	H
Aggregate H				
550	H	H	H	H
5800	H	H	H	H
16800	H	H	H	H
34000	H	H	H	H
Aggregate M				
550	H	M	H	H
5800	M	L	H	H
16800	M	L	H	H
34000	M	L	M	M

SKID ANALYSIS OF ASPHALT PAVEMENTS (SAAP)

A computer program was developed using Visual Basic programming language to execute the steps needed to calculate the skid resistance of asphalt pavements as a function of traffic. The program is included on a compact disk labeled as Product 0-5627-P1 in a sleeve on the last page of this report. This section describes the program and the steps needed to calculate the pavement skid resistance.

In the first step (Figure 19), the user needs to input the username and proceed to next window. In the second step (Figure 20), the mixture gradation is inputted to the software. The user can either enter the gradation or select one of the standard mixture gradations used in the State of Texas. If the user selects to enter gradation manually by clicking on <input gradation> button, a window pops up (Figure 21) where the amount of percent passing for selected sieves are entered. The user can select any number of sieves and enter the percent passing values for each selected sieve.

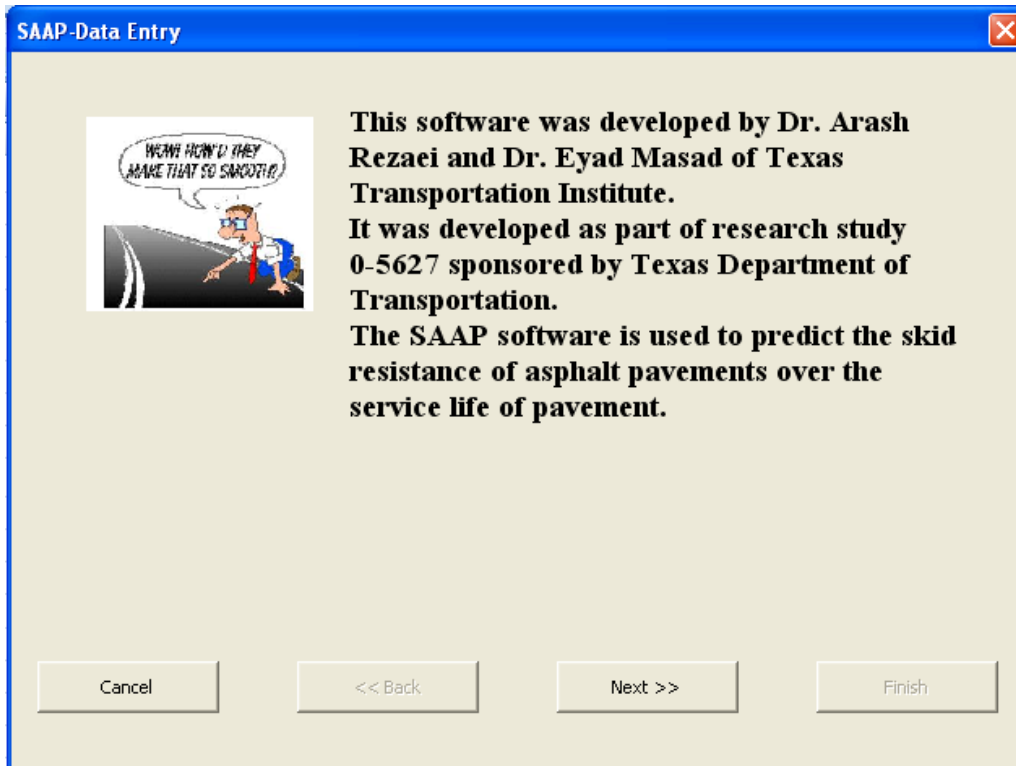


Figure 19. Initial Window of the Program.

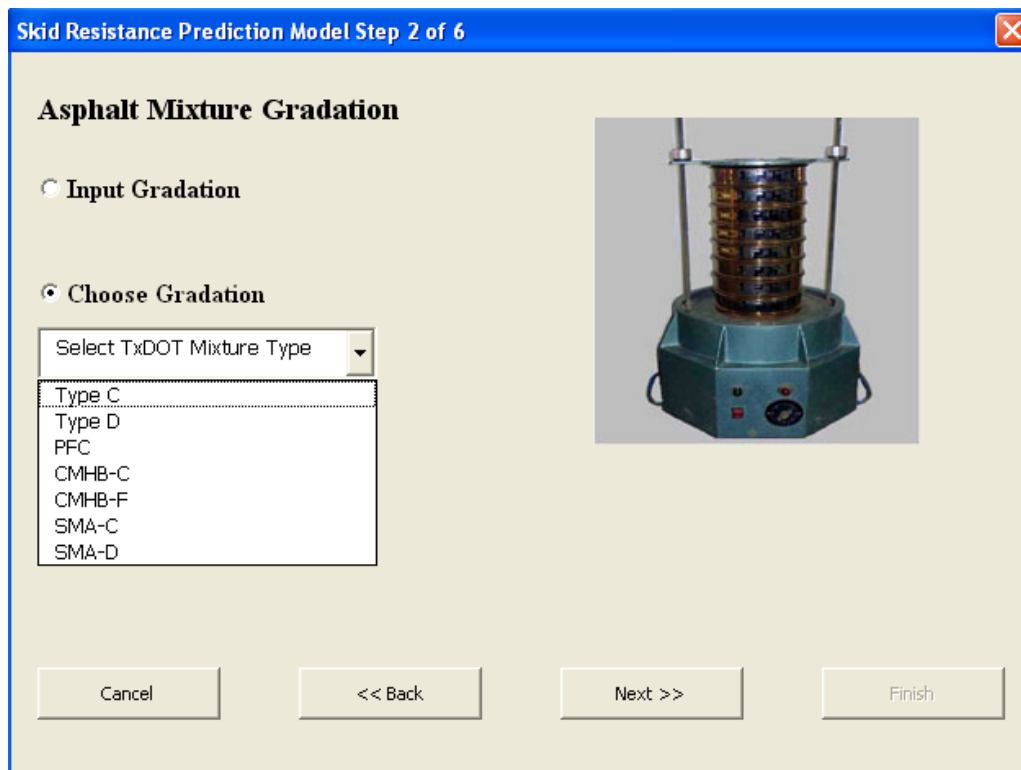


Figure 20. Aggregate Gradation Input.

Sieve Size		Percent Passing
in.	mm	
<input checked="" type="checkbox"/>	1	25
<input checked="" type="checkbox"/>	7/8	22.4
<input checked="" type="checkbox"/>	3/4	19
<input type="checkbox"/>	5/8	16
<input type="checkbox"/>	1/2	12.5
<input type="checkbox"/>	3/8	9.5
<input type="checkbox"/>	#4	4.75
<input type="checkbox"/>	#8	2.36
<input type="checkbox"/>	#10	2
<input type="checkbox"/>	#40	0.425
<input type="checkbox"/>	#60	0.18
<input type="checkbox"/>	#200	0.075

Figure 21. Manual Aggregate Gradation.

In the next step, the aggregate texture values measured using AIMS are entered (Figure 22). Here the user has options to input either the texture measured at two points (before polishing and after polishing for 105 minutes in the Micro-Deval), or texture measured at three points (before polishing, after polishing for 105 minutes, and 180 minutes in the Micro-Deval) (Figure 23). The use of three data points provides more accurate estimation of aggregate resistance to polishing. This step will be followed by windows to enter the texture data of aggregates from one or more sources. User can select up to three aggregate sources used in the mixture. As shown in Figures 22 and 23 users can input the texture value of component aggregate source(s).

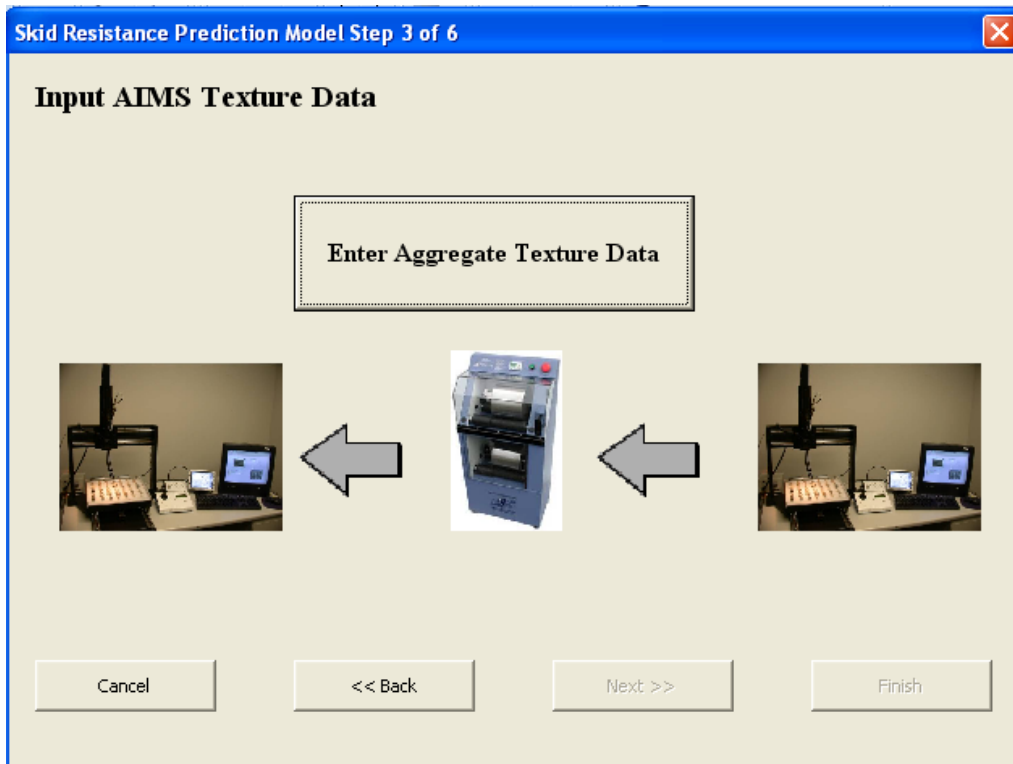


Figure 22. AIMS Texture Data Input Window.

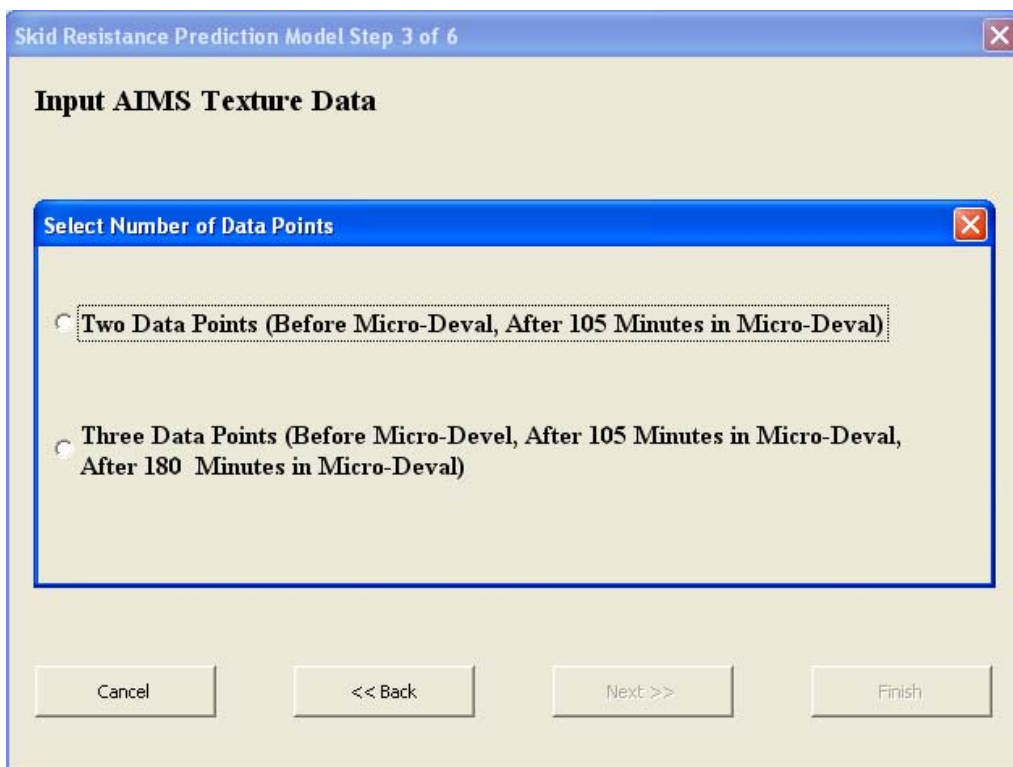


Figure 23. Texture Data Points Select.

Figure 24. Two Point Texture Measurement.

Figure 25. Three Point Texture Measurement.

By clicking on <Next > button, the MPD value is entered or calculated (Figure 26). The MPD value can be either entered by the user from the measured MPD value for that particular mix or estimated by the software based on gradation. The following step is when the user inputs the traffic data. In this step, users enter the information about the highway type, total number of through traffic lanes, total AADT for both directions, and percent truck traffic (Figure 27).

Skid Resistance Prediction Model Step 4 of 6

Input Pavement Texture Data

Measured Mean Profile Depth (MPD) in mm

Use SAAP Estimation of Mean Profile Depth (MPD) in mm Based on Mixture Gradation



Figure 26. Input MPD Value.

Skid Resistance Prediction Model Step 5 of 6

Input Traffic data:

Highway Type

 Divided
 Undivided

Total Number of Through Traffic Lanes

 Two Lanes
 Four Lanes
 Six Lanes
 Eight Lanes or More

Average Annual Daily Traffic (AADT) for Both Directions:

Percent Truck Traffic:

Figure 27. Traffic Data Input.

The next step in the software provides the options on how the user wants to see the output. One option is to obtain a prediction of skid resistance as a function of years in service; the other option is to get a classification of the pavement section based on its skid resistance after a specified number of years (Figure 28).

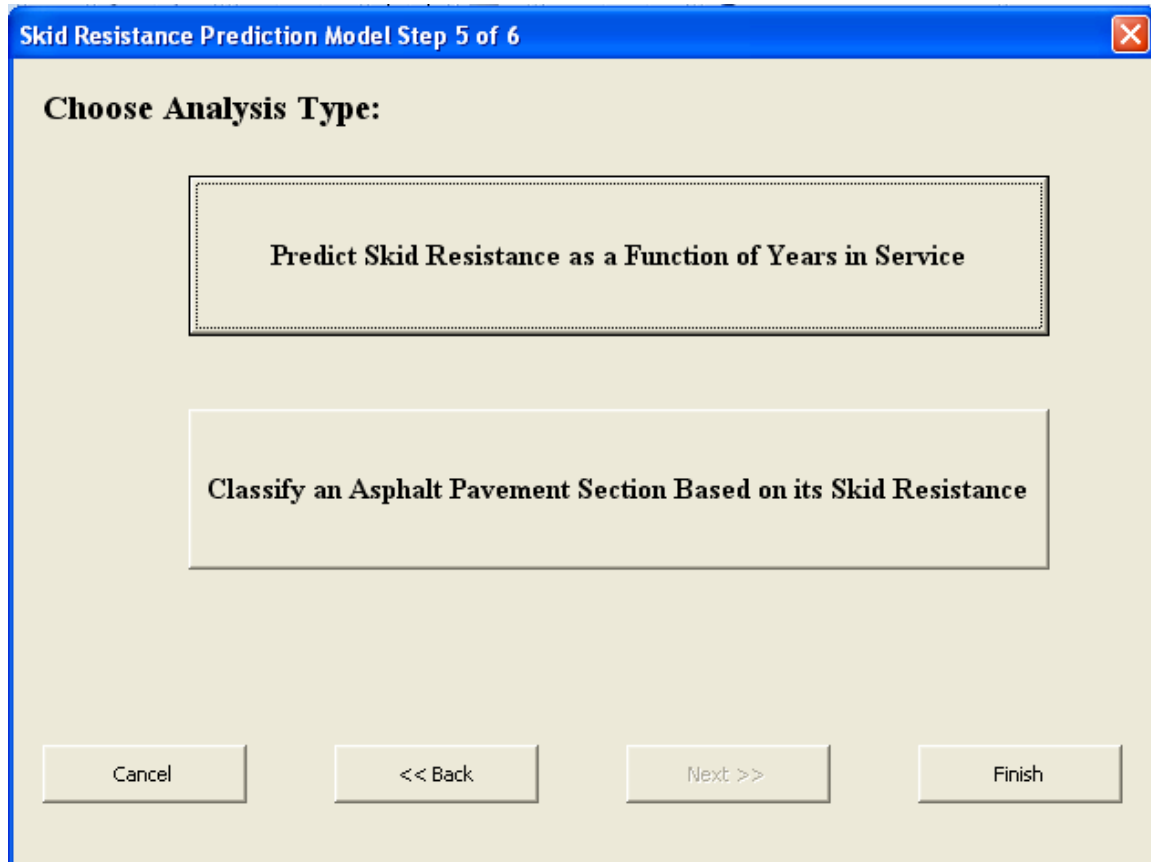


Figure 28. Analysis Type.

If the user chooses <Skid Resistance Prediction Model>, the software will provide a plot of skid number over the service life (Figure 29). If the user selects the <Aggregate Classification>, a window pops up in which the user needs to input some additional information required for pavement classification (Figure 30). These input parameters are:

- The length of service life in years for which a pavement section will be classified.
- The skid resistance thresholds values based on which a pavement section will be classified (Figure 30). The first threshold value is the acceptable skid number above which designer is not concerned. The second threshold value is the skid number above which (but below the acceptable value) one should monitor the

surface condition more frequently and below which one should take corrective measure to restore surface friction.

After clicking on <Set> button a window with the pavement classification will be presented (Figure 31). Depending on the predicted skid number at the end of service life and designer selected threshold values the pavement is classified as high, medium, or low. By clicking on the <Finish> button, the program will be terminated, and Microsoft® Excel will be closed. A set of example input data and corresponding output charts are provided in the Appendix C for clarity.

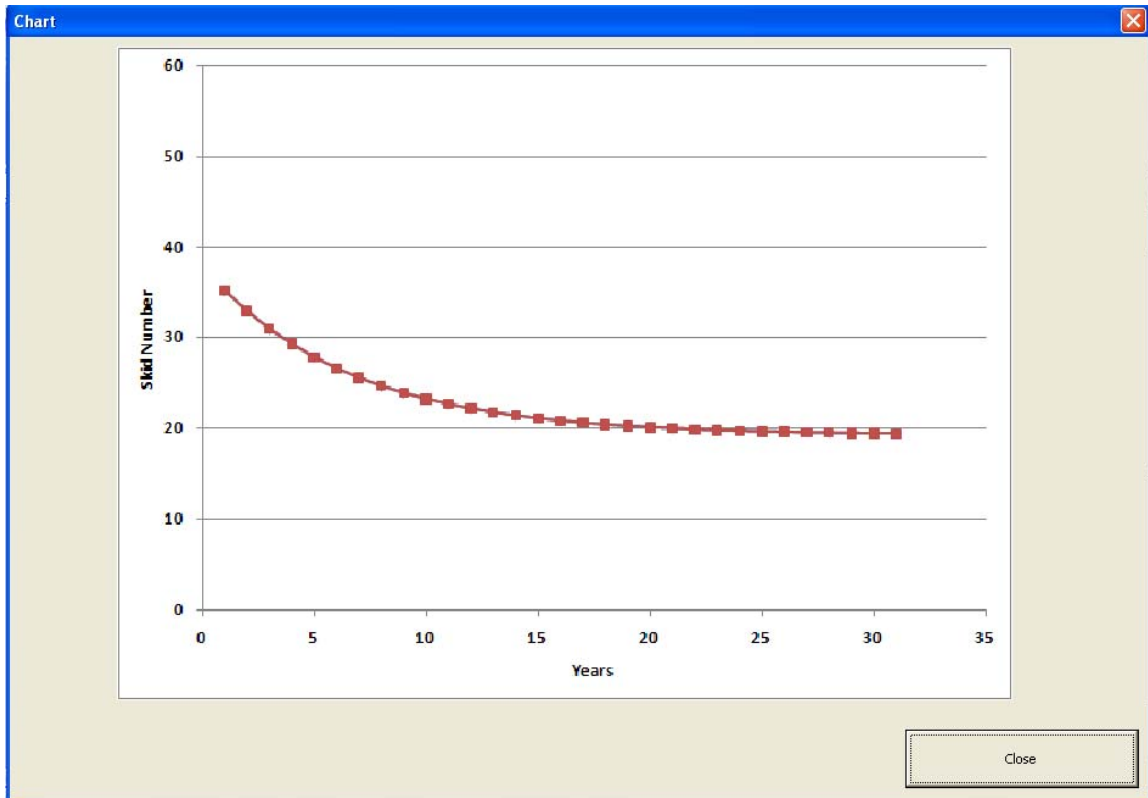


Figure 29. A Sample Plot of Skid Number over the Service Years.

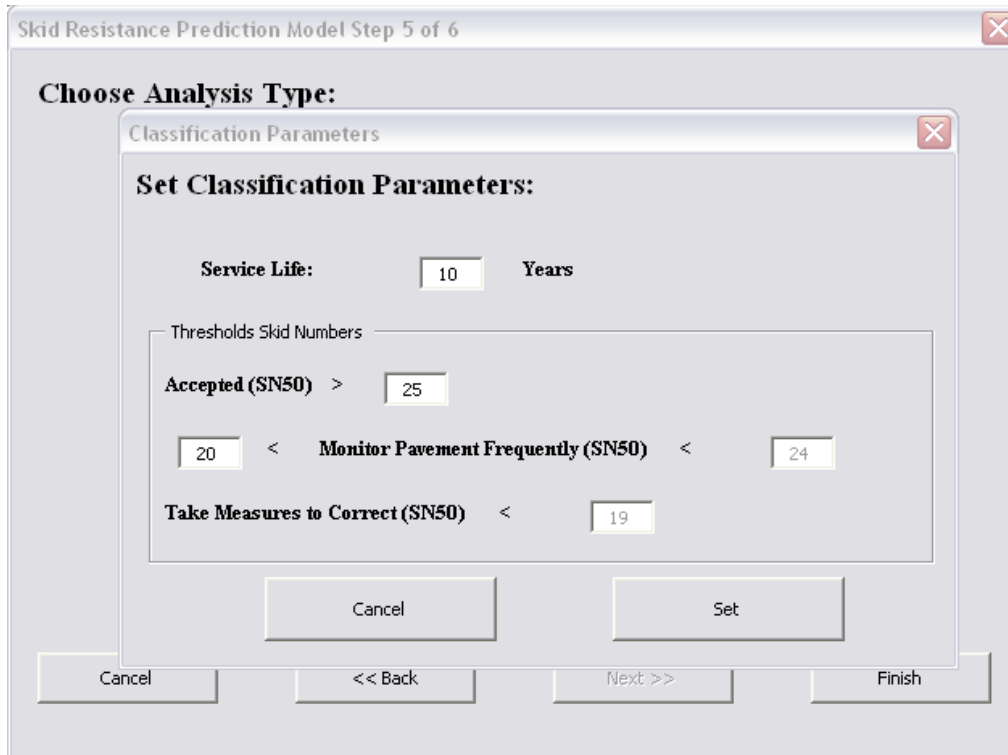


Figure 30. Classification Setting Values.

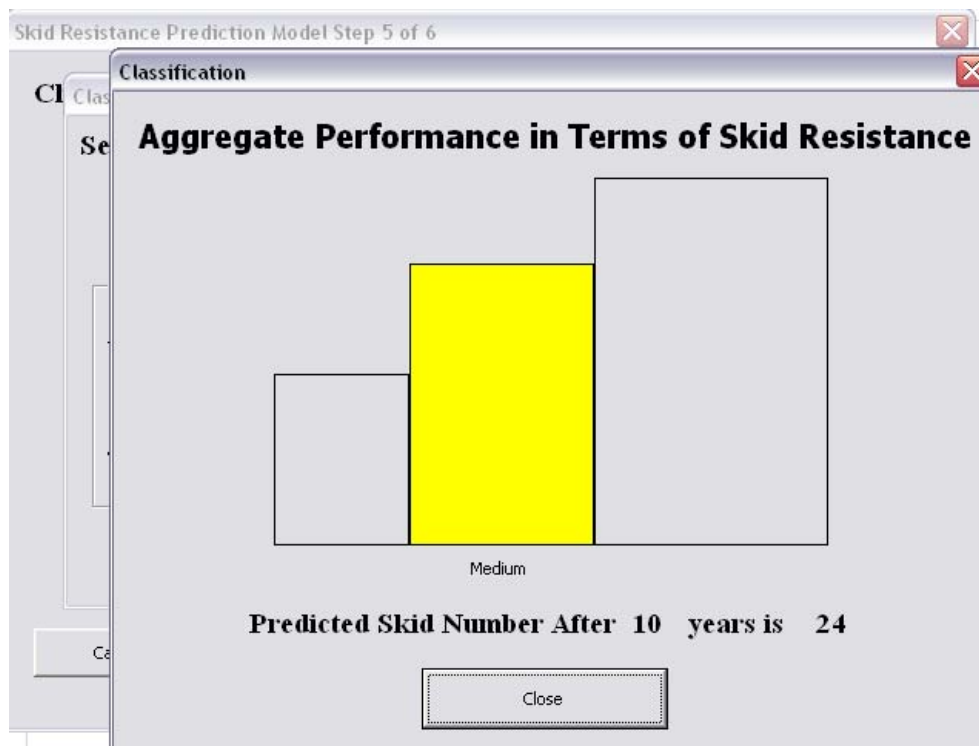


Figure 31. Classification Sample.

CHAPTER VI – CONCLUSIONS AND RECOMMENDATIONS

SUMMARY OF THE RESULTS OF THE FIELD DATA ANALYSIS

In Phase I of this study, researchers conducted laboratory experiments to determine the influence of aggregate properties and mixture design on the skid resistance of asphalt mixture slabs. The work in Phase I led to the development of a method to predict IFI as a function of aggregate gradation and aggregate texture measured using AIMS.

In Phase II of the project, skid data from different road sections with different material and mix types were collected. Traffic, mix type, and aggregate type were the main factors that were considered in the analysis of the measured skid numbers. To facilitate comparing different road categories in their current service life, a single factor denoted TMF was defined. This factor is the multiplication of AADT in the design lane and years in service divided by 1000. TMF considers both traffic level and years of operation.

The results of the data analysis showed the measured skid number to decrease as TMF increased. The measured skid numbers had less variation at higher TMF levels. This phenomenon could be attributed to mixtures reaching close to terminal skid condition that is associated with aggregates approaching their equilibrium (or terminal) state of texture after a high number of polishing or loading cycles.

Field measurements of skid number for four surface types (surface treatment Grade 3, surface treatment Grade 4, PFC, and Type C) were included in data analysis. The results showed that surface treatments generally had higher skid numbers than Type C, which is a conventional dense graded mix. Additionally, PFC mixes exhibited better skid resistance than Type C mixes and surface treatment mixes. The results showed the PFC mixes had the lowest variation in skid number, while surface treatment mixes had the highest variability.

The effect of aggregate type was studied, and the results showed that there was high interaction between aggregate performance, mix type in which aggregate is used, and traffic level. In general, it is hard to classify aggregates without specifying mixture

type and traffic levels. Some aggregate types performed poorly in certain mixtures, while their performance was acceptable in other mixtures.

For the most part, the results of the field data analysis were in agreement with the laboratory findings in Phase I. The same equation form (i.e., Equation 1) that was used to describe aggregate rate of polishing can be used to describe skid number versus TMF values in the field and to describe skid number versus polishing cycles in the laboratory.

In Phase II, 64 road sections were selected for testing using DFT and CTMeter devices. The selection considered covering a wide range of material type and traffic conditions, and more importantly to include some of the mixtures that were tested in the laboratory in Phase I of this study. CTMeter and DFT devices were used to take measurements from the left wheelpath of the outside lane and from the shoulder.

The results showed there was no correlation between the MPD values and measured skid number. The results also indicated that there was a fair correlation between friction and measured skid number for all mixes.

The data collected in Phases I and II were analyzed, and a system was developed to predict the skid number of asphalt mixtures as a function of traffic level. This system requires input parameters that can be easily obtained. These input parameters are aggregate texture measured using AIMS before Micro-Deval, aggregate texture measured using AIMS after Micro-Deval polishing, and aggregate gradation.

RECOMMENDATIONS

The system that was developed in this study is very promising and has been verified using the data collected in this study. Although the 0-5627 research team conducted extensive field testing on hot mix asphalt (HMA) surfaces, the evaluation of surface treatment skid resistance was limited to the analyses of corresponding data from the PMIS database. Further testing is needed so that the HMA asphalt prediction model can be tailored to the skid prediction model of surface treatment. There is also a need for validation of the skid prediction model at a wide variety of conditions and for more asphalt mixtures types.

The current model developed in 0-5627 uses a simple parameter, TMF, to account for the influence of traffic on skid resistance. This parameter only describes the total

number of traffic on the outer lane of the pavement without making a distinction between different traffic categories. An analysis is needed to evaluate the influence of traffic distribution on skid number and subsequent assessment of developing a new method for including the influence of traffic and its distribution on skid resistance.

Researchers recommend creation of an implementation project to verify and implement the system state wide. Research Project 0-5627 primarily focused on developing a skid prediction of an HMA surface. The prediction model should be modified so it can also be applied for surface treatments. Using the data from testing on surface treatments, the necessary adjustment in the model and the software can be made to accommodate the method to be used for surface treatments. There is also a need for validation of a skid prediction model at a wide variety of conditions and for more asphalt mixtures.

Researchers further recommend developing a rational method for setting the acceptable values of skid resistance based on climatic data and pavement geometry. This can be achieved by studying the relationship between accident data, skid resistance, climatic data, and pavement and highway geometry.

REFERENCES

- 1 Noyce D.A., Bahia, H.U., Yambó, J.M., and Kim, G. “Incorporating Road Safety into Pavement Management: Maximizing Asphalt Pavement Surface Friction for Road Safety Improvements.” Midwest Regional University Transportation Center Traffic Operations and Safety (TOPS) Laboratory, 2005.
- 2 Smith, H. “Pavement Contributions to Wet-Weather Skidding Accident Reduction.” *Transportation Research Record 622*, Transportation Research Board, TRB, National Research Council, Washington, D.C., 1976.
- 3 Davis, R.M., Flintsch, G.W., Al-Qadi, I.L.K., and McGhee, K. “Effect of Wearing Surface Characteristics on Measured Pavement Skid Resistance and Texture.” *Presented at 81st Transportation Research Board Annual Meeting*, Washington, D.C., 2002.
- 4 FHWA. Nationwide Personal Transportation Survey. NPTS Databook, *FHWA-Report FHWA-PL-94-010*, Federal Highway Administration, U.S. Department of Transportation, 1990.
- 5 Rizenbergs, R.L., Burchett, J.L., and Napier, C.T. “Skid Resistance of Pavements.” *Report No.KYHPR-64-24, Part II*, Kentucky Department of Highways, Lexington, KY, 1972.
- 6 Giles, C.G., Sabey, B.E., and Cardew, K.H.F. “Development and Performance of the Portable Skid Resistance Tester.” *ASTM Special Technical Publication No.326*, American Society of Testing and Materials (ASTM), Philadelphia, PA, 1962.
- 7 McCullough, B.V. and Hankins, K.D. “Skid Resistance Guidelines for Surface Improvements on Texas Highways.” *Transportation Research Record 131*, Transportation Research Board, TRB, National Research Council, Washington, D.C., 1966.
- 8 Kummer, H.W. and Meyer, W.E. “Penn State Road Surface Friction Tester as Adapted to Routine Measurement of Pavement Skid Resistance.” *Road Surface Properties, 42nd Annual Meeting*, January, 1963.
- 9 NAPA. “Hot Mix Asphalt Materials, Mixture Design, and Construction.” National Asphalt Pavement Association, NAPA Education Foundation, Lanham, MD, 1996.

- 10 Jayawickrama, P.W., Prasanna, R., and Senadheera, S.P. "Survey of State Practices to Control Skid Resistance on Hot-Mix Asphalt Concrete Pavements." *Transportation Research Record 1536*, Transportation Research Board, TRB, National Research Council, Washington, D.C., 1996.
- 11 Flintsch, G.W., Luo, Y., and Al-Qadi, I.L. "Analysis of the Effect of Pavement Temperature on the Frictional Properties of Flexible Pavement Surfaces." *Presented at 84th Transportation Research Board Annual Meeting*, Washington, D.C., 2005.
- 12 Kennedy, C.K., Young, A.E., and Buttler, I.C. "Measurement of Skidding Resistance and Surface Texture and the Use of Results in the United Kingdom." *Symposium: Surface Characteristics of Roadways*. American Society of Testing and Materials (ASTM), Philadelphia, PA, 1990.
- 13 Harald, A. "Skid Resistance and Road Surface Texture." *Symposium: Surface Characteristics of Roadways*, American Society of Testing and Materials (ASTM), Philadelphia, PA, 1990.
- 14 Forster, S.W. "Pavement Microtexture and its Relation to Skid Resistance." *Transportation Research Record 1215*, Transportation Research Board, TRB, National Research Council, Washington D.C., 1989.
- 15 Lay, C. and Judith, B. "Friction and Surface Texture Characterization of 14 Pavement Test Sections in Greenville, North Carolina." *Transportation Research Record 1639*, Transportation Research Board, TRB, National Research Council, Washington, D.C., 1998.
- 16 Saito, K., Horiguchi, T., Kasahara, A., Abe, H., and Henry, J.J. "Development of Portable Tester for Measuring Skid Resistance and Its Speed Dependency on Pavement Surfaces." *Transportation Research Record 1536*, Transportation Research Board, TRB, National Research Council, Washington D.C., 1996.
- 17 Chelliah, T., Stephanos P., Shah, M.G., and Smith, T. "Developing a Design Policy to Improve Pavement Surface Characteristics." *Presented in Transportation Research Board 82nd Annual Meeting*, Washington, D.C., 2003.
- 18 Shupe, J.W. "Pavement Slipperiness." *Section 20 of the Highway Engineering Handbook* by K.B. Woods, McGraw-Hill Book Co., Inc., New York, NY, 1960.

- 19 Bloem, D.L. "Skid-Resistance: The Role of Aggregates and Other Factors." *National Sand and Gravel Association Circular 109*, Silver Spring, MD, 1971.
- 20 Goodman, S.N., Hassan, Y., and Abd El Halim, A.O. "Preliminary Estimation of Asphalt Pavement Frictional Properties from Superpave Gyrotory Specimen and Mix Parameters." *Transportation Research Record 1949*, Transportation Research Board, TRB, National Research Council, Washington, D.C., 2006.
- 21 Roberts, A.D. "Rubber Adhesion at High Rolling Speeds." *Journal of Natural Rubber Research*, Vol. 3, No. 4, 1988.
- 22 Wasilewska, M. and Gardziejczyk, W. "Polishing Resistance of Road Aggregates Applied in Wearing Course." *Proceedings of the 3rd International Conference of Modern Technologies in Highway Engineering*, Poznan, Poland, September 8–9, 2005.
- 23 Csathy, T.I., Burnett, W.C., and Armstrong, M.D. "State-of-the-Art of Skid Resistance Research." *Highway Research Board Special Report 95*, Highway Research Board, National Research Council, Washington, D.C., 1968.
- 24 Liang, R.Y. and Chyi, L.L. "Polishing and Friction Characteristics of Aggregates Produced in Ohio." *FHWA Report FHWA/OH-2000/001*, Federal Highway Administration, Columbus, OH, 2000.
- 25 Gray, J.E. and Renninger, F.A. "The Skid Resistant Properties of Carbonate Aggregates." *Highway Research Record 120*, Highway Research Board, National Research Council, Washington, D.C., 1965.
- 26 Crouch, L.K., Shirley, G., Head, G., and Goodwin, W.A. "Aggregate Polishing Resistance Pre-Evaluation." *Transportation Research Record 1530*, Transportation Research Board, TRB, National Research Council, Washington, D.C., 1996.
- 27 West, T.R., Choi, J.C., Bruner, D.W., Park, H.J., and Cho, K.H. "Evaluation of Dolomite and Related Aggregates Used in Bituminous Overlays for Indiana Pavements." *Transportation Research Record 1757*, Transportation Research Board, TRB, National Research Council, Washington, D.C., 2001.
- 28 Fulop, I.A., Bogardi, I., Gulyas, A., and Csicsely-Tarpay, M. "Use of Friction and Texture in Pavement Performance Modeling." *ASCE Journal of Transportation Engineering*, Vol. 126, No. 3, 2000.

- 29 Henry, J.J. and Dahir, S. "Effects of Textures and the Aggregates That Produce Them on the Performance of Bituminous Surfaces." *Transportation Research Record 712*, Transportation Research Board, National Research Council, Washington, D.C., 1979.
- 30 Fwa, T.F., Choo, Y.S., and Liu, Y.R. "Effect of Aggregate Spacing on Skid Resistance of Asphalt Pavement." *Journal of Transportation Engineering, Vol. 129, No. 4*, American Society of Civil Engineering, ASCE, 2003.
- 31 Liu, Y., Fwa, T.F., and Choo, Y.S. "Effect of Surface Macrotexture on Skid Resistance Measurements by the British Pendulum Test." *Journal of Testing and Evaluation, Vol. 32, No. 4*, American Society of Civil Engineering, ASCE, 2004.
- 32 Prowell, B.D., Zhang, J., and Brown, E.R. "Aggregate Properties and the Performance of Superpave-Designed Hot Mix Asphalt." National Cooperative Highway Research Program, *NCHRP Report 539*, Transportation Research Board, National Research Council, Washington, D.C., 2005.
- 33 Mahmoud, E. and E. Masad. "Experimental Methods for the Evaluation of Aggregate Resistance to Polishing, Abrasion and Breakage." *Journal of Materials in Civil Engineering*, ASCE, Vol.19, No.11, 2007, pp. 977–985.
- 34 Al-Rousan, T.M. "Characterization of Aggregate Shape Properties Using a Computer Automated System." *Ph.D. Dissertation*, College Station, TX, 2004.
- 35 Txhotmix. <http://www.txhotmix.org>.2008. Access date: 02/18/08.
- 36 Vollor, T.W. and Hanson, D.I. "Development of Laboratory Procedure for Measuring Friction of HMA Mixtures-Phase 1." *NCAT Report 06-06*, National Center of Asphalt Technology, Auburn University, AL, 2006.
- 37 ASTM, *Annual Book of ASTM Standards*, Vol. 04.03, American Society for Testing and Materials, West Conshohocken, PA, 2006.
- 38 Dynamic Friction Tester, *Product Guide*,
<http://www.nippou.com/en/products/dft.html>. Accessed Feb. 23, 2008.
- 39 Hall, J.W., Glover, L.T., Smith, K.L., Evans, L.D., Wambold, J.C., Yager, T.J., and Rado, Z. "Guide for Pavement Friction." *Project No. 1-43*, Final Guide, National Cooperative Highway Research Program, Transportation Research Board, National Research Council, Washington, D.C., 2006.
- 40 *Circular Texture Meter*, <http://www.tics.hu/CTMeter.htm>. Accessed Feb. 23, 2008.

- 41 Wambold, J.C., Antle, C.E., Henry J.J., and Rado, Z. PIARC (Permanent International Association of Road Congress) Report. International PIARC Experiment to Compare and Harmonize Texture and Skid Resistance Measurement, C-1 PIARC Technical Committee on Surface Characteristics, France, 1995.
- 42 Henry, J.J., Abe, H., Kameyama, S., Tamai, A., Kasahara, A., and Saito, K. "Determination of the International Friction Index Using the Circular Track Meter and the Dynamic Friction Tester." *Proceedings of SURF 2000*, the World Road Association. Paris, France, 2000.

**APPENDIX A – STANDARD PROCEDURES FOR MEASURING
DEGRADATION OF AGGREGATE BY MICRO-DEVAL ABRASION AND
TEXTURE MEASUREMENT BY AIMS**

Tex-461-A, Degradation of Coarse Aggregate by Micro-Deval Abrasion

Section 1

Overview

Use this test method to test coarse aggregate for resistance to abrasion and weathering using the Micro-Deval apparatus.

Units of Measurement

The values given in parentheses (if provided) are not standard and may not be exact mathematical conversions. Use each system of units separately. Combining values from the two systems may result in nonconformance with the standard.

Section 2

Definitions

The following term is referenced in this test procedure.

◆ **Constant weight.** Constant weight is defined as aggregates other than limestone rock asphalt that are dried at a temperature of $230 \pm 9^{\circ}\text{F}$ ($110 \pm 5^{\circ}\text{C}$) to a condition such that they will not lose more than 0.1% moisture after 2 hr. of drying. Limestone rock asphalt samples will be dried at a temperature of $140 \pm 5^{\circ}\text{F}$ ($60 \pm 3^{\circ}\text{C}$) to a condition such that they will not lose more than 0.1% moisture after 2 hr. of drying. Such a condition of dryness can be verified by weighing the sample before and after successive 2-hr. drying periods. In lieu of such determination, samples may be considered to have reached constant weight when they have dried at a temperature of $230 \pm 9^{\circ}\text{F}$ ($110 \pm 5^{\circ}\text{C}$) for an equal or longer period than that previously found adequate for producing the desired constant condition under equal or heavier loading conditions of the oven.

Section 3

Apparatus

Use the following apparatus:

- ◆ Micro-Deval Abrasion machine and accessories that meet department specification No. 845-49-40.
- ◆ Standard U.S. sieves and pans, meeting the requirements of “Tex-907-K, Verifying the

Accuracy of Wire Cloth Sieves,” including:

- 3/4 in. (19.0 mm).
- 1/2 in. (12.5 mm).
- 3/8 in. (9.5 mm).
- 1/4 in. (6.3 mm).
- No. 4 (4.75 mm).
- ◆ Oven, capable of maintaining a temperature of $230 \pm 9^\circ\text{F}$ ($110 \pm 5^\circ\text{C}$).
- ◆ Balance, accurate and readable to 0.1 g or 0.1% of the mass of the test sample, whichever is greater.

Section 4

Preparing Sample

Wash and dry the test sample to constant weight. Separate the sample into individual size fractions according to “Tex 401-A, Sieve Analysis of Fine and Coarse Aggregate,” and recombine to meet the grading as shown. Dry limestone rock asphalt to constant weight at $140 \pm 9^\circ\text{F}$ ($60 \pm 5^\circ\text{C}$).

- ◆ For bituminous aggregate, use the following standard gradation:

Bituminous Aggregate		
Passing	Retained	Wt. (g)
1/2 in. (12.5 mm)	3/8 in. (9.5 mm)	750 ±5
3/8 in. (9.5 mm)	1/4 in. (6.3 mm)	375 ±5
1/4 in. (6.3 mm)	No. 4 (4.75 mm)	375 ±5

- ◆ For concrete aggregate, use the following standard gradation:

Concrete Aggregate		
Passing	Retained	Wt. (g)
3/4 in. (19.0 mm)	1/2 in. (12.5 mm)	660 ±5
1/2 in. (12.5 mm)	3/8 in. (9.5 mm)	330 ±5
3/8 in. (9.5 mm)	1/4 in. (6.3 mm)	330 ±5
1/4 in. (6.3 mm)	No. 4 (4.75 mm)	180 ±5

Section 5

Procedure

The following table outlines the procedure for testing coarse aggregate for resistance to abrasion and weathering using the Micro-Deval apparatus.

Testing Coarse Aggregate	
Step	Action
1	<ul style="list-style-type: none"> ◆ Prepare a representative 1500 ±5 g sample according to the applicable standard grading. A maximum of 10% of an adjacent size material from the standard grading may be substituted if the sample does not contain appropriate weights. Crush parent material to obtain sizes if necessary. ◆ Record the weight to the nearest 1.0 g, as 'A' under 'Calculations.'
2	Saturate the sample in 0.5 gal. (2000 ±500 mL) of tap water (temperature 68 ±9°F [20 ±5°C]) for a minimum of 1 hr. either in the Micro-Deval container or in another suitable container.
3	<ul style="list-style-type: none"> ◆ Place the sample, water, and 5000 ±5 g of stainless steel balls in the Micro-Deval container. ◆ Place the Micro-Deval container on the machine.
4	<ul style="list-style-type: none"> ◆ Set the timer and start the machine. <ul style="list-style-type: none"> ◆ Test concrete aggregate samples at 100 ±5 rpm for 120 ±1 min. ◆ Test bituminous aggregate samples at 100 ±5 rpm for 105 ±1 min. ◆ Record the rpms registered by the tachometer at the end of the test period.
5	<ul style="list-style-type: none"> ◆ Stack a No. 4 (4.75 mm) and a No. 16 (1.18 mm) sieve together and carefully decant the sample over them. Take care to remove the entire sample from the stainless steel jar. ◆ Wash the retained material with water until the wash water is clear and all materials smaller than No. 16 (1.18 mm) pass the sieve.
6	<ul style="list-style-type: none"> ◆ Remove the stainless steel balls using a magnet or other suitable means. ◆ Discard material passing the No. 16 (1.18 mm) sieve.
7	<ul style="list-style-type: none"> ◆ Oven-dry the sample to constant weight at 230 ±9°F (110 ±5°C). ◆ Oven-dry limestone rock asphalt to constant weight at 140 ±9°F (60 ±5°C).
8	<ul style="list-style-type: none"> ◆ Weigh the sample to the nearest 1.0 gm. ◆ Record the oven-dry weight as 'B' under 'Calculations.'

Section 6

Calculations

Calculate the Micro-Deval abrasion loss as follows:

$$\text{Percent loss} = (A - B) / A \times 100$$

Record the nearest whole percentage point.

Determining Aggregate Shape Properties by Means of Digital Image Analysis

AASHTO Designation: xx-xx

1. SCOPE

- 1.1. This standard covers the measurement of aggregate shape properties using the Digital Image Analysis techniques.
- 1.2. This standard may involve hazardous materials, operations, and equipment. This standard does not purport to address all of the safety problems associated with its use. It is the responsibility of the user of this standard to establish appropriate safety and health practices and determine the applicability of regulatory limitations prior to use.
-

2. REFERENCED DOCUMENTS

2.1. *AASHTO Standards:*

- M 92 Standard Specification for Wire-Cloth Sieves for Testing Purposes
- T 2 Sampling of Aggregates
- T 11 Amount of Material Finer Than 75 μ m in Aggregate
- T 27 Standard Method of Test for Sieve Analysis of Fine and Coarse Aggregates
- T 84 Standard Method of Test for Specific Gravity and Absorption of Fine Aggregate
- T 85 Standard Method of Test for Specific Gravity and Absorption of Coarse Aggregate
- T 248 Standard Method of Test for Reducing Samples of Aggregate to Testing Size

2.2. *Other References:*

- ASTM C 802, "Standard Practice for Conducting an Interlaboratory Test Program to Determine the Precision of Test Methods for Construction Materials."
 - ASTM C 670 "Standard Practice for Preparing Precision and Bias Statements for Test Methods for Construction Materials."
-

3. TERMINOLOGY

- 3.1. Aggregate size—sieve size in which material is retained after passing the next larger sieve.
- 3.1.1. Fine Aggregate—Aggregate material passing 4.75 mm (#4) sieve.
sieve sizes: 2.36 mm (#8), 1.18 mm (#16), 0.60 mm (#30), 0.30 mm (#50), 0.15 mm (#100), 0.075 mm (#200)
- 3.1.2. Coarse Aggregate—Aggregate material retained on 4.75 mm (#4) sieve.
sieve sizes: 25.0 mm (1"), 19.0 mm (3/4"), 12.5 mm (1/2"), 9.5 mm (3/8"), 4.75 mm (#4)
- 3.2. Shape Properties for each retained sieve (x)
- 3.2.1. Gradient Angularity (GA)—Applies to both fine and coarse aggregate sizes and is related to the sharpness of the corners of 2-dimensional images of aggregate particles. The gradient angularity quantifies changes along a particle boundary with higher gradient values indicating a more angular

shape. Gradient angularity has a relative scale of 0 to 10,000 with a perfect circle having a value of 0.

$$\text{Gradient Angularity: } GA = \frac{1}{\frac{n}{3} - 1} \sum_{i=1}^{n-3} |\theta_i - \theta_{i+3}| \quad (1)$$

where: θ angle of orientation of the edge points.

n is the total number of points.

subscript i denoting the i^{th} point on the edge of the particle.

3.2.2.

Texture or Micro-Texture (TX)—Applies to coarse aggregate sizes only describing relative smoothness or roughness of surface features less than roughly 0.5 mm in size which are too small to affect the overall shape. Texture has a relative scale of 0 to 1000 with a smooth polished surface approaching a value of 0.

$$TX = \frac{1}{3N} \sum_{i=1}^3 \sum_{j=1}^N (D_{i,j}(x, y))^2 \quad (2)$$

where:

D = decomposition function.

n = decomposition level.

N = total number of coefficients in an image.

$i = 1, 2, \text{ or } 3$ for detailed images.

j = wavelet index.

x, y = location of the coefficients in transformed domain.

3.2.3.

Sphericity (SP)—Applies to coarse aggregate sizes only and describes the overall 3-dimensional shape of a particle. Sphericity has a relative scale of 0 to 1. A sphericity value of one indicates a particle has equal dimensions (cubical).

$$SP = \sqrt[3]{\frac{d_s * d_l}{d_L^2}} \quad (3)$$

where: d_s = particle shortest dimension.

d_l = particle intermediate dimension.

d_L = particle longest dimension.

3.2.4.

Form 2D—Applies to fine aggregate sizes only and is used to quantify the relative form from 2-dimensional images of aggregate particles. Form2D has a relative scale of 0 to 20. A perfect circle has a Form 2D value of zero.

$$\text{Form2D} = \sum_{\theta=0}^{\theta=360-\Delta\theta} \left[\frac{R_{\theta+\Delta\theta} - R_{\theta}}{R_{\theta}} \right] \quad (4)$$

where: R_{θ} is the radius of the particle at an angle of θ .

$\Delta\theta$ is the incremental difference in the angle.

3.2.5.

Flat and Elongated—those particles having a ratio of longest dimension to shortest dimension greater than a specified value.

Aggregate particle dimensions in an x, y, z coordinate system.

d_s = particle shortest dimension.

d_i = particle intermediate.

d_L = particle longest dimension.

$$\text{Flatness Ratio (S/L): } \textit{Flatness} = \frac{d_s}{d_i} \quad (5)$$

$$\text{Elongation Ratio (I/L): } \textit{Elongation} = \frac{d_i}{d_L} \quad (6)$$

$$\text{Flat and Elongated Value (F\&E): } L/S = \frac{d_L}{d_s} \quad (7)$$

- 3.2.6. Flat or Elongated—those particles having a ratio of intermediate dimension to shortest dimension or longest dimension to intermediate dimension greater than a specified value.

$$\text{Flat or Elongated Value (ForE): } \frac{d_i}{d_s} \textit{ or } \frac{d_L}{d_i} > \textit{Ratio} \text{ (i.e.: 1, 2, 3...)} \quad (8)$$

4. SIGNIFICANCE AND USE

- 4.1. Shape, angularity, and surface texture of aggregates have been shown to directly affect the engineering properties of highway construction materials such as hot mix asphalt concrete, Portland cement concrete, and unbound aggregate layers. This standard provides direct measurement of aggregate shape, angularity, and texture. For coarse aggregates, the shape properties include: Gradient Angularity, Sphericity, Texture, and Flat and Elongated value. For fine aggregates the shape properties include: Gradient Angularity and Form 2D.

Note 1—The National Cooperative Highway Research Program Report 555 provides background information relevant to characterizing aggregate shape, texture, and angularity.

- 4.2. This test method may be used to characterize and monitor the shape properties of aggregate material samples sizes 0.075 mm (#200) through 25.0 mm (1"). This method may be used to characterize a single size within a material source or all sizes within the source.

5. APPARATUS

- 5.1. *Digital Image Acquisition and Analysis System*—A computer controlled electro-mechanical instrument for capturing digital images at variable magnification and software for image analysis. Instrumentation and analysis software shall include algorithms for Gradient Angularity, Form 2D, Flat and Elongated, Sphericity, and Texture.
- 5.1.1. A camera and optic system capable of providing the required resolutions over the range of particles being analyzed.
- 5.1.2. A system for positioning the particle for imaging. This can be a movable camera, a movable support tray, or a combination thereof.
- 5.1.3. A system for auto-focusing the image.
- 5.1.4. A system for determining particle three dimensional measurements x, y, z in millimeters.
- 5.1.5. A system for detecting and removing touching particles from the analysis.

- 5.1.6. A system for presenting the particles for imaging consisting of trays or other support surface for aggregate sizes from 0.075 mm (#200) through 25.0 mm (1"). The particles shall be presented for imaging on a flat surface. A small recess for aligning particles is acceptable.
- 5.1.7. A variable lighting system for backlighting and/or top lighting the material sample.
Note 2—The Aggregate Image Measurement System and the associated AIMS SOFTWARE algorithms for image analysis computations have proven to be an acceptable system for this analysis.
- 5.2. *Balance*—A balance meeting the requirements of M 231, Class G 5, for determining the mass of aggregates.
- 5.3. *Oven*—An oven of appropriate size capable of maintaining a uniform temperature of $110\pm 5^{\circ}\text{C}$ ($290\pm 9^{\circ}\text{F}$)
- 5.4. *Miscellaneous*— Equipment to perform sample preparation methods AASHTO T 2, T 11, T 27, T 248.

6. HAZARDS

- 6.1. Use standard safety precautions and protective clothing when handling materials and preparing material samples.

7. STANDARDIZATION

- 7.1. Confirm the image acquisition system has been standardized. Frequency and method of standardization shall follow manufacturer's instructions.

8. PREPARATION OF APPARATUS

- 8.1. Confirm the system has been standardized by verifying the standardization date.
- 8.2. Confirm the machine operation settings are correct for the analysis to be performed.

9. SAMPLE PREPARATION

- 9.1. Sample the aggregate according to procedures in AASHTO T 2.
Note 3—Material samples obtained for AASHTO T 84 and T85 specific gravity determinations have proven to be acceptable.
- 9.2. Thoroughly mix the sample and reduce it to the approximate quantity needed using the applicable procedures in AASHTO T 248.
- 9.3. Determine the amount of material finer than 0.075 mm (#200) by AASHTO T 11.
- 9.4. Oven dry the sample at $110\pm 5^{\circ}\text{C}$ ($230\pm 9^{\circ}\text{F}$) to substantially constant mass.
- 9.5. Determine the sample grading on the washed, dry sample in accordance with AASHTO T 27. Calculate the percentage of material in each size fraction. Maintain sample material as separate retained sieve sizes.

- 9.6. Obtain the required aggregate of each size from the sample using the procedures described in AASHTO T 248.
- 9.7. Maintain the necessary size fractions obtained in a dry condition in separate containers for each size.
- The following list provides suggested sample mass to achieve the required minimum particle count for each size fraction:

Size	Approx. Mass	Minimum Number of Particles
0.075 mm (#200)	200 g	150
0.15 mm (#100)	200 g	150
0.3 mm (#50)	200 g	150
0.6 mm (#30)	200 g	150
1.18 mm (#16)	200 g	150
2.36 mm (#8)	200 g	150
4.75 mm (#4)	2 kg	50
9.5 mm (3/8 inch)	2 kg	50
12.5 mm (1/2 inch)	2 kg	50
19.0 mm (3/4 inch)	2 kg	50
25.0 mm (1 inch)	5 kg	50

10. PROCEDURE FOR COARSE AGGREGATE

- 10.1. Position the coarse aggregate sample for image acquisition by size fraction. Each size fraction of retained material may be run separately.
- 10.2. Distribute the coarse aggregate sample over the support surface in a manner that provides separation of at least 1.0 mm between particles. Particle orientation shall be determined by permitting them to come to rest randomly.
- 10.3. Initiate the image acquisition sequence and analysis algorithms. This process is typically automated. The operator inputs the material size, and the system automatically captures the required images and calculates the shape properties for each particle.
- 10.4. Each characterization requires the minimum number of particles for each size fraction listed in Section 9.7 to be analyzed. If the required particle count is not achieved in one sequence, repeat the sequence with additional particles until the required number of images is acquired.
- For sizes that contain inadequate percent retained mass to achieve minimum particle count use the shape value obtained from the next larger or the next smaller size, whichever is present.

11. PROCEDURE FOR FINE AGGREGATE

- 11.1. Position the fine aggregate sample for image acquisition by size fraction. Each size fraction of retained material may be run separately.
- Note 4—Most fine aggregate materials are analyzed using backlighting. However, some translucent materials may require a dark background and top lighting to achieve the appropriate image contrast. If the system fails to capture usable images with backlighting, use a dark background and top lighting. A dark background is typically required for 0.30 mm (#50) and smaller sizes.

- 11.2. Distribute the fine aggregate sample over the support surface in a manner that provides separation between particles. Typically only a very light coating is needed. Particles orientation shall be determined by permitting them to come to rest randomly.
- 11.3. Initiate the image acquisition sequence, and run the analysis routines. This process is typically automated. The operator selects the material size, and the system automatically captures the required images and calculates the shape properties for each particle.
- 11.4. Each characterization requires the minimum number of particles for each size fraction listed in Section 9.7 to be analyzed. If the required particle count is not achieved in one sequence, repeat the sequence until the required number of images is acquired.
For sizes that contain inadequate percent retained mass to achieve minimum particle count use the shape value obtained from the next larger or the next smaller size, whichever is present.

12. CALCULATIONS

- 12.1. Calculate gradient angularity value for each fine and coarse aggregate particle.
- 12.1.1. Calculate the gradient angularity mean and standard deviation for each size fraction.
- 12.2. Calculate the texture (TX) value for each coarse particle.
- 12.2.1. Calculate the texture mean and standard deviation for each coarse size fraction.
- 12.3. Calculate the sphericity (SP) for each coarse aggregate particle.
- 12.3.1. Calculate the sphericity mean and standard deviation for each coarse size fraction.
- 12.4. Calculate the Form 2D value for each fine particle.
- 12.4.1. Calculate the Form 2D mean and standard deviation for each fine size fraction.
- 12.5. Calculate the percent distribution of Flat and Elongated at the following ratios:
 $\geq 1:1, >2:1, >3:1, >4:1, >5:1$
 $\%L/S(\geq 1)_x = \% \text{ of Particles with } d_l/d_s \geq 1$
 $\%L/S(>2)_x = \% \text{ of Particles with } d_l/d_s > 2$
 $\%L/S(>3)_x = \% \text{ of Particles with } d_l/d_s > 3$
 $\%L/S(>4)_x = \% \text{ of Particles with } d_l/d_s > 4$
 $\%L/S(>5)_x = \% \text{ of Particles with } d_l/d_s > 5$
 where: x designates the retained sieve size
- 12.6. Calculate the percent distribution of Flat or Elongated at the following ratios:
 $\geq 1:1, >2:1, >3:1, >4:1, >5:1$
 $\%F_{or}E(\geq 1)_x = \% \text{ of Particles with } d_l/d_s \text{ or } d_l/d_l \geq 1$
 $\%F_{or}E(>2)_x = \% \text{ of Particles with } d_l/d_s \text{ or } d_l/d_l > 2$
 $\%F_{or}E(>3)_x = \% \text{ of Particles with } d_l/d_s \text{ or } d_l/d_l \leq 3$
 $\%F_{or}E(>4)_x = \% \text{ of Particles with } d_l/d_s \text{ or } d_l/d_l > 4$
 $\%F_{or}E(>5)_x = \% \text{ of Particles with } d_l/d_s \text{ or } d_l/d_l > 5$
 where: x designates the retained sieve size

13. REPORT

- 13.1. Report the following information:
A sample report format is presented in Appendix X1
- 13.1.1. Procedure used
- 13.1.2. Date of the analysis
- 13.1.3. Material sample identification: type, source, and size
- 13.1.4. Number of particles analyzed
- 13.1.5. Material shape property mean and standard deviation. Graphical representations of the property distributions may be included.

14. PRECISION AND BIAS

- 14.1. *Precision*—An Inter-Laboratory Study (ILS) was conducted in 2009 in accordance with ASTM C802, “Standard Practice for Conducting an Inter-Laboratory Test Program to Determine the Precision of Test Methods for Construction Materials.” The ILS results were used to develop a precision statement for the test method using ASTM C670, “Standard Practice for Preparing Precision and Bias Statements for Test Methods for Construction Materials.” The ILS featured eight systems, 32 Laboratories, and three material sources.

Table 14.1: Precision for Sizes 25 mm, 19 mm, 12.5 mm, 9.5 mm, 4.75 mm, 2.36 mm, 1.18 mm, 0.60 mm, 0.30 mm, and 0.15 mm.

Aggregate Shape Characteristic	Within Laboratory		Between Laboratory	
	Coefficient of Variation (% of mean)	Acceptable Range of Two Results (% of mean)	Coefficient of Variation (% of mean)	Acceptable Range of Two Results (% of mean)
Angularity	2.9%	8.2%	4.3%	12.1%
Texture	4.5%	12.7%	7.1%	19.8%
Sphericity	1.2%	3.4%	2.6%	7.2%
Flat or Elongated	2.1%	5.9%	3.4%	9.6%
2D Form	2.8%	7.7%	3.5%	9.9%

- 14.2. *Bias*—Since there is no accepted reference device suitable for determining the bias in this method, no statement of bias is made.

15. KEYWORDS

- 15.1. Aggregate, angularity, consensus property, shape, texture, form, elongated

Appendix X1: Sample Report

Material Information

Date:

Project:

Technician:

Workbook Name:

Description:

Include	Samples	Size	Comment
<input checked="" type="checkbox"/>	12.5 (0.50) 33 LS 1	12.5	
<input checked="" type="checkbox"/>	12.5 (0.50) 41 GRT 1	12.5	
<input checked="" type="checkbox"/>	12.5 (0.50) 41 GRV 1	12.5	
<input checked="" type="checkbox"/>	12.5 (0.50) 17 GRT 1	12.5	
<input checked="" type="checkbox"/>	12.5 (0.50) 17 GRV 1	12.5	
<input checked="" type="checkbox"/>	12.5 (0.50) 17 LS 1	12.5	
<input type="checkbox"/>			
<input type="checkbox"/>			

AIMS Material Summary

Project Name: Date:

Workbook: Technician:

Description:

Form2D

Sample	Size	Particles in Range	Average	Standard Deviation	Low (≤ 6)		(≤ 6)		Medium (6 - 12)		(≤ 12)		High (12 - 20)		(≤ 20)		Out of Range
					#	%	#	%	#	%	#	%	#	%	#	%	

Angularity

Sample	Size	Particles in Range	Average	Standard Deviation	Low (≤ 3300)		(≤ 3300)		Medium (3300-6600)		(≤ 6600)		High (6600-10000)		(≤ 10000)		Out of Range
					#	%	#	%	#	%	#	%	#	%			
12.5 (0.50) 33 LS 1	12.5	50	2784.3	669.0	37	74.0%	74.0%	13	26.0%	100.0%	0	0.0%	100.0%	0	0		
12.5 (0.50) 41 GRT 1	12.5	50	3138.7	597.3	28	56.0%	56.0%	22	44.0%	100.0%	0	0.0%	100.0%	0	0		
12.5 (0.50) 41 GRV 1	12.5	50	2791.7	978.7	35	70.0%	70.0%	15	30.0%	100.0%	0	0.0%	100.0%	0	0		
12.5 (0.50) 17 GRT 1	12.5	50	3118.7	655.3	33	66.0%	66.0%	17	34.0%	100.0%	0	0.0%	100.0%	0	0		
12.5 (0.50) 17 GRV 1	12.5	50	2623.1	862.9	40	80.0%	80.0%	10	20.0%	100.0%	0	0.0%	100.0%	0	0		
12.5 (0.50) 17 LS 1	12.5	50	2670.4	726.4	42	84.0%	84.0%	8	16.0%	100.0%	0	0.0%	100.0%	0	0		

Texture

Sample	Size	Particles in Range	Average	Standard Deviation	Low (≤ 260)		(≤ 260)		Medium (260-550)		(≤ 550)		High (550 - 1000)		(≤ 1000)		Out of Range
					#	%	#	%	#	%	#	%	#	%			
12.5 (0.50) 33 LS 1	12.5	50	281.8	98.1	22	44.0%	44.0%	28	56.0%	100.0%	0	0.0%	100.0%	0	0		
12.5 (0.50) 41 GRT 1	12.5	50	455.5	119.8	1	2.0%	2.0%	41	82.0%	84.0%	8	16.0%	100.0%	0	0		
12.5 (0.50) 41 GRV 1	12.5	49	211.8	131.9	35	71.4%	71.4%	14	28.6%	100.0%	0	0.0%	100.0%	1	1		
12.5 (0.50) 17 GRT 1	12.5	50	457.4	88.6	0	0.0%	0.0%	43	86.0%	86.0%	7	14.0%	100.0%	0	0		
12.5 (0.50) 17 GRV 1	12.5	50	224.4	141.9	35	70.0%	70.0%	14	28.0%	98.0%	1	2.0%	100.0%	0	0		
12.5 (0.50) 17 LS 1	12.5	50	252.3	84.4	32	64.0%	64.0%	17	34.0%	98.0%	1	2.0%	100.0%	0	0		

AIMS Material Summary

Project Name:	Coarse Aggregate Sample	Date:	5/20/09
Workbook:	AIMS_Shape_3.6.xlsm	Technician:	TEC
Description:			

Sphericity														
Sample	Size	Particles in Range	Average	Standard Deviation	Low (≤ 0.3)		(≤ 0.3)	Medium (0.3-0.7)		(≤ 0.7)	High (0.7 - 1.0)		(≤ 1.0)	Out of Range
					#	%	Cum. %	#	%	Cum. %	#	%	Cum. %	
12.5 (0.50)_33_LS_1	12.5	50	0.69	0.10	0	0.0%	0.0%	28	56.0%	56.0%	22	44.0%	100.0%	0
12.5 (0.50)_41_GRT_1	12.5	49	0.62	0.09	0	0.0%	0.0%	37	75.5%	75.5%	12	24.5%	100.0%	1
12.5 (0.50)_41_GRV_1	12.5	49	0.69	0.08	0	0.0%	0.0%	24	49.0%	49.0%	25	51.0%	100.0%	1
12.5 (0.50)_17_GRT_1	12.5	50	0.63	0.11	0	0.0%	0.0%	37	74.0%	74.0%	13	26.0%	100.0%	0
12.5 (0.50)_17_GRV_1	12.5	50	0.69	0.08	0	0.0%	0.0%	27	54.0%	54.0%	23	46.0%	100.0%	0
12.5 (0.50)_17_LS_1	12.5	50	0.69	0.09	0	0.0%	0.0%	27	54.0%	54.0%	23	46.0%	100.0%	0

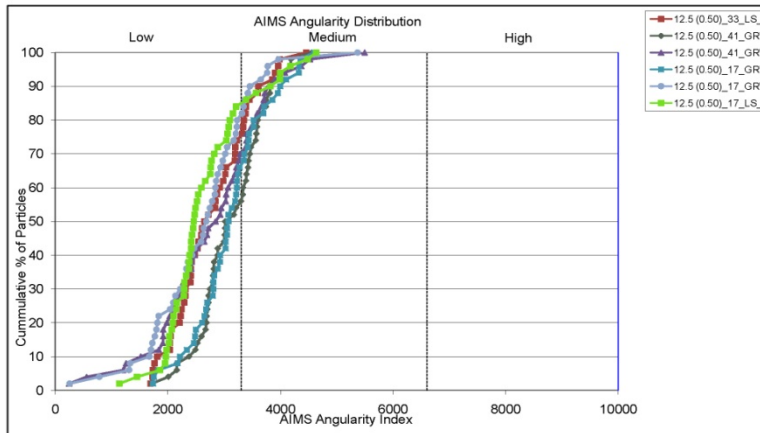
Flat and Elongated Distribution													
Sample	Size	Particles in Range	L/S $\geq 1:1$		L/S $> 2:1$		L/S $> 3:1$		L/S $> 4:1$		L/S $> 5:1$		Out of Range
			#	%	#	%	#	%	#	%	#	%	
12.5 (0.50)_33_LS_1	12.5	50	50	100.0%	28	56.0%	6	12.0%	1	2.0%	0	0.0%	0
12.5 (0.50)_41_GRT_1	12.5	49	49	100.0%	43	87.8%	21	42.9%	6	12.2%	1	2.0%	1
12.5 (0.50)_41_GRV_1	12.5	49	49	100.0%	29	59.2%	5	10.2%	1	2.0%	0	0.0%	1
12.5 (0.50)_17_GRT_1	12.5	50	50	100.0%	40	80.0%	22	44.0%	9	18.0%	1	2.0%	0
12.5 (0.50)_17_GRV_1	12.5	50	50	100.0%	26	52.0%	4	8.0%	2	4.0%	0	0.0%	0
12.5 (0.50)_17_LS_1	12.5	50	50	100.0%	33	66.0%	7	14.0%	1	2.0%	0	0.0%	0

Flat or Elongated Distribution													
Sample	Size	Particles in Range	F or E $\geq 1:1$		F or E $> 2:1$		F or E $> 3:1$		F or E $> 4:1$		F or E $> 5:1$		Out of Range
			#	%	#	%	#	%	#	%	#	%	
12.5 (0.50)_33_LS_1	12.5	50	50	100.0%	10	20.0%	0	0.0%	0	0.0%	0	0.0%	0
12.5 (0.50)_41_GRT_1	12.5	49	49	100.0%	23	46.9%	4	8.2%	0	0.0%	0	0.0%	1
12.5 (0.50)_41_GRV_1	12.5	49	49	100.0%	8	16.3%	0	0.0%	0	0.0%	0	0.0%	1
12.5 (0.50)_17_GRT_1	12.5	50	50	100.0%	24	48.0%	5	10.0%	0	0.0%	0	0.0%	0
12.5 (0.50)_17_GRV_1	12.5	50	50	100.0%	6	12.0%	1	2.0%	0	0.0%	0	0.0%	0
12.5 (0.50)_17_LS_1	12.5	50	50	100.0%	13	26.0%	1	2.0%	0	0.0%	0	0.0%	0

AIMS Angularity

Project Name:	Coarse Aggregate Sample	Date:	5/20/09
Workbook:	AIMS_Shape_3.6.xlsm	Technician:	TEC
Description:			

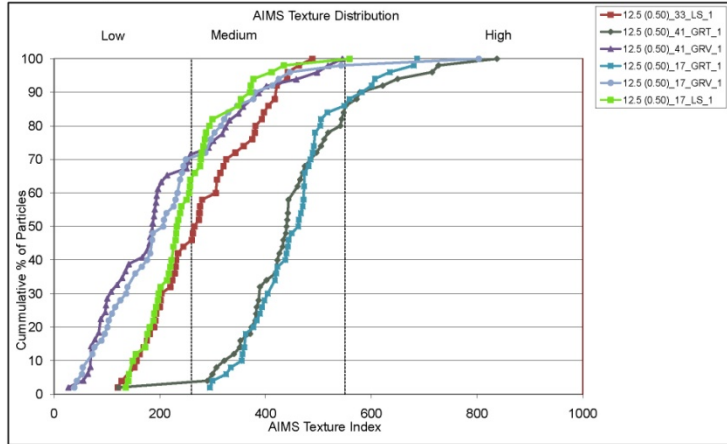
Particles in Range	Average	Std. Deviation	Median	Mode	#	%	Cum. %	#	%
Low (≤ 3300)	2854.5	786.4	2837.8	#N/A	215	71.7%	71.7%	210	70.0%
Medium (3300 - 6600)					85	28.3%	100.0%	285	95.0%
High (6600 - 10000)					0	0.0%	100.0%	296	98.7%
Out of Range					0			4	1.3%



AIMS Texture

Project Name:	Coarse Aggregate Sample	Date:	5/20/09
Workbook:	AIMS_Shape_3.6.xlsm	Technician:	TEC
Description:			

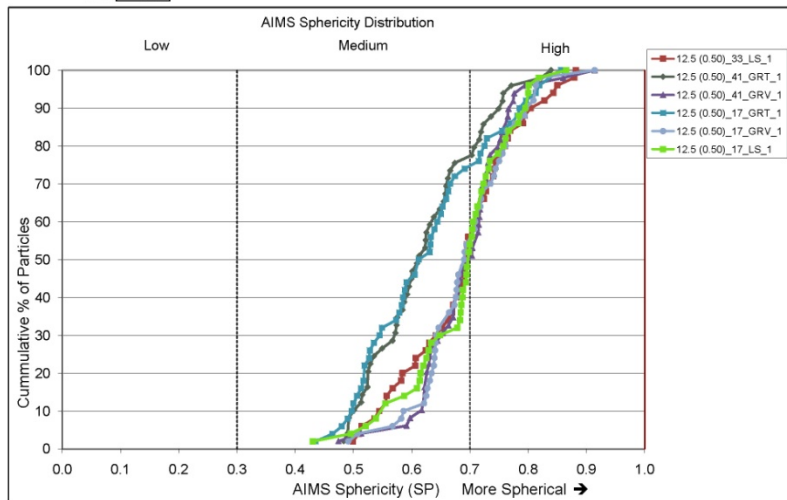
Particles in Range	#	%	Cum. %	#	%		
Average	299						
Std. Deviation	152.9						
Median	300.9						
Mode	175.6						
Low (≤ 280)	125	41.8%	(≤ 280)	41.8%	-σ < n < σ	202	67.8%
Medium (280 - 550)	167	52.8%	(≤ 550)	84.3%	-2σ < n < 2σ	290	97.0%
High (550 - 1000)	17	5.7%	(≤ 1000)	100.0%	-3σ < n < 3σ	297	98.3%
Out of Range	1				n < -3σ or n > 3σ	2	0.7%



AIMS Sphericity

Project Name:	Coarse Aggregate Sample	Date:	5/20/09
Workbook:	AIMS_Shape_3.6.xlsm	Technician:	TEC
Description:			

Particles in Range	#	%	Cum. %	#	%		
Average	298						
Std. Deviation	0.669						
Median	0.678						
Mode	0.694						
Low (≤ 0.3)	0	0.0%	(≤ 0.3)	0.0%	-σ < n < σ	202	67.8%
Medium (0.3 - 0.7)	180	60.4%	(≤ 0.7)	60.4%	-2σ < n < 2σ	288	96.6%
High (0.7 - 1.0)	118	39.6%	(≤ 1.0)	100.0%	-3σ < n < 3σ	298	100.0%
Out of Range	2				n < -3σ or n > 3σ	0	0.0%



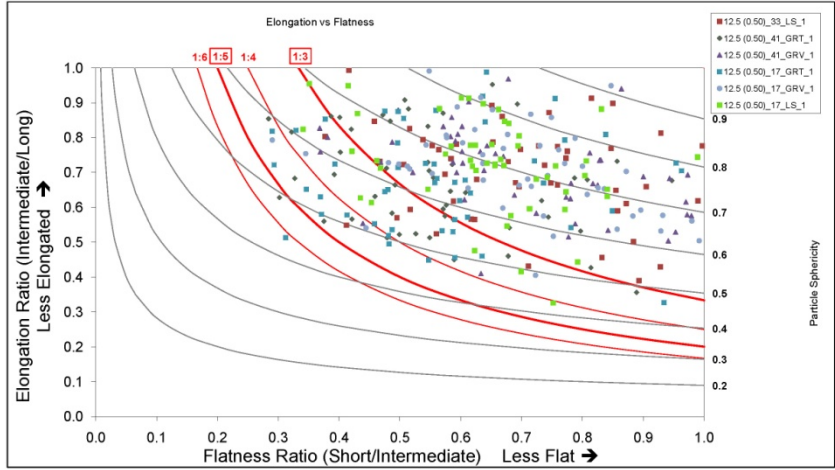
AIMS Flat and Elongated

Project Name: Coarse Aggregate Sample Date: 5/20/09
 Workbook: AIMS_Shape_3.6.xlsm Technician: TEC
 Description:

F & E		Sphericity	
Particles in Range	#	%	
Average	2.481	0.668	
Std. Deviation	0.819	0.096	
Median	2.273	0.678	
Mode	2.316	0.684	

F & E		Sphericity	
Ratio	#	%	
L/S ≥ 1:1	298	100.0%	
L/S > 2:1	199	66.8%	
L/S > 3:1	65	21.8%	
L/S > 4:1	20	6.7%	
L/S > 5:1	2	0.7%	

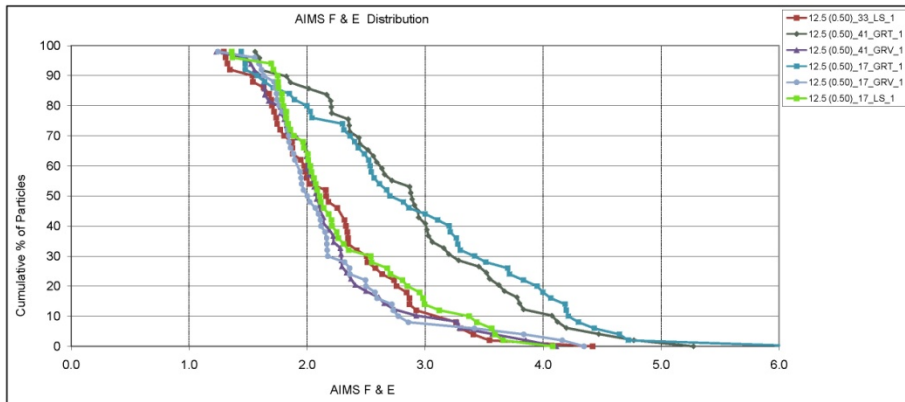
Sphericity		F & E		Sphericity		
Low (≤ 0.3)	#	%	#	%	#	%
Low (≤ 0.3)	0	0.0%	219	73.5%	202	67.8%
Medium (0.3 - 0.7)	190	60.4%	282	94.6%	288	100.0%
High (0.7 - 1.0)	118	39.6%	296	99.3%	298	100.0%
Out of Range	2		2	0.7%	0	0.0%



AIMS Flat and Elongated Distribution

Project Name: Coarse Aggregate Sample Date: 5/20/09
 Workbook: AIMS_Shape_3.6.xlsm Technician: TEC
 Description:

F and E		
Ratio	#	Cum. %
L/S ≥ 1:1	298	100.0%
L/S > 2:1	199	66.8%
L/S > 3:1	65	21.8%
L/S > 4:1	20	6.7%
L/S > 5:1	2	0.7%



Standard Practice for

Determining Aggregate Source Shape Values from Digital Image Analysis Shape Properties

AASHTO Designation: xx-xx

16. SCOPE

- 16.1. This standard covers the determination of aggregate source and source blend shape characteristics using gradation analysis and shape properties determined by means of digital image analysis.
- 16.2. This standard may involve hazardous materials, operations, and equipment. This standard does not purport to address all of the safety problems associated with its use. It is the responsibility of the user of this standard to establish appropriate safety and health practices and determine the applicability of regulatory limitations prior to use.

17. REFERENCED DOCUMENTS

17.1. *AASHTO Standards:*

- T 11 Amount of Material Finer Than 75 μ m in Aggregate
- T 27 Standard Method of Test for Sieve Analysis of Fine and Coarse Aggregates
- T 84 Standard Method of Test for Specific Gravity and Absorption of Fine Aggregate
- T 85 Standard Method of Test for Specific Gravity and Absorption of Coarse Aggregate
- TP XX Standard Method of Test for Determining Aggregate Shape Properties by Means of Digital Image Analysis

18. TERMINOLOGY

- 18.1. Aggregate size—material retained on a given sieve size after passing the next larger sieve.
- 18.1.1. Fine Aggregate—Aggregate material passing 4.75 mm (#4) sieve.
sieve sizes: 2.36 mm (#8), 1.18 mm (#16), 0.60 mm (#30), 0.30 mm (#50), 0.15 mm (#100), 0.075 mm (#200)
- 18.1.2. Coarse Aggregate—Aggregate material retained on 4.75 mm (#4) sieve.
sieve sizes: 25.0 mm (1"), 19.0 mm (3/4"), 12.5 mm (1/2"), 9.5 mm (3/8"), 4.75 mm (#4)
- 18.2. Shape Properties for each retained sieve (x)
- 18.2.1. Gradient Angularity (*GA*)—Applies to both fine and coarse aggregate sizes and is related to the sharpness of the corners of 2-dimensional images of aggregate particles. The gradient angularity quantifies changes along a particle boundary with higher gradient values indicating a more angular shape. Gradient angularity has a relative range of 0 to 10,000 with a perfect circle having a value of 0.

$$\text{Gradient Angularity: } GA = \frac{1}{\frac{n}{3} - 1} \sum_{i=1}^{n-3} |\theta_i - \theta_{i+3}| \quad (1)$$

where: θ angle of orientation of the edge points.

n is the total number of points,

subscript i denoting the i^{th} point on the edge of the particle.

18.2.2. Texture (or Micro-Texture) (TX)—Applies to coarse aggregate sizes only and describes the relative smoothness or roughness of surface features less than roughly 0.5 mm in size that are too small to affect the overall shape. Texture has a relative scale of 0 to 1000 with a smooth polished surface approaching a value of 0.

$$TX = \frac{1}{3N} \sum_{i=1}^3 \sum_{j=1}^N (D_{i,j}(x, y))^2 \quad (2)$$

where:

D = decomposition function.

n = decomposition level.

N = total number of coefficients in an image.

$i = 1, 2, \text{ or } 3$ for detailed images.

j = wavelet index.

x, y = location of the coefficients in transformed domain.

18.2.3. Sphericity (SP)—Applies to coarse aggregate sizes only and describes the overall 3-dimensional shape of a particle. Sphericity has a relative scale of 0 to 1. A sphericity value of one indicates a particle has equal dimensions (cubical).

$$SP = \sqrt[3]{\frac{d_s * d_l}{d_L^2}} \quad (3)$$

where: d_s = particle shortest dimension.

d_l = particle intermediate dimension.

d_L = particle longest dimension.

18.2.4. Form 2D—Applies to fine aggregate sizes only and is used to quantify the relative form from 2-dimensional images of aggregate particles. Form 2D has a relative scale of 0 to 20. A perfect circle has a Form 2D value of zero.

$$\text{Form2D} = \sum_{\theta=0}^{\theta=360-\Delta\theta} \left[\frac{R_{\theta+\Delta\theta} - R_{\theta}}{R_{\theta}} \right] \quad (4)$$

where: R_{θ} is the radius of the particle at an angle of θ .

$\Delta\theta$ is the incremental difference in the angle.

18.2.5. Flat and Elongated—those particles having a ratio of longest dimension to shortest dimension greater than a specified value.

Aggregate particle dimensions in an x, y, z coordinate system.

d_s = particle shortest dimension.

d_l = particle intermediate.

d_L = particle longest dimension.

$$\text{Flatness Ratio (S/L): } \textit{Flatness} = \frac{d_s}{d_l} \quad (5)$$

$$\text{Elongation Ratio (I/L): } \textit{Elongation} = \frac{d_l}{d_L} \quad (6)$$

$$\text{Flat and Elongated Value (F\&E): } L/S = \frac{d_L}{d_s} \quad (7)$$

- 18.2.6. Flat or Elongated—those particles having a ratio of intermediate dimension to shortest dimension or longest dimension to intermediate dimension greater than a specified value.

$$\text{Flat or Elongated (ForE): } \frac{d_l}{d_s} \textit{ or } \frac{d_L}{d_l} > \textit{Ratio} \text{ (i.e.: 1, 2, 3...)} \quad (8)$$

- 18.2.7. %Pass_x = % passing sieve x

- 18.2.8. %R_x = % retained on sieve x (passing sieve x+1)

19. SIGNIFICANCE AND USE

- 19.1. Shape, angularity, and surface texture of aggregates have been shown to directly affect the engineering properties of highway construction materials such as hot mix asphalt concrete, Portland cement concrete, and unbound aggregate layers. This standard is used to characterize the combined shape values for an aggregate source from the individual particle shape properties determined by digital image analysis from AASHTO Test Method xx-xx. The aggregate shape characterization includes Gradient Angularity, Form 2D, Sphericity, Texture, and Flat and Elongated value.

Note 1—The National Cooperative Highway Research Program Report 555 provides background information relevant to characterizing aggregate shape, texture, and angularity.

- 19.2. This practice may be used to characterize the shape characteristics of single source aggregate materials and multiple source aggregate material blends.

20. PROCEDURE

- 20.1. Determine the aggregate sample grading according to AASHTO T27 and the amount finer than 75 μ m according to AASHTO T11.
- 20.2. Determine the aggregate sample specific gravities according to AASHTO T84 and T85.
- 20.3. Determine the material sample shape values for Form 2D, Gradient Angularity, Sphericity, Form Ratios (F&E, F or E), and Texture according to AASHTO TP XX.

21. CALCULATIONS – SINGLE SOURCE

- 21.1. The material sample is typically characterized by individual evaluation of material retained on each sieve size, passing the next larger sieve. For the purpose of calculating the combined shape

values, consider any sizes that contain inadequate percent retained mass to achieve minimum particle count to have the same shape value as the average of the next larger or the next smaller size, whichever is present.

- 21.2. Calculate the Percent Retained for the aggregate sample on each sieve using the AASHTO T27 results.:

Sieve Sizes (x):

Coarse: 25.0 mm (1"), 19.0 mm (3/4"), 12.5 mm (1/2"), 9.5 mm (3/8"), 4.75 mm (#4)

Fine: 2.36 mm (#8), 1.18 mm (#16), 0.60 mm (#30), 0.30 mm (#50), 0.15 mm (#100), 0.075 mm (#200)

Percent Passing: $\%Pass_x = \% \text{ passing sieve } x$

Percent Retained: $\%R_x = \% \text{ retained on sieve } x$

$$\%R_x = \%Pass_{x+1} - \%Pass_x \quad (9)$$

- 21.3. Calculate average particle size, volume, and surface area for each sieve size x for unit mass.

For the purposes of shape characterization, volume and surface area of an average particle is estimated by using a cubical shape with side dimensions estimated by the average of the retained sieve and next larger sieve dimension.

$$\text{Average Particle Size: } D_x = \frac{(\text{Sieve}_x + \text{Sieve}_{x+1})}{2} \text{ (mm)} \quad (10)$$

$$\text{Average Particle Surface Area (cubical): } PSA_x = 6 * D_x^2 \text{ (mm}^2\text{)} \quad (11)$$

$$\text{Average Particle Volume (cubical): } V_x = D_x^3 \text{ (mm}^3\text{)} \quad (12)$$

- 21.4. Calculate number of particles per sample unit mass for each sieve size from the size distribution of AASHTO T27 and the respective specific gravities from AASHTO T84 and T85.

$$\text{Number of particles per sieve size: } \#P_x = \frac{\%R_x * 1000}{G_{sb} * V_x} \quad (13)$$

Note 2—A mass of 1 is assumed in Eq 13. This calculation determines the weighting factor applied to each sieve size for a material sample, therefore, actual mass is not required.

- 21.5. Calculate total particle surface area for each sieve size per sample unit mass.

$$\text{Particle Surface Area (each sieve x) (mm}^2\text{): } SSA_x = PSA_x * \#P_x \quad (14)$$

- 21.6. Calculate Sample Surface Area (per unit mass):

$$\text{Total Surface Area (mm}^2\text{): } TSA = \sum_{x=0.075}^{25.0} SSA_x \quad (15)$$

$$\text{Coarse Surface Area (mm}^2\text{): } CSA = \sum_{x=4.75}^{25.0} SSA_x \quad (16)$$

$$\text{Fine Surface Area (mm}^2\text{): } FSA = \sum_{x=0.075}^{2.36} SSA_x \quad (17)$$

21.7. Calculate Sample Particles Count (per unit mass):

$$\text{Total Particles: } \#TP = \sum_{x=0.075}^{25.0} \#P_x \quad (18)$$

$$\# \text{ Coarse Particles: } \#CP = \sum_{x=4.75}^{25.0} \#P_x \quad (19)$$

$$\# \text{ Fine Particles: } \#FP = \sum_{x=0.075}^{2.36} \#P_x \quad (20)$$

21.8. Calculate Sample Gradient Angularity (weighted by surface area):

$$\text{Fine Gradient Angularity: } FGA = \frac{1}{FSA} \sum_{x=0.075}^{2.36} [SSA_x * GA_x] \quad (21)$$

$$\text{Coarse Gradient Angularity: } CGA = \frac{1}{CSA} \sum_{x=4.75}^{25.0} [SSA_x * GA_x] \quad (22)$$

$$\text{Overall Gradient Angularity: } GA = \frac{1}{TSA} \sum_{x=0.075}^{25.0} [SSA_x * GA_x] \quad (23)$$

21.9. Calculate Sample Fine Aggregate Form 2D (weighted by surface area):

$$Form2D = \frac{1}{FSA} \sum_{x=0.075}^{2.36} [SSA_x * 2D_x] \quad (24)$$

21.10. Calculate Sample Coarse Aggregate Texture (weighted by surface area):

$$TX = \frac{1}{CSA} \sum_{x=4.75}^{25.0} [SSA_x * TX_x] \quad (25)$$

21.11. Calculate Sample Coarse Aggregate Sphericity (weighted by particle count):

$$SP = \frac{1}{\#CP} \sum_{x=4.75}^{25.0} [\#P_x * SP_x] \quad (26)$$

21.12. Calculate Sample Sphericity Range Distribution (weighted by particle count):

% of Particles with Sphericity ≤ 0.3 :

$$SP(0.3) = \frac{1}{\#CP} \sum_{x=4.75}^{25.0} [\#P_x * SP(0.3)_x] \quad (27)$$

% of Particles with Sphericity $0.3 < SP \leq 0.7$:

$$SP(0.7) = \frac{1}{\#CP} \sum_{x=4.75}^{25.0} [\#P_x * SP(0.7)_x] \quad (28)$$

% of Particles with Sphericity $0.7 < SP \leq 1.0$:

$$SP(1.0) = \frac{1}{\#CP} \sum_{x=4.75}^{25.0} [\#P_x * SP(1.0)_x] \quad (29)$$

- 21.13. Calculate sample weighted percentages of coarse aggregate Flat and Elongated Values (weighted by mass fraction) at the following ratios: $\geq 1:1$, $>2:1$, $>3:1$, $>4:1$, $>5:1$

$$\% d_L/d_S \geq 1 : \%L/S(\geq 1) = \sum_{x=4.75}^{25.0} \left[\frac{\%R_x * \%L/S(\geq 1)_x}{100} \right] \quad (30)$$

$$\% d_L/d_S > 2 : \%L/S(> 2) = \sum_{x=4.75}^{25.0} \left[\frac{\%R_x * \%L/S(> 2)_x}{100} \right] \quad (31)$$

$$\% d_L/d_S > 3 : \%L/S(> 3) = \sum_{x=4.75}^{25.0} \left[\frac{\%R_x * \%L/S(> 3)_x}{100} \right] \quad (32)$$

$$\% d_L/d_S > 4 : \%L/S(> 4) = \sum_{x=4.75}^{25.0} \left[\frac{\%R_x * \%L/S(> 4)_x}{100} \right] \quad (33)$$

$$\% d_L/d_S > 5 : \%L/S(> 5) = \sum_{x=4.75}^{25.0} \left[\frac{\%R_x * \%L/S(> 5)_x}{100} \right] \quad (34)$$

- 21.13.1. Calculate the sample weighted percentages of Coarse Aggregate Flat or Elongated (weighted by mass fraction) at the following ratios: $\geq 1:1$, $>2:1$, $>3:1$, $>4:1$, $>5:1$

$$\% d_L/d_S \text{ or } d_L/d_L \geq 1 : \%ForE(\geq 1) = \sum_{x=4.75}^{25.0} \left[\frac{\%R_x * \%ForE(\geq 1)_x}{100} \right] \quad (35)$$

$$\% d_L/d_S \text{ or } d_L/d_L > 2 : \%ForE(> 2) = \sum_{x=4.75}^{25.0} \left[\frac{\%R_x * \%ForE(> 2)_x}{100} \right] \quad (36)$$

$$\% d_L/d_S \text{ or } d_L/d_L > 3 : \%ForE(> 3) = \sum_{x=4.75}^{25.0} \left[\frac{\%R_x * \%ForE(> 3)_x}{100} \right] \quad (37)$$

$$\% d_L/d_S \text{ or } d_L/d_L > 4 : \%ForE(> 4) = \sum_{x=4.75}^{25.0} \left[\frac{\%R_x * \%ForE(> 4)_x}{100} \right] \quad (38)$$

$$\% d_L/d_S \text{ or } d_L/d_L > 5 : \%ForE(> 5) = \sum_{x=4.75}^{25.0} \left[\frac{\%R_x * \%ForE(> 5)_x}{100} \right] \quad (39)$$

22. CALCULATIONS – MULTIPLE SOURCE BLEND

- 22.1. Use the calculations in this section to estimate the shape characteristics of multiple material source blends. Each source must be sampled and characterized according to Section 21 calculations.

- 22.2. Determine Blend Composition Percentages

$\%AS_n$ = Percent Aggregate Source n

$$\sum_{i=1}^n \%AS_i = 100 \quad (40)$$

where: n = # of aggregate sources.

- 22.3. Calculate Blend Surface Area

Blend Total Surface Area (each sieve):

$$SSA_{Blend_x} = \sum_{i=1}^n \sum_{x=0.075}^{37.5} \left[\frac{\%AS_i * SSA_{ix}}{100} \right] \quad (1)$$

where: $x = 0.075$ to 25.0 mm

$n = \#$ of aggregate sources

Total Surface Area Blend (all sieves $x = 0.075$ to 25.0 mm)

$$TSA_{Blend} = \sum_{x=0.075}^{25.0} SSA_{Blend_x} \quad (41)$$

Coarse Surface Area Blend (sieve $x = 4.75$ to 25.0):

$$CSA_{Blend} = \sum_{x=4.75}^{25.0} SSA_{Blend_x} \quad (42)$$

Fine Surface Area Blend (sieve $x = 0.075$ to 2.36):

$$FSA_{Blend} = \sum_{x=0.075}^{2.36} SSA_{Blend_x} \quad (43)$$

22.4. Calculate number of particles per blend unit mass for each sieve size:

$$\#P_{Blend_x} = \sum_{i=1}^n \sum_{x=0.075}^{25.0} \left[\frac{\%AS_i * \#P_{ix}}{100} \right] \quad (44)$$

22.5. Calculate number of particles per blend unit mass

Total Particle Count Blend:

$$\#TP_{Blend} = \sum_{x=0.075}^{25.0} \#P_{Blend_x} \quad (45)$$

Coarse Particles Blend:

$$\#CP_{Blend} = \sum_{x=4.75}^{25.0} \#P_{Blend_x} \quad (46)$$

Fine Particles Blend:

$$\#FP_{Blend} = \sum_{x=0.075}^{2.36} \#P_{Blend_x} \quad (47)$$

22.6. Calculate Blend Gradient Angularity for each size $x = 0.075$ to 25.0 mm and combined (weighted by surface area):

$$GA_{Blend_x} = \frac{1}{SSA_{Blend_x}} \left[\sum_{i=1}^i \left[\frac{\%AS_i * SSA_{ix} * GA_{ix}}{100} \right] \right] \quad (48)$$

Blend Fine Gradient Angularity:

$$FGA_{Blend} = \frac{1}{FSA_{Blend}} \left[\sum_{x=0.075}^{2.36} [SSA_{Blend_x} * GA_{Blend_x}] \right] \quad (49)$$

Blend Coarse Gradient Angularity:

$$CGA_{Blend} = \frac{1}{CSA_{Blend}} \left[\sum_{x=4.75}^{25.0} [SSA_{Blend_x} * GA_{Blend_x}] \right] \quad (50)$$

Blend Overall Gradient Angularity:

$$GA_{Blend} = \frac{1}{TSA_{Blend}} \left[\sum_{x=0.075}^{25.0} [SSA_{Blend_x} * GA_{Blend_x}] \right] \quad (51)$$

22.7. Calculate Blend Fine Aggregate Form 2D for each size $x = 0.075$ to 2.36 mm and combined (weighted by surface area):

$$Form2D_{Blend_x} = \frac{1}{SSA_{Blend_x}} \left[\sum_{i=1}^n \left[\frac{\%AS_i * SSA_{ix} * 2D_{ix}}{100} \right] \right] \quad (52)$$

Blend Form 2D:

$$Form2D_{Blend} = \frac{1}{FSA_{Blend}} \left[\sum_{x=0.075}^{2.36} [SSA_{Blend_x} * 2D_{Blend_x}] \right] \quad (53)$$

22.8. Calculate Blend Texture for each size $x = 4.75$ to 25.0 mm and combined (weighted by coarse aggregate surface area):

$$TX_{Blend_x} = \frac{1}{SSA_{Blend_x}} \left[\sum_{i=1}^n \left[\frac{\%AS_i * SSA_{ix} * TX_{ix}}{100} \right] \right] \quad (54)$$

Blend Texture:

$$TX_{Blend} = \frac{1}{CSA_{Blend}} \left[\sum_{x=4.75}^{25.0} [SSA_{Blend_x} * TX_{Blend_x}] \right] \quad (55)$$

22.9. Calculate Average Blend Sphericity for each size 4.75 to 25.0 and blend (weighted by coarse particle count):

$$SP_{Blend_x} = \frac{1}{\#P_{Blend_x}} \left[\sum_{i=1}^n \left[\frac{\%AS_i * \#P_{ix} * SP_{ix}}{100} \right] \right] \quad (56)$$

Blend Sphericity:

$$SP_{Blend} = \frac{1}{\#CP_{Blend}} \left[\sum_{x=4.75}^{25.0} [\#P_{Blend_x} * SP_{Blend_x}] \right] \quad (57)$$

22.10. Calculate Blend Sphericity Distribution for each sieve 4.75 to 25.0 mm and blend (weighted by coarse particle count):

% of Particles with Sphericity ≤ 0.3 (Blend):

$$SP(0.3)_{Blend_x} = \frac{1}{\#P_{Blend_x}} \left[\sum_{i=1}^n \left[\frac{\%AS_i * \#P_{ix} * SP(0.3)_{ix}}{100} \right] \right] \quad (58)$$

$$SP(0.3)_{Blend} = \frac{1}{\#CP_{Blend}} \left[\sum_{x=4.75}^{25.0} \left[\#P_{Blend_x} * SP(0.3)_{Blend_x} \right] \right] \quad (59)$$

% of Particles with Sphericity $0.3 < SP \leq 0.7$ (Blend):

$$SP(0.7)_{Blend_x} = \frac{1}{\#P_{Blend_x}} \left[\sum_{i=1}^n \left[\frac{\%AS_i * \#P_{ix} * SP(0.7)_{ix}}{100} \right] \right] \quad (60)$$

$$SP(0.7)_{Blend} = \frac{1}{\#CP_{Blend}} \left[\sum_{x=4.75}^{25.0} \left[\#P_{Blend_x} * SP(0.7)_{Blend_x} \right] \right] \quad (61)$$

% of Particles with Sphericity $0.7 < SP \leq 1.0$ (Blend):

$$SP(1.0)_{Blend_x} = \frac{1}{\#P_{Blend_x}} \left[\sum_{i=1}^n \left[\frac{\%AS_i * \#P_{ix} * SP(1.0)_{ix}}{100} \right] \right] \quad (62)$$

$$SP(1.0)_{Blend} = \frac{1}{\#CP_{Blend}} \left[\sum_{x=4.75}^{25.0} \left[\#P_{Blend_x} * SP(1.0)_{Blend_x} \right] \right] \quad (63)$$

22.11. Calculate combined Flat and Elongated Values for each sieve 4.75 to 25.0 mm and blend (weighted by mass fraction):

% $d_L/d_S \geq 1$ (Blend):

$$\%L/S(\geq 1)_{Blend_x} = \left[\sum_{i=1}^n \left[\frac{\%AS_i * \%R_{ix} * \%L/S(\geq 1)_{ix}}{100^2} \right] \right] \quad (64)$$

$$\%L/S(\geq 1)_{Blend} = \left[\sum_{x=4.75}^{25.0} \left[\%L/S(\geq 1)_{Blend_x} \right] \right] \quad (65)$$

% $d_L/d_S > 2$ (Blend):

$$\%L/S(> 2)_{Blend_x} = \left[\sum_{i=1}^n \left[\frac{\%AS_i * \%R_{ix} * \%L/S(> 2)_{ix}}{100^2} \right] \right] \quad (66)$$

$$\%L/S(> 2)_{Blend} = \left[\sum_{x=4.75}^{25.0} \left[\%L/S(> 2)_{Blend_x} \right] \right] \quad (67)$$

% $d_L/d_S > 3$ (Blend):

$$\%L/S(> 3)_{Blend_x} = \left[\sum_{i=1}^n \left[\frac{\%AS_i * \%R_{ix} * \%L/S(> 3)_{ix}}{100^2} \right] \right] \quad (68)$$

$$\%L/S(> 3)_{Blend} = \left[\sum_{x=4.75}^{25.0} \left[\%L/S(> 3)_{Blend_x} \right] \right] \quad (69)$$

% d_L/d_S > 4 (Blend):

$$\%L/S(>4)_{Blend_x} = \left[\sum_{i=1}^n \left[\frac{\%AS_i * \%R_{ix} * \%L/S(>4)_{ix}}{100^2} \right] \right] \quad (70)$$

$$\%L/S(>4)_{Blend} = \left[\sum_{x=4.75}^{25.0} [\%L/S(>4)_{Blend_x}] \right] \quad (71)$$

% d_L/d_S ≤ 5 (Blend):

$$\%L/S(>5)_{Blend_x} = \left[\sum_{i=1}^n \left[\frac{\%AS_i * \%R_{ix} * \%L/S(>5)_{ix}}{100^2} \right] \right] \quad (72)$$

$$\%L/S(>5)_{Blend} = \left[\sum_{x=4.75}^{37.5} [\%L/S(>5)_{Blend_x}] \right] \quad (73)$$

22.12.

Calculate Flat or Elongated Values for each sieve 4.75 to 25.0 mm and blend (weighted by mass fraction):

% d_L/d_S or d_L/d_I ≥ 1 : (Blend):

$$\%ForE(\geq 1)_{Blend_x} = \left[\sum_{i=1}^n \left[\frac{\%AS_i * \%R_{ix} * \%ForE(\geq 1)_{ix}}{100^2} \right] \right] \quad (74)$$

$$\%ForE(\geq 1)_{Blend} = \left[\sum_{x=4.75}^{25.0} [\%ForE(\geq 1)_{Blend_x}] \right] \quad (75)$$

% d_L/d_S or d_L/d_I > 2 : (Blend):

$$\%ForE(> 2)_{Blend_x} = \left[\sum_{i=1}^n \left[\frac{\%AS_i * \%R_{ix} * \%ForE(> 2)_{ix}}{100^2} \right] \right] \quad (76)$$

$$\%ForE(> 2)_{Blend} = \left[\sum_{x=4.75}^{25.0} [\%ForE(> 2)_{Blend_x}] \right] \quad (77)$$

% d_L/d_S or d_L/d_I > 3 : (Blend):

$$\%ForE(> 3)_{Blend_x} = \left[\sum_{i=1}^n \left[\frac{\%AS_i * \%R_{ix} * \%ForE(> 3)_{ix}}{100^2} \right] \right] \quad (78)$$

$$\%ForE(> 3)_{Blend} = \left[\sum_{x=4.75}^{25.0} [\%ForE(> 3)_{Blend_x}] \right] \quad (79)$$

% d_L/d_S or d_L/d_I > 4 : (Blend):

$$\%ForE(> 4)_{Blend_x} = \left[\sum_{i=1}^i \left[\frac{\%AS_i * \%R_{ix} * \%ForE(> 4)_{ix}}{100^2} \right] \right] \quad (80)$$

$$\%ForE(> 4)_{Blend} = \left[\sum_{x=4.75}^{25.0} [\%ForE(> 4)_{Blend_x}] \right] \quad (81)$$

% d_i/d_s or $d_i/d_l > 5$: (Blend):

$$\%ForE(> 5)_{Blend_x} = \left[\sum_{i=1}^n \left[\frac{\%AS_i * \%R_{ix} * \%ForE(> 5)_{ix}}{100^2} \right] \right] \quad (82)$$

$$\%ForE(> 5)_{Blend} = \left[\sum_{x=4.75}^{25.0} [\%ForE(> 5)_{Blend_x}] \right] \quad (83)$$

23. REPORT

23.1. Report the following information:

A sample report format is presented in Appendix X1.

23.1.1. Project name.

23.1.2. Date of the analysis.

23.1.3. Material sample identifications: type, source, size, gradation.

23.1.4. Number of particles analyzed for each size.

23.1.5. Material shape property mean and standard deviation. Graphical representations of the property distributions may be included.

24. PRECISION AND BIAS

24.1. *Precision*—This practice uses data generated from other testing methods to develop cumulative information, therefore the precision of the values generated in this practice are established by the precision of the standards used to collect the raw data.

24.2. *Bias*—Since there is no accepted reference device suitable for determining the bias in this method, no statement of bias is made.

25. KEYWORDS

25.1. Aggregate, angularity, consensus property, shape, texture, form, elongation

Appendix X1: Determining Aggregate Source Shape Values from Digital Image Analysis Shape Properties

Stockpile Information

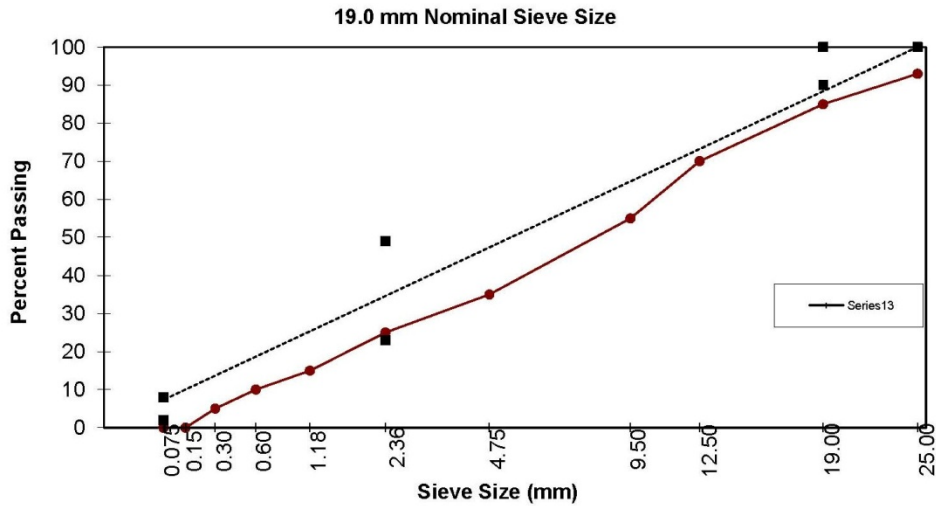
Date:
 Project:
 Technician:
 Workbook Name:

Description:

	Include Estimate	Nominal Sieve	●	○
		Size	% Passing	% Retained
	<input type="checkbox"/>	37.5 (1.5")	100.0%	0.0%
Coarse	<input checked="" type="checkbox"/>	25.0 (1.0")	93.0%	7.0%
	<input checked="" type="checkbox"/>	19.0 (3/4")	85.0%	8.0%
	<input checked="" type="checkbox"/>	12.5 (1/2")	70.0%	15.0%
	<input checked="" type="checkbox"/>	9.5 (3/8")	55.0%	15.0%
	<input checked="" type="checkbox"/>	4.75 (#4)	35.0%	20.0%
Fine	<input checked="" type="checkbox"/>	2.36 (#8)	25.0%	10.0%
	<input checked="" type="checkbox"/>	1.18 (#16)	15.0%	10.0%
	<input checked="" type="checkbox"/>	0.60 (#30)	10.0%	5.0%
	<input checked="" type="checkbox"/>	0.30 (#50)	5.0%	5.0%
	<input checked="" type="checkbox"/>	0.15 (#100)	0.0%	5.0%
	<input checked="" type="checkbox"/>	0.075 (#200)	0.0%	0.0%
		Passing #200	0.0%	0.0%

Gsb(Coarse)=

Gsb (Fine)=



AIMS Stockpile Summary

Project Name:	41_Granite_1	Date:	2/5/09
Workbook:	41_Granite1_AIMS_Stockpile_v3.6.xlsm	Technician:	mjg
Description:			

Combined Properties (weighted)

2D Form (Fine)	7.95	Sphericity (Coarse)		Flat & Elongated Ratio (Coarse)		Flat or Elongated Ratio (Coarse)	
Angularity (Coarse & Fine)	3457.5	Low (≤ 0.3)	0.0%	L/S ≥ 1:1	65.0%	F or E ≥ 1:1	65.0%
Fine Angularity	3501.3	Medium (0.3 - 0.7)	44.3%	L/S > 2:1	48.0%	F or E > 1:2	25.7%
Coarse Angularity	3039.7	High (0.7 - 1.0)	20.7%	L/S > 3:1	23.3%	F or E > 1:3	4.8%
Texture (Coarse)	387.6	Sphericity (Coarse)	0.67	L/S > 4:1	7.3%	F or E > 1:4	0.8%
				L/S > 5:1	2.0%	F or E > 1:5	0.8%

Form2D

Size	Particles in Range	Average	Standard Deviation	Low (≤ 6)		(≤ 6)	Medium (6 - 12)		(≤ 12)	High (12 - 20)		(≤ 20)	Out of Range #
				#	%	Cum. %	#	%	Cum. %	#	%	Cum. %	
2.36 (#8)	151	7.7	1.9	33	21.9%	21.9%	113	74.8%	96.7%	5	3.3%	100.0%	0
1.18 (#16)	150	7.5	1.8	32	21.3%	21.3%	116	77.3%	98.7%	2	1.3%	100.0%	0
0.60 (#30)	150	8.0	2.1	26	17.3%	17.3%	119	79.3%	96.7%	5	3.3%	100.0%	0
0.30 (#50)	151	8.0	2.2	28	18.5%	18.5%	115	76.2%	94.7%	8	5.3%	100.0%	0
0.15 (#100)	151	8.1	2.0	17	11.3%	11.3%	128	84.8%	96.0%	6	4.0%	100.0%	0
0.075 (#200)	146	8.9	2.8	19	13.0%	13.0%	104	71.2%	84.2%	23	15.8%	100.0%	5

Angularity

Size	Particles in Range	Average	Standard Deviation	Low (≤ 3300)		(≤ 3300)	Medium(3300-6600)		(≤ 6600)	High(6600-10000)		(≤ 10000)	Out of Range #
				#	%	Cum. %	#	%	Cum. %	#	%	Cum. %	
37.5 (1.5")													
25.0 (1.0")	50	2873.0	493.1	37	74.0%	74.0%	13	26.0%	100.0%	0	0.0%	100.0%	0
19.0 (3/4")	50	2841.5	639.0	41	82.0%	82.0%	9	18.0%	100.0%	0	0.0%	100.0%	0
12.5 (1/2")	50	3138.7	597.3	28	56.0%	56.0%	22	44.0%	100.0%	0	0.0%	100.0%	0
9.5 (3/8")	50	3251.6	694.5	27	54.0%	54.0%	23	46.0%	100.0%	0	0.0%	100.0%	0
4.75 (#4)	50	2963.7	590.8	37	74.0%	74.0%	13	26.0%	100.0%	0	0.0%	100.0%	0
2.36 (#8)	151	3454.8	918.6	71	47.0%	47.0%	79	52.3%	99.3%	1	0.7%	100.0%	0
1.18 (#16)	150	3288.5	802.0	81	54.0%	54.0%	69	46.0%	100.0%	0	0.0%	100.0%	0
0.60 (#30)	150	3642.0	949.7	58	38.7%	38.7%	90	60.0%	98.7%	2	1.3%	100.0%	0
0.30 (#50)	151	3650.0	984.1	62	41.1%	41.1%	89	58.9%	100.0%	0	0.0%	100.0%	0
0.150 (#100)	151	3451.5	1060.6	83	55.0%	55.0%	66	43.7%	98.7%	2	1.3%	100.0%	0
0.075 (#200)	151	2595.7	1241.4	126	83.4%	83.4%	24	15.9%	99.3%	1	0.7%	100.0%	0

AIMS Stockpile Summary

Project Name:	41_Granite_1	Date:	2/5/09
Workbook:	41_Granite1_AIMS_Stockpile_v3.6.xlsm	Technician:	mjg
Description:			

Texture													
Size	Particles in Range	Average	Standard Deviation	Low (≤ 260)		(≤ 260)	Medium (260 - 550)		(≤ 550)	High (550 - 1000)		(≤ 1000)	Out of Range #
				#	%	Cum. %	#	%	Cum. %	#	%	Cum. %	
37.5 (1.5")													
25.0 (1.0")	50	461.0	84.8	0	0.0%	0.0%	45	90.0%	90.0%	5	10.0%	100.0%	0
19.0 (3/4")	50	480.4	90.5	1	2.0%	2.0%	39	78.0%	80.0%	10	20.0%	100.0%	0
12.5 (1/2")	50	455.5	119.8	1	2.0%	2.0%	41	82.0%	84.0%	8	16.0%	100.0%	0
9.5 (3/8")	50	430.5	128.8	5	10.0%	10.0%	38	76.0%	86.0%	7	14.0%	100.0%	0
4.75 (#4)	50	342.5	135.2	13	26.0%	26.0%	33	66.0%	92.0%	4	8.0%	100.0%	0

Sphericity													
Size	Particles in Range	Average	Standard Deviation	Low (≤ 0.3)		(≤ 0.3)	Medium (0.3 - 0.7)		(≤ 0.7)	High (0.7 - 1.0)		(≤ 1.0)	Out of Range #
				#	%	Cum. %	#	%	Cum. %	#	%	Cum. %	
37.5 (1.5")													
25.0 (1.0")	49	0.68	0.08	0	0.0%	0.0%	30	61.2%	61.2%	19	38.8%	100.0%	1
19.0 (3/4")	49	0.62	0.09	0	0.0%	0.0%	39	79.6%	79.6%	10	20.4%	100.0%	1
12.5 (1/2")	49	0.62	0.09	0	0.0%	0.0%	37	75.5%	75.5%	12	24.5%	100.0%	1
9.5 (3/8")	50	0.61	0.10	0	0.0%	0.0%	37	74.0%	74.0%	13	26.0%	100.0%	0
4.75 (#4)	50	0.67	0.12	0	0.0%	0.0%	28	56.0%	56.0%	22	44.0%	100.0%	0

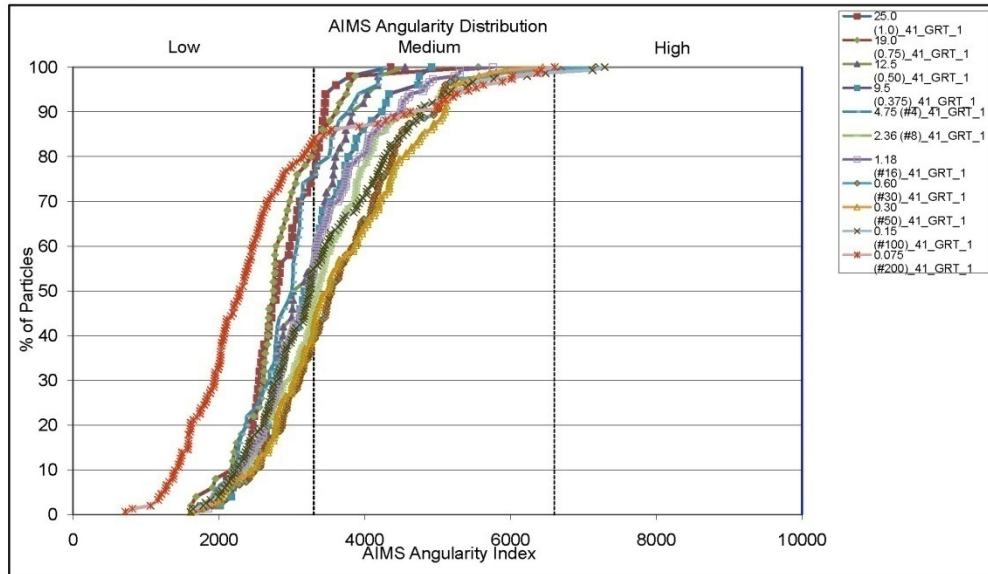
Flat and Elongated Distribution												
Size	Particles in Range	L/S ≥ 1:1		L/S > 2:1		L/S > 3:1		L/S > 4:1		L/S > 5:1		Out of Range #
		#	%	#	%	#	%	#	%	#	%	
37.5 (1.5")												
25.0 (1.0")	49	49	100.0%	33	67.3%	9	18.4%	1	2.0%	0	0.0%	1
19.0 (3/4")	49	49	100.0%	42	86.7%	20	40.8%	5	10.2%	1	2.0%	1
12.5 (1/2")	49	49	100.0%	43	87.8%	21	42.9%	6	12.2%	1	2.0%	1
9.5 (3/8")	50	50	100.0%	39	78.0%	25	50.0%	7	14.0%	1	2.0%	0
4.75 (#4)	50	50	100.0%	29	58.0%	12	24.0%	6	12.0%	3	6.0%	0

Flat or Elongated Distribution												
Size	Particles in Range	F or E ≥ 1:1		F or E > 2:1		F or E > 3:1		F or E > 4:1		F or E > 5:1		Out of Range #
		#	%	#	%	#	%	#	%	#	%	
37.5 (1.5")												
25.0 (1.0")	49	49	100.0%	12	24.5%	2	4.1%	0	0.0%	0	0.0%	1
19.0 (3/4")	49	49	100.0%	23	46.9%	4	8.2%	0	0.0%	0	0.0%	1
12.5 (1/2")	49	49	100.0%	23	46.9%	4	8.2%	0	0.0%	0	0.0%	1
9.5 (3/8")	50	50	100.0%	24	48.0%	2	4.0%	0	0.0%	0	0.0%	0
4.75 (#4)	50	50	100.0%	15	30.0%	5	10.0%	2	4.0%	2	4.0%	0

AIMS Angularity

Project Name:	41_Granite_1	Date:	2/5/09
Workbook:	41_Granite1_AIMS_Stockpile_v3.6.xlsm	Technician:	mjg
Description:			

Particles in Range	1154								
Average	3274.7	Low (≤ 3300)	651	56.4%	(≤ 3300)	56.4%	-σ < n < σ	814	70.5%
Std. Deviation	995.6	Medium (3300 - 6600)	497	43.1%	(≤ 6600)	99.5%	-2σ < n < 2σ	1105	95.8%
Median	3170.6	High (6600 - 10000)	6	0.5%	(≤ 10000)	100.0%	-3σ < n < 3σ	1144	99.1%
Mode	3330.1	Out of Range	0				n < -3σ or n > 3σ	10	0.9%



**APPENDIX B – SAMPLE ILLUSTRATION OF SURFACE
CHARACTERISTICS FOR DIFFERENT MIX TYPES**



Mix: Type D
Highway: SH 36
District: Yoakum
Age: 4 Years
AADT: 4800
MPD: 0.48 mm
DFT 20: 0.331
DFT 80: 0.307
Aggregate: Colorado
Materials
Skid Number: 21

Figure B1. Type D Mixture on Wheelpath of SH 36 in Yoakum District.



Mix: Type D
Highway: SH 36
District: Yoakum
Age: 4 Years
AADT: 4800
MPD: 0.49 mm
DFT 20: 0.643
DFT 80: 0.535
Aggregate: Colorado
Materials
Skid Number: N.A

Figure B2. Type D Mixture on Shoulder of SH 36 in Yoakum District.



Mix: CMHB-C
Highway: US 87
District: Lubbock
Age: 5 Years
AADT: 2905
MPD: 0.98 mm
DFT 20:0.498
DFT 80:0.411
Aggregate:
Vulcan/Brownwood,
Hanson/Davis
Skid Number: 38

Figure B3. CMHB Mixture on Wheelpath of US 87 in Lubbock.



Mix: CMHB-C
Highway: US 87
District: Lubbock
Age: 5 Years
AADT: 2905
MPD: 1.2 mm
DFT 20:0.502
DFT 80:0.418
Aggregate:
Vulcan/Brownwood,
Hanson/Davis
Skid Number: 51

Figure B4. CMHB Mixture on Shoulder of US 87 in Lubbock.



Mix: SMA-C
Highway: IH 20
District: Atlanta
Age: 7 Years
AADT: 15610
MPD: 0.86 mm
DFT 20: 0.505
DFT 80:0.423
Aggregate: Martin
Marietta/Jones Mill,
Malvern Ark
Skid Number: 31

Figure B5. SMA-C Mixture on Wheelpath of IH 20 in Atlanta District.



Mix: SMA-C
Highway: IH 20
District: Atlanta
Age: 7 Years
AADT: 15610
MPD: 0.86 mm
DFT 20: 0.485
DFT 80:0.402
Aggregate: Martin
Marietta/Jones Mill,
Malvern Ark
Skid Number: 37

Figure B6. SMA-C Mixture on Shoulder of IH 20 in Atlanta District.



Mix: Type C
Highway: SH 16
District: San Antonio
Age: 6 Years
AADT: 6400
MPD: 0.61 mm
DFT 20:0.294
DFT 80:0.282
Aggregate: Martin
Marietta/Beckman
Skid Number: 13

Figure B7. Type C Mixture on Wheelpath of SH 16 in San Antonio.



Mix: Type C
Highway: SH 16
District: San Antonio
Age: 6 Years
AADT: 6400
MPD: 0.46 mm
DFT 20:0.424
DFT 80:0.420
Aggregate: Martin
Marietta/Beckman
Skid Number: 20

Figure B8. Type C Mixture on Shoulder of SH 16 in San Antonio.



Mix: PFC
Highway: IH 35
District: San Antonio
Age: 4 Years
AADT: 107000
MPD: 1.15 mm
DFT 20:0.437
DFT 80:0.360
Aggregate: Martin
Marietta/Beckman,
Delta/Brownlee
Skid Number: 24

Figure B9. PFC Mixture on Wheelpath of IH 35 in San Antonio.



Mix: PFC
Highway: IH 35
District: San Antonio
Age: 4 Years
AADT: 107000
MPD: 1.37 mm
DFT 20:0.547
DFT 80:0.468
Aggregate: Martin
Marietta/Beckman,
Delta/Brownlee
Skid Number: 31

Figure B10. PFC Mixture on Wheelpath of IH 35 in San Antonio.



Mix: Superpave
Highway: IH 20
District: Abilene
Age: 7 Years
AADT: 9535
MPD: 0.56 mm
DFT 20:0.218
DFT 80:0.255
Aggregate:
Vulcan/Black Lease
Skid Number: 15

Figure B11. Superpave Mixture on Wheelpath of IH 20 in Abilene.



Mix: Superpave
Highway: IH 20
District: Abilene
Age: 7 Years
AADT: 9535
MPD: 0.61 mm
DFT 20:0.682
DFT 80:0.629
Aggregate:
Vulcan/Black Lease
Skid Number: 31

Figure B12. Superpave Mixture on Shoulder of IH 20 in Abilene.

APPENDIX C – EXAMPLE DATA AND SENSITIVITY ANALYSIS

Table C1. Example Input Data.

Input Category	Input Parameters	Value
Asphalt mixture gradation	Choose gradation	Type C
AIMS texture data	Number of data points	2
	Number of aggregate sources	2
	Name of aggregate source 1	ABC
	Name of aggregate source 2	XYZ
	Source 1: Proportion of aggregate in the mix (%)	60
	Source 1: Percent Passing #4	30
	Source1: Texture before Micro-Deval	220
	Source 1: Texture after 105 minutes Micro-Deval	100
	Source 2: Proportion of aggregate in the mix (%)	40
	Source 2: Percent Passing #4	85
	Source2: Texture before Micro-Deval	180
	Source 2: Texture after 105 minutes Micro-Deval	80
Pavement texture data	Use SAAP estimation of MPD in mm	0.76 (Default)
Traffic data	Highway type	Divided
	Number of traffic lanes	Four Lanes
	Average annual daily traffic	20,000
	Percentage of truck traffic	10
Analysis type	Predict skid resistance as a function of years in service	Figure A1 as output
Analysis type	Classify an asphalt pavement section based on its skid resistance	Figure A2 as output
	Service life	15 years
	Accepted SN50	28
	Monitor pavement frequently	22< SN50<27

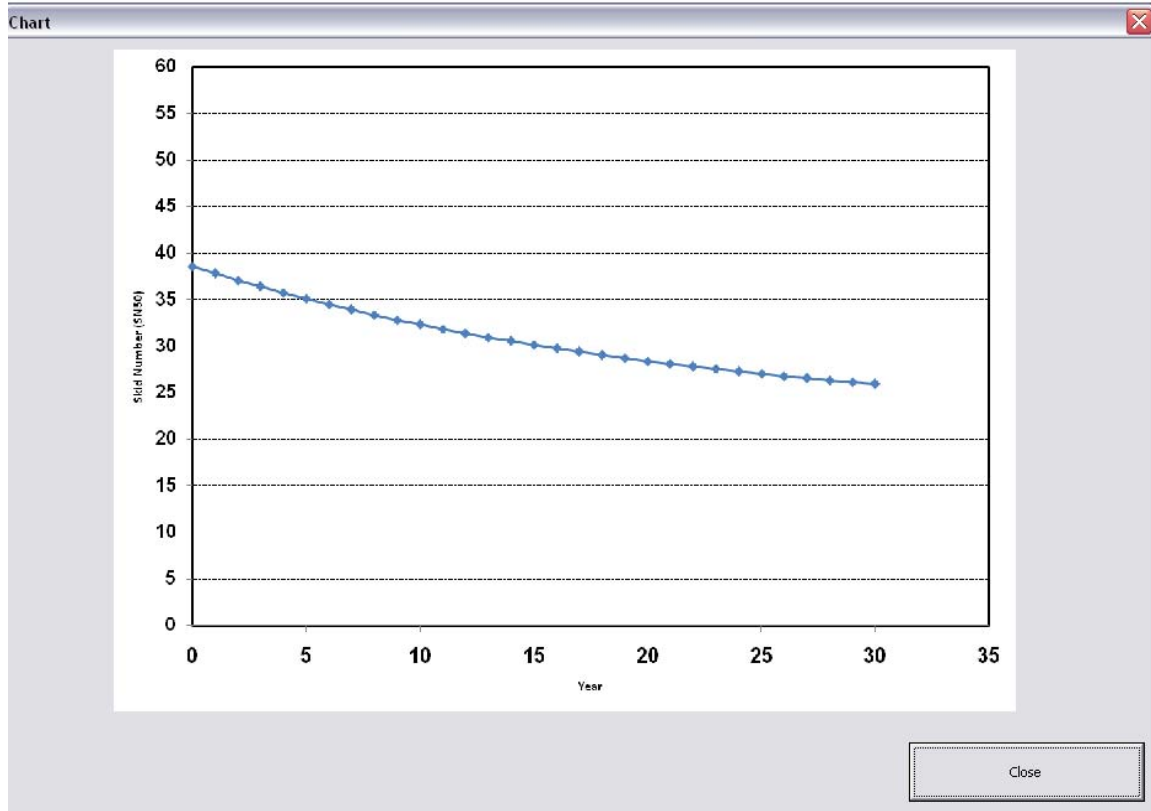


Figure C1. Example Output Chart for Skid Prediction.

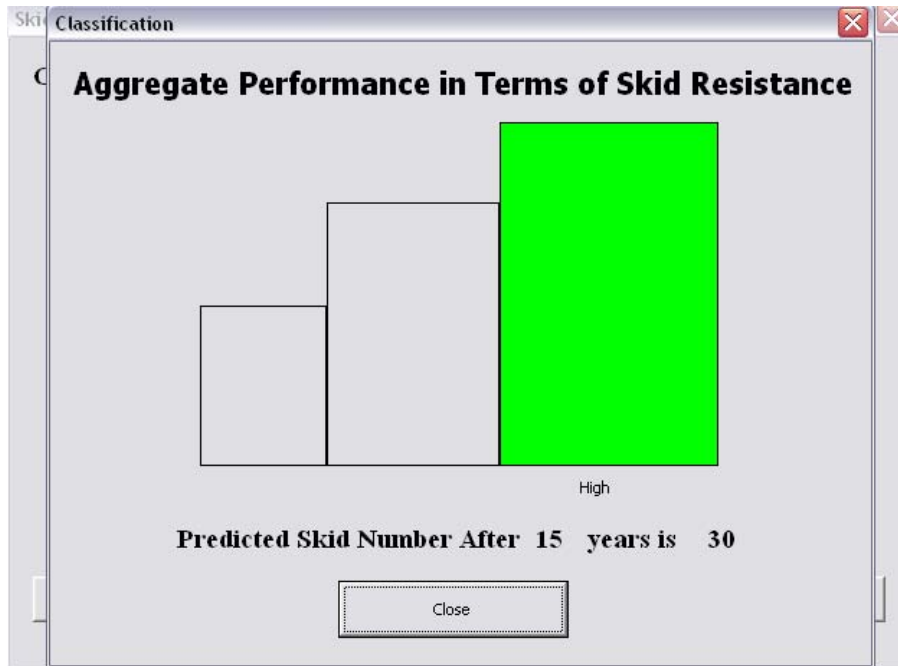


Figure C2. Example Output Chart for Pavement Classification.

A small scale simple sensitivity analysis was performed to show the variation of skid number along the service life of the pavement with the change of major variables. The input parameters that were varied are mixture type, aggregate type (texture), and traffic. The input variables were changed one at a time.

Figure C3 shows the change skid numbers with the service life of pavement for different type of surface mixtures. SMA and CMHB-C exhibit the highest initial skid number followed by PFC and Type C mixture. Type D mixture exhibits lowest skid numbers. Over time the loss of skid number for PFC mixture is lowest among all the mixtures. This graph shows that the skid number along the service life is very sensitive to the mixture type or mixture gradation.

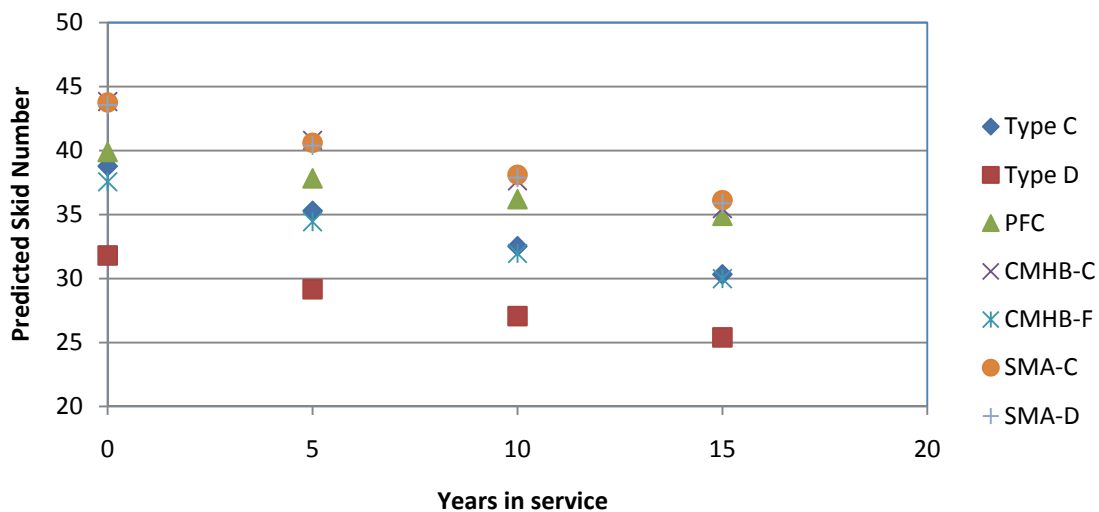


Figure C3. Variation of Predicted Skid Number for Different Mixture Type.

Figure C4 shows the change of skid numbers with the service life for different traffic levels. Loss of skid number is sensitive to traffic level. At low traffic level (500 ADT) the skid number virtually remains unchanged over the service life. The level of truck traffic was not changed as in the current program the effect of truck traffic on skid resistance is not calculated. Figure C5 presents the variation of skid number of the service life for three different levels of aggregate texture loss. Loss of aggregate texture due to Micro-Deval polishing has the most dramatic effect on loss of skid number. Typically, aggregates with high initial texture value shows high initial skid number. But the skid number loses rapidly if the measured texture loss is high. The skid number was not sensitive to the mean profile depth for given mixture type.

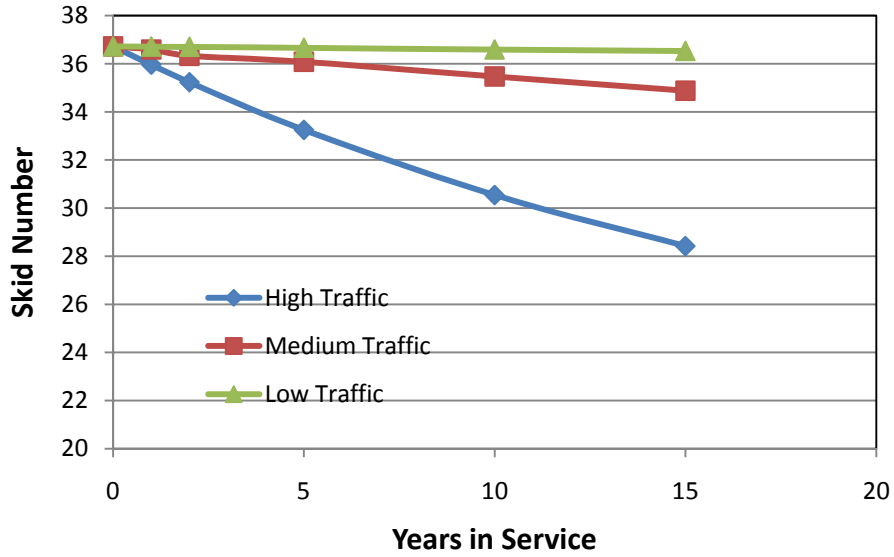


Figure C4. Variation of Skid Number for Different Traffic Levels.

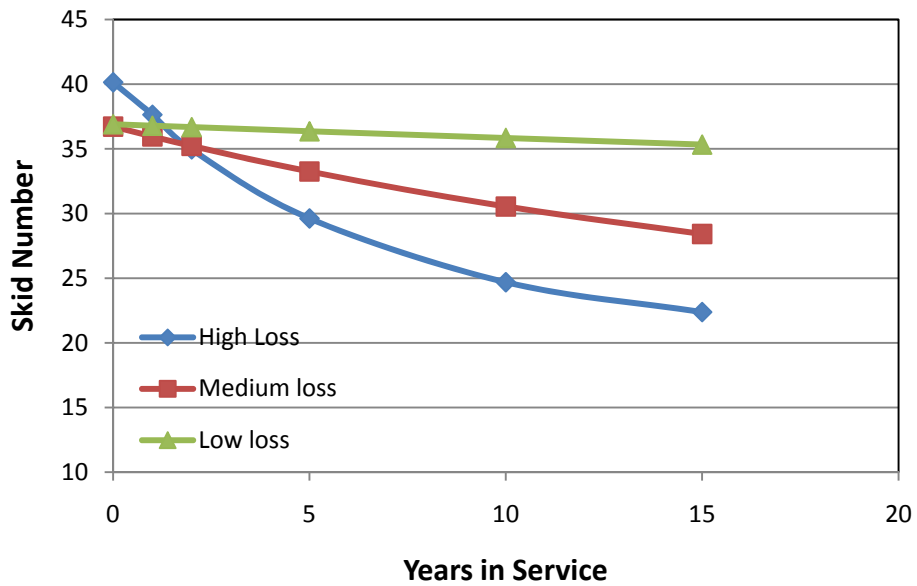


Figure C5. Variation of Skid Number for Different Traffic Levels.